

Design and Implementation of a Tribological Module

Design of a Testing Device for the Qualitative Evaluation
of Laser Cladded Coatings in Deep Drawing Applications

Master Thesis
at
Graz University of Technology

submitted by
Marina Kofler



Institute for Tools and Forming (T&F)
Graz University of Technology
A-8010 Graz, Austria

Advisor: Univ.-Prof. Dr.-Ing. Ralf Kolleck
Dipl.-Ing. Robert Vollmer

March 28, 2012



© Copyright Marina Kofler 2012

Entwicklung und Implementierung eines Tribo-Moduls

Entwicklung einer Testkonfiguration zur qualitativen
Bewertung von laserauftraggeschweißten
Beschichtungen in der Umformtechnik

Diplomarbeit
an der
Technischen Universität Graz

vorgelegt von
Marina Kofler



Institut für Werkzeugtechnik & Spanlose Produktion
Technische Universität Graz
A-8010 Graz, Österreich

Betreuer: Univ.-Prof. Dr.-Ing. Ralf Kolleck
Dipl.-Ing. Robert Vollmer

28. März 2012



Diese Arbeit wurde in englischer Sprache verfasst.

© Copyright Marina Kofler 2012

STATUTORY DECLARATION

I declare that I have authored this thesis independently, that I have not used other than the declared sources/resources, and that I have explicitly marked all material which has been quoted either literally or by content from the used sources.

EIDESSTATTLICHE ERKLÄRUNG

Ich erkläre an Eides statt, dass ich die vorliegende Arbeit selbstständig verfasst, andere als die angegebenen Quellen/Hilfsmittel nicht benutzt, und die den benutzten Quellen wörtlich und inhaltlich entnommenen Stellen als solche kenntlich gemacht habe.

Marina Kofler
Graz, Austria, March 2012

Abstract

Aside from the physical disruption of a forming tool, tool wear is considered the most important failure mode in forming applications, as it has a direct impact on the dimension accuracy, shape and quality of the processed parts. Thus, its progress has to be monitored and - if possible - anticipated thoroughly. The wear of forming tools is mainly caused by the co-occurrence and overlapping mechanisms of adhesion and abrasion. At elevated temperatures tribochemical reactions also have to be considered. Since high-strength and ultra high-strength materials have become a dominant constant in deep drawing operations, the tribological strain on forming tools has ever been increasing. In order to meet these demanding requirements, while maintaining appropriate cost levels, critical tool areas are covered with functional graded coatings. This master thesis aims at designing a device to pretest and evaluate these coatings, as well as innovative material pairings, before they are transferred to actual forming applications.

The practical part of this thesis emphasizes the development of a suitable testing configuration that is specifically adapted to the distinct characteristics of deep drawing applications. In common test configurations - often referred to as Pin/Disc or Pin/Flat tribometer - mostly recurring contact movements (circular, translational) are realized. The repeated contact of the two friction partners leads to an alteration of the initial material surfaces and, for example, destroys passive layers. The presented paper describes a tribometric system in which the test pin meanders on a large-area sheet metal, and therefore simulates the deep drawing process in a more accurate way, as it is always in contact with intact surface areas.

Such a constellation naturally reproduces the *Stop-and-Go* peculiarity (the sequential occurrence of acceleration, steady speed and deceleration) that is featured by all deep drawing operations. The generated surface pressures are derived from state-of-the-art drawing applications and also contribute to the significance of the obtained test results for deep drawing applications. Furthermore, a cooling system is incorporated into the design, enabling the simulation of high temperature forming processes as well. This thesis comprises the concept generation, the design of the tribological module and a thorough documentation of the test set-up. In addition, basic knowledge of the science of tribology is provided, and its implications for forming technologies are highlighted.

Kurzfassung

Neben der effektiven Materialermüdung von Umformwerkzeugen, zählt Werkzeugverschleiß zu den wichtigsten Versagensarten im Umformprozess, da er direkten Einfluss auf die Maßgenauigkeit, die Form und die Qualität der hergestellten Bauteile ausübt. Es ist daher essentiell dessen Fortschreiten genauestens zu überwachen und - sofern möglich - vorherzusagen. Der Verschleiß in Umformwerkzeugen wird hauptsächlich durch das Vorkommen und die Überlagerung der Verschleißmechanismen Adhäsion und Abrasion verursacht. Bei erhöhten Temperaturen müssen zusätzlich auch tribochemische Reaktionen berücksichtigt werden. Durch den vermehrten Einsatz von hochfesten und ultra-hochfesten Materialien in Tiefziehprozessen, hat sich die tribologische Belastung der betreffenden Werkzeuge in den letzten Jahren kontinuierlich erhöht. Um diesen anspruchsvollen Anforderungen, auf einem dennoch akzeptablen Kostenniveau, gerecht zu werden, werden kritische Werkzeugbereiche mittels Laserauftragsschweißen beschichtet und dadurch verschleißbeständiger gemacht.

Das Ziel der vorgestellten Diplomarbeit besteht darin eine Testkonfiguration zu entwerfen, mit der man diese Beschichtungen, sowie neuartige Materialkonzepte, evaluieren und vorab testen kann - bevor man sie dann auf den eigentlichen Umformprozess überträgt.

Der Kern dieser Arbeit besteht aus der Entwicklung eines neuartigen Versuchskonzeptes, welches speziell auf die besonderen Charakteristiken in der Umformtechnik ausgelegt wurde. In üblichen Testkonfigurationen, bekannt als Pin/Disk oder Pin/Flat Tribometer, werden vorwiegend wiederkehrende Kontaktbewegungen (kreisförmig/translatorisch) realisiert. Durch den wiederholten Kontakt der beiden Reibpartner werden die Ausgangsoberflächen verändert und, beispielsweise, Passivschichten zerstört. In der vorliegenden Arbeit wurde ein tribometrisches System entwickelt, das - im Gegensatz dazu - den zu bewertenden Teststift mäanderförmig auf einem großflächigen Blechbauteil bahngesteuert bewegt. Dadurch steht dieser ständig mit intakten Ausgangsmaterialien in Berührung und simuliert somit den Tiefziehprozess sehr realitätsnah. Aber auch der signifikante *Stop-and-Go* Faktor des Tiefziehens (das Aufeinanderfolgen von Beschleunigung, konstanter Geschwindigkeit und Verzögerung), sowie die abbildbaren Flächenpressungen, die auf dem derzeitigen Stand der Technik basieren, erhöhen die Aussagekraft der Testergebnisse für den Tiefziehprozess.

Da zusätzlich ein Kühlsystem in das Design eingearbeitet wurde, ist auch das Vorhersagen komplizierter Verschleißprozesse in Hochtemperaturprozessen möglich. Neben der Konzeptentwicklung, der Konstruktion des Tribomoduls und der gründlichen Beschreibung des Versuchsaufbaus, beinhaltet die vorliegende Diplomarbeit grundlegendes Theoriewissen der Tribologie und deren Signifikanz für die Umformtechnik.

Acknowledgements

A master thesis marks the ending of an academic study. In my case this final project was far more than just the mandatory composition of a chosen topic. It gave me the possibility to apply knowledge I gathered throughout the years of study, to refresh facts and information that got lost along the way, and to acquire a new understanding for the scientific study of tribology. I am very grateful for being given such an opportunity in form of a truly interesting master thesis. I am therefore deeply indebted to Univ.-Prof. Dr.-Ing. Ralf Kolleck and my advisor Dipl.-Ing. Robert Vollmer. I would like to thank for the support and patience during the elaboration of this thesis.

The fact that I could combine my master thesis with my employment at the Institute for Tools and Forming (T&F) was a truly fortunate coincidence. I was always surrounded with people that would generously provide invaluable *words of wisdom*, in both, technical and general, aspects. Listing every person individually that helped me in some way or another, would inevitably result in an enumeration of all employees at the T&F. I would like to substitutionally thank *ALL* colleagues at the T&F for their inestimable support. In this context, special thanks have to go to Heinz Fasching for his technical insights throughout the course of the project, and Florian Krall for his assistance during the pilot test sequence.

I am profoundly grateful for the thorough and exerted revision of this paper by Dipl.-Ing. Cornelia Hoisl, even though tribometric devices are not her area of expertise.

Concluding, I would like to acknowledge the debt I owe to my family. Without their unalienable support and encouragement I would have not been able to complete this study. My mother, Barbara, and my grandparents, Adelheid and Thomas, provided moral support throughout the course my studies. I feel also very much indebted to my siblings, Marlen and Matthias, as well as my partner, Manuel, for listening to my endless disquisitions on emerging problems or progress made. - I will be, forever, thankful for your understanding.

Symbols and Abbreviations

List of Symbols

A	Geometric Contact Area	[mm ²]
a	Half Contact Width (Hertzian Pressure)	[mm]
A_i	Surface Area of Micro Contact	[mm ²]
A_{Real}	Real Contact Area	[mm ²]
d_0	Blank Diameter before Forming	[mm]
d_1	Inner Diameter of Cup (Punch Diameter)	[mm]
d_a	Diameter of Wear Scar Perpendicular to Sliding Direction	[mm]
d_p	Diameter of Wear Scar Parallel to Sliding Direction	[mm]
d_p	Punch Diameter	[mm]
E	Modulus of Elasticity	[MPa]
F_{BH}	Blank Holder Force	[N]
F_N	Normal Force	[N]
F_P	Punch Force	[N]
F_R	Friction Force	[N]
F_{Rdyn}	Dynamic/Kinetic Friction Force	[N]
F_{Rstat}	Static Friction Force	[N]
G	Shear Modulus of Elasticity	[MPa]
I	Moment of Inertia	[mm ⁴]
k_f	Flow Stress	[MPa]
p	Surface Pressure	[N/mm ²]
R	Spring Rate	[N/mm]
r	Vertical Anisotropy	[-]
r	Radius	[mm]
r_{fd}	Die Radius	[mm]
r_{fp}	Punch Radius	[mm]

R_m	Tensile Strength	[MPa]
s	Sheet Thickness	[mm]
s_n	Nominal Spring Deflection	[mm]
T_R	Recrystallisation Temperature	[K]
T_S	Melting Temperature	[K]
U	Strain Energy	[Nmm]
v	Velocity	[m/s]
$W_{V;b}$	Wear Volume of a Ball	[m ³]
β	Drawing Ratio	[-]
β_0	Initial Drawing Ratio	[-]
β_{max}	Maximum Drawing Ratio	[-]
β_n	Subsequent Drawing Ratio	[-]
δ	Flattening (Hertzian Pressure)	[mm]
ε	Elongation (Strain)	[-]
η	Viscosity	[kg/ms]
φ	Natural Strain (True Elongation, Natural Logarithmic Strain)	[-]
$\varphi_1; \varphi_2; \varphi_3$	Main Natural Strains	[-]
φ_b	Widthwise Natural Strain	[-]
φ_s	Latitudinal Natural Strain	[-]
φ_v	Effective Strain	[-]
γ	Shear Strain (Shearing Angle)	[°]
λ	Proportionality Factor	[-]
$\dot{\lambda}$	Proportionality Factor	[-]
μ	Friction Coefficient	[-]
ρ	Density	[kg/m ³]
σ	Normal Stress	[MPa]
τ	Shear Stress	[MPa]

Acronyms

AHSS	Advanced High-Strength Steel
AVC	Advanced Vehicle Concepts
bcc	Body-Centred Cubic
BH	Bake Hardenable (Steel)
CMn	Carbon-Manganese (Steel)
CVD	Chemical Vapour Deposition
DP	Dual Phase (Steel)
EHL	ElastoHydrodynamic Lubrication
fcc	Face-Centred Cubic
FLC	Forming Limit Curve
FLD	Forming Limit Diagram
GfT	Deutsche Gesellschaft für Tribologie
HAZ	Heat Affected Zone
hcp	Hexagonal Closest Packed
HL	Hydrodynamic Lubrication
HSLA	High Strength, Low Alloy (Steel)
HSS	High-Strength Steel
IF	Interstitial Free (Steel)
IS	Isotropic (Steel)
Mart	Martensite (Steel)
MGPG	Measurement Good Practice Guide
NPL	National Physical Laboratory
PVD	Physical Vapour Deposition
T&F	Institute for Tools and Forming
TRIP	Transformation Induced Plasticity (Steel)
TTS	Tribotechnical System
UHSS	Ultra High-Strength Steel
ULSAB	Ultra-Light Steel Auto Body

Contents

Symbols and Abbreviations	iii
1 Introduction	1
2 Tribology	5
2.1 Significance	5
2.2 Tribotechnical System	6
2.3 Friction	8
2.3.1 Historical Review	8
2.3.2 Classification of Friction	9
2.3.3 Mechanisms of Friction	11
2.4 Wear	14
2.4.1 Wear Types	14
2.4.2 Wear Mechanisms	14
2.4.3 Wear Quantification	18
2.5 Testing Equipment	20
2.5.1 Levels of Tribological Testing	21
2.5.2 Tribometry	22
3 Forming Technologies	27
3.1 Introduction	27
3.1.1 Historical Development	27
3.1.2 Economic Relevance	28
3.1.3 Classification of Forming Technologies	28
3.2 Deep Drawing	30
3.2.1 Procedural Principle	30
3.2.2 Characterizing Parameters	32
3.3 Tribology in Forming Applications	35
3.3.1 Tribosystem	35
3.3.2 Friction	36
3.3.3 Wear	37
3.4 Wear Slowing Tool Coatings	38
3.4.1 Surface Treatments of Critical Tool Areas	38
3.4.2 Laser Cladding	39
4 Project Content	43

5	Determination of Concept	45
5.1	Generation of Concept Variants	45
5.2	Assessment of Concepts	45
5.3	Selection of Concept	51
6	Technical Realisation	53
6.1	Determination of Basic Dimensions	53
6.2	Holding Fixture	54
6.3	Adjustment of Surface Pressure	55
6.4	Guiding System	58
6.5	Cooling System	58
6.6	Housing	59
7	Test Set-up	61
7.1	Pin Preparation	61
7.2	Fixation of Metal Sheet	61
7.3	Assembly of Tribo-Module	63
7.4	Calibration	65
7.5	Pilot Test Sequence	66
7.6	Obtained Results	68
8	Concluding Remarks and Outlook	69
A	Wear related Terms and Definitions	71
B	Technical Drawings	77
	List of Figures	86
	List of Tables	87
	Bibliography	89

Chapter 1

Introduction

When reviewing general trends and ongoing research in the peripheral fields of automotive industries, there are two catchphrases that have become ubiquitous during the last period of years: *lightweight construction* and *high-strength materials*. Not many papers and publications can be found that lack these attractive slogans. Whether the main focus is the reduction of CO_2 emissions, the improvement of crash performances and passenger safety, or the positive economic aspect in general, - at one point or another, the concept of lightweight design, and consequently high-strength materials, is introduced to the topic. It is this aspiration for highly efficient and, at the same time, safe vehicles that result in innovative material concepts that compete for the highest realizable strengths.

The tensile strengths of new materials are increasing constantly. In order to give some kind of reference regarding the strength behaviour of this specific material group, new prefixes have been introduced, because the sole description by adjectives is no longer sufficient. High-strength (HSS), advanced high-strength (AHSS), ultra high-strength steels (UHSS) - though the distinction is not easily made¹, the problems for manufacturing processes are very much alike.

In order to meet the increasing demands that arise from the elevated mechanical (and often thermal) exposure, tool concepts need to be improved eventually. The field of metal forming is no exception to this rule. In order to plastically deform ultra high-strength sheet materials - that frequently feature tensile strengths (R_m) of up to 1,400 MPa - the forming tools have to be adapted. As a complete replacement is highly uneconomical, critical tool areas are often coated with high-strength, wear-resisting layers.

Laser cladding, as applied at the T&F, is one approach to cope with these augmented demands. This innovative coating technique combines the advantages of laser welding and powder metallurgy. This way, high bonding strengths between the coating and the substrate can be achieved, while maintaining small heat affected zones (HAZ). Moreover, there are nearly no constraints regarding the coating materials.

Even though, the possibilities of different powder combinations are endless, it is crucial to verify various compositions before applying them to actual tool surfaces. Also, new and

¹See Figure 1.1

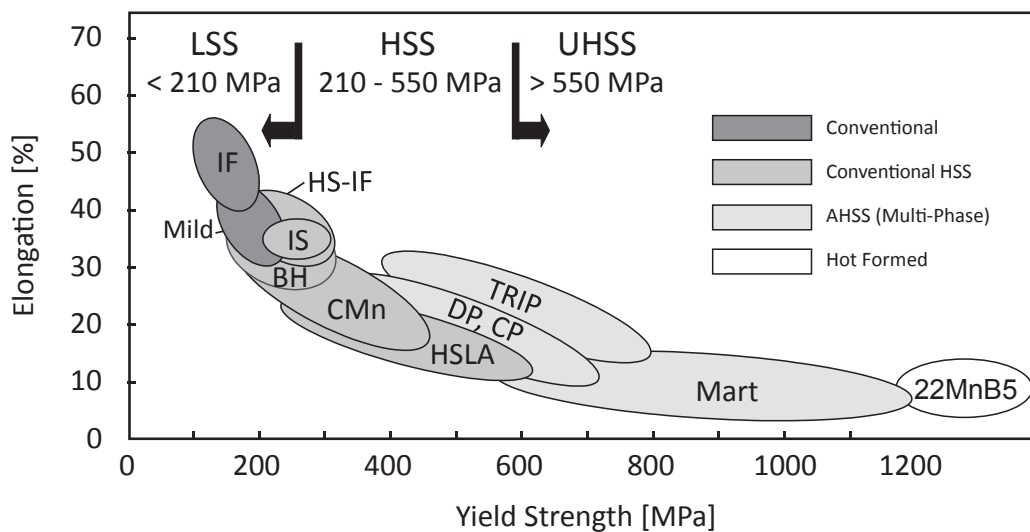


Figure 1.1: Yield strength in relation to the maximal elongation of common steel grades [ULSAB-AVC, 2001, p. 2]

innovative coating materials should be tested and evaluated before being transferred to large scale applications.

This diploma thesis aims at conceptualizing and designing a suitable pretesting device for this specific purpose.

The mechanical and thermal loads that were mentioned before, are also referred to as *tribological strains*. Even though many people might not be familiar with the term *tribology*, the mechanisms and effects comprised by this expression are omnipresent and well perceived. DIN 50323² defines tribology as the science and technology of interacting surfaces in relative motion. It comprises the areas of friction, wear and lubrication, including associated boundary layer interactions between solids as well as between fluids or gases.

Both, friction and especially wear, are mainly associated with unfavourable energy and material losses that need to be prevented by all means necessary. Though, this is true for the majority of technical systems, there are also some positive effects worth mentioning. Friction, for example, is beneficially applied in clutches, brakes, bolts and nuts. And even the material removing effect of wear mechanisms can sometimes be desired: for instance, when writing with a pencil on a piece of paper.

²All referenced standards and guidelines can be obtained from Appendix 'Bibliography'.

One part of this paper aims at introducing the basic terms and fundamentals, as well as its causes and effects of the rather *young*, interdisciplinary science of tribology. The gained knowledge is then applied to the deep drawing process and is ultimately incorporated in the designed tribological testing device.

Chapter 2

Tribology

Relative motion between two or more interacting surfaces - a setting that can be observed in the vast majority of technical applications - inevitably results in a resistance to that motion. This resistance, or friction, will eventually lead to energy and material losses and therefore causes wear. In order to minimize the destructive and expensive effects of wear, numerous lubrication concepts have been introduced into modern engineering operations.

Tribology is the interdisciplinary science that comprises the configuration described above. It is the connective study of the fields of friction, wear and lubrication.

2.1 Significance

The study of tribology has been established to explore and fully understand the complex mechanisms that take place in a tribological system, combining - for the first time ever - all major disciplines involving friction and wear.

Originally derived from the Greek term '*tribos - to rub*', the term *Tribology* was coined by Prof. H. Peter Jost in a UK Government Report in March 1966. [Jost, 1996] The so-called *Jost Report* highlighted the immense saving potential that lies within this branch of study. The fact that tribology is mainly based on already existing knowledge and only requires some comparatively low research efforts contributed to the rapid expansion of this new idea, resulting in over 40 national tribology societies or committees and another several hundred corresponding chairs in 2011. [International Tribology Council, 2011]

The promising cost reduction is still the main driving force behind ongoing research. The *German Society of Tribology* (Deutsche Gesellschaft für Tribologie (GfT)) points out that about 5 % of the German annual gross national product is lost due to friction and wear. This equals a total of 35 billion € /year. The consistent implementation of the already gathered knowledge on tribology could economize an amount of 5 billion € /year, further measures from ongoing research activities not even included. [Gesellschaft für Tribologie, 2012]

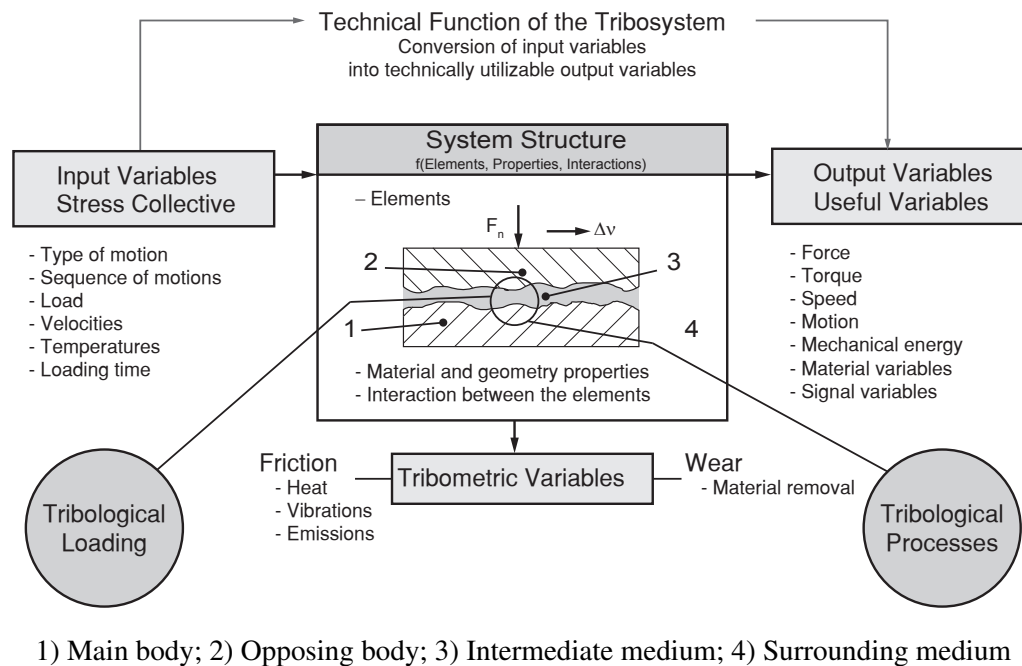


Figure 2.1: Schematic description of a tribotechnical system (adapted from Czichos and Habig [1992, p. 13] and Grote and Antonsson [2009, p.296])

2.2 Tribotechnical System

The tribotechnical system (TTS) is a simplified model of a real technical application, detaching all elements involved in friction and wear from their surrounding.

Figure 2.1 highlights all elements and parameters of a tribotechnical system. Accordingly, Czichos and Habig [1992, pp. 13-14] define the characterizing properties of a tribosystem:

1. Function and Output Variables
2. System Structure
 - Components subjected to tribological strains
 - Relevant properties of elements
 - Interactions of and interdependencies between parts
3. Stress Collective or Input Variables
4. Tribological Loading
5. Tribological Processes
6. Tribometric Parameters

Function and Output Variables

Every TTS exists to fulfil a certain function that can be described by the obtained output variables. Prevalent output variables include motions, forces/torques, material and signal

variables.

Systems Structure

Base body, opposing body, intermediate and surrounding medium - these are the basic components that define the system structure. Even the most complex technical configurations can be reduced to this comprehensive model. Table 2.1 shows examples of system structures of common tribosystems. Note that while the main and opposing bodies are principal elements and can be found in every tribosystem, intermediate and surrounding media can be missing in certain cases. An additional classification can be made according the system boundary. A *closed* system consists of two bodies whose stressed areas are repeatedly in contact. In an *open* system, on the other hand, the main body is continuously stressed by new material zones of the counter body. [Grote and Antonsson, 2009, p. 296]

The relevant properties of the elements can be separated into material, geometry and physical parameters.

Input Variables

The input (or operating) variables are characterized by the progress and duration of mechanical loads, temperatures, velocities, types of movement (sliding, rolling, flowing, impact) as well as patterns of movement (continuous, oscillating, intermitting).

Tribological Loading

The tribological load originates in the stress collective and describes its impact on the system structure. The representing parameters are dynamic, highly influenceable by the system configuration and only present when the TTS is operating. Above all, it is important to state that the characterizing variables, like contact geometry, surface pressure or lubrication thickness, can *not* be anticipated by considering the engaged system elements individually.

Tribological Processes

Friction and wear mechanisms and their interdependencies are commonly referred to as tribological processes. They are caused by the tribological loading and ultimately result in wear induced material losses and friction induced energy losses.

Tribometric Parameters

Tribometric parameters are numeral values that epitomize material and energy losses as well as changes in the system structure.

The above explanations highlight that the tribological behaviour of a TTS is rather a system response to the occurring loads, than an accumulation of material properties. Complex and irreversible processes take place - especially in the boundary layers - and influence each

Table 2.1: System structure of common tribosystems [Grote and Antonsson, 2009, p. 297]

TTS	Base Body	Counter-body	Interfacial Medium	Ambient Medium	System Type
Press and shrink joints	Shaft	Hub	-	Air	Closed
Sliding bearing	Journal	Bearing bush	Oil	Air	Closed
Mechanical face seal	Seal head	Seat	Liquid or gas	Air	Closed
Gear train	Pinion	Wheel	Gear oil	Air	Closed
Wheel/Rail	Wheel	Rail	Moisture, dust, ...	Air	Open
Excavator bucket/ Excavated material	Bucket	Material	-	Air	Open
Turning tool	Cutting edge	Workpiece	Lubricant	Air	Open

other. Thus, a thorough and systematical description can only result from obtaining friction and wear parameters. Details on friction and wear, including their characterizing values, can be found in the following sections.

Appendix A ‘Wear related Terms and Definitions’ features an abundant list of terms and definitions regarding friction and wear, including the German translation, a general classification and a short explanation.

2.3 Friction

From a macroscopic point of view, friction is perceived as the collectivity of forces and mechanisms that opposes the relative movement of two subtended bodies. This notion is perspicuous and taught at a very early stage of any technical study programme.

However, the real complexity that is comprised by the well known equation

$$F_R = F_N \cdot \mu \quad (2.1)$$

(μ = friction coefficient), is disguised by its simplicity. The mechanisms responsible for friction are complex, highly system dependant and, above all, they are amplifying and manipulating each other. Various mathematical models and respective theories enable and facilitate a description of single processes. A relevant anticipation of the overlapping and interdependence of various mechanisms is not yet realizable. Friction, as defined by Equation 2.1, can therefore be understood as the substitutional solution for the mathematical problem of friction.

2.3.1 Historical Review

Friction is a dominant in nearly every aspect of life - influencing nature as well as engineering applications. Consequentially, early records of the methodic use of friction exist, dating back 400,000 years.

Although systematically applied throughout history (Neanderthals using flint stones - 200,000 B.C.; Egyptians and Sumerians applying lubricants to move heavy objects - 2,400 B.C.)¹, it was not until Leonardo da Vinci (1452-1519) that first analytical studies were performed. Even though the concept of *Force* was not adequately defined for another 200 years (Sir Isaac Newton, 1687 *Principia*²), Da Vinci already formulated the following statements³:

“The friction made by the same weight will be of equal resistance at the beginning of its movement although the contact may be of different breadth and length.

Friction produces double the amount of effort if the weight is doubled.”

[Leonardo da Vinci, 1452 - 1519]

These two observations, as well as da Vinci’s introduction of the friction coefficient as the ratio between the friction force and the normal force are still valid today. That is with some limitations. Equation 2.1, often also referred to as *Amontons’* or *Coulomb’s Friction Law* indicates that the friction force is independent from the contact area and the relative velocity between the two bodies engaged in the tribological process.

It is true that minimizing the geometric contact area ($A = a \cdot b$) by half, while leaving the normal force constant, the friction force will not change in value. In real technical applications the asperities of materials lead to a discrete number of micro contacts (A_i), which increases with rising surface pressure. That means that while the geometric contact area is bisected, the real contact area A_{real}

$$A_{real} = \sum_{i=1}^n A_r^i, \quad (\text{with } A \gg A_{real}) \quad (2.2)$$

increases due to elevated surface pressure. Thus an influence of the contact area can not be neglected categorically. [Sommer et al., 2010, pp. 8-9]

For an extensive disquisition on the history of friction see Dowson [1998].

2.3.2 Classification of Friction

Friction occurs in numerous forms and variations. The following section gives an overview on the prevalent types of categorization in accordance with the GfT [2002]. Identifying the nature of the exerting friction is crucial, as it gives information on the prospective wear behaviour and needs to be simulated accurately in eventual testing configurations.

General Classification

Apart from the obvious and general classification of friction in friction of two separate bodies (*external* friction) and friction between material sectors belonging to the same body (*internal* friction), a further distinction whether an external force/torque results in actual motion is

¹[Dowson, 1998]

²[Pourciau, 2006]

³[Persson, 1998, p. 10]

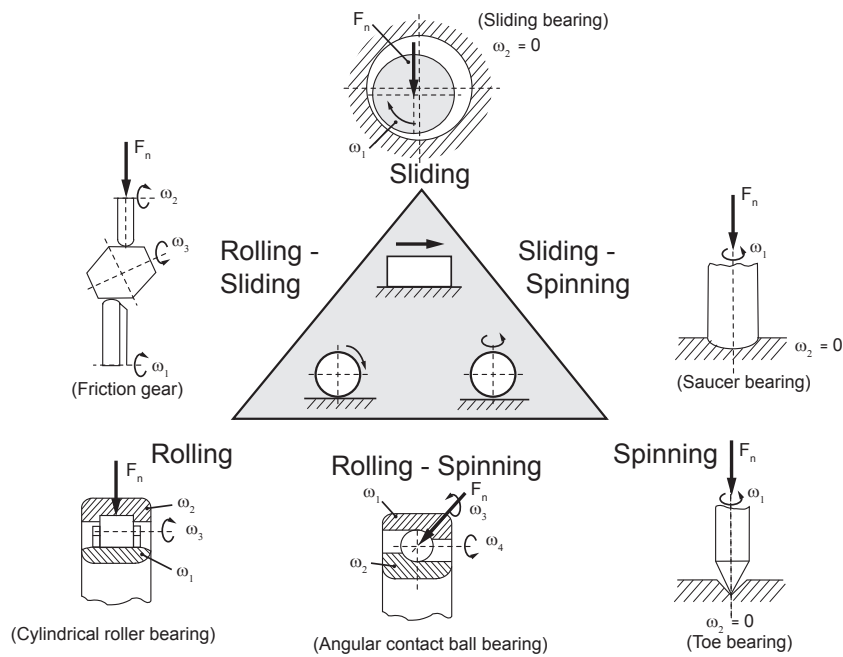


Figure 2.2: Friction according to motion types [Grote and Antonsson, 2009, p. 302]

made. *Static* friction (F_{Rstat}) occurs at the very beginning of relative motion or if the applied external force is not big enough to initialize motion at all. Either way, F_{Rstat} does not cause energy dissipation and is therefore regarded loss-free. [Sommer et al., 2010, p. 10] As soon as motion sets in, the minimal force needed to sustain that motion is referred to as *kinetic/dynamic* friction (F_{Rdyn}). The dynamic friction force acts tangentially in the interface between the two bodies moving relatively to each other and is opposed to the direction of the movement.

Friction Type

Dynamic friction can be further divided according to the type of movement. The main motion types are *rolling*, *sliding* and *spinning*. Figure 2.2 illustrates these principal types of movement on the basis of practical applications. Additionally, mixed variations are depicted. One friction type that is not shown in Figure 2.2 is *impact* friction. It is caused by the striking of one body against another.

All types of kinetic friction are subjected to mechanical losses. The main part of the energy loss can be attributed to heat conversion. While minor fractions of energy are saved in the material as lattice defects or are emitted through vibrations, wear mechanisms also contribute to this energy dissipation. [Sommer et al., 2010, p. 10]

Friction State

Even though friction is desired in some cases (for instance for friction couplings, brakes, self-locking of screws), in most cases friction is tried to be minimized. This can be achieved by lubricating the contact area. Depending on how effective this separation of the two solid bodies is, another classification of friction can be made.

The main friction states are solid, fluid, gas and mixed friction. *Solid* friction exists between materials that possess solid properties and are in direct contact. There are two subcategories. If the solid friction partners also feature boundary layers (with modified properties compared to the base material), it is referred to as *boundary-layer* friction. *Boundary* friction, on the other hand, prevails if the boundary layer is composed of molecules derived from a lubricant. The difference between boundary friction and fluid friction is the neglecting of the lubricant's hydrodynamic effects due to little velocities and/or quantities in boundary friction. *Fluid* friction is a version of internal friction. It occurs either between liquids or if solid bodies are entirely separated by a fluid (lubrication film). *Gas* friction characterises a friction state similar to fluid friction, with a gaseous film separating the rigid material zones. *Mixed* friction is a combination of other friction states, usually of solid friction (boundary friction) and fluid friction.

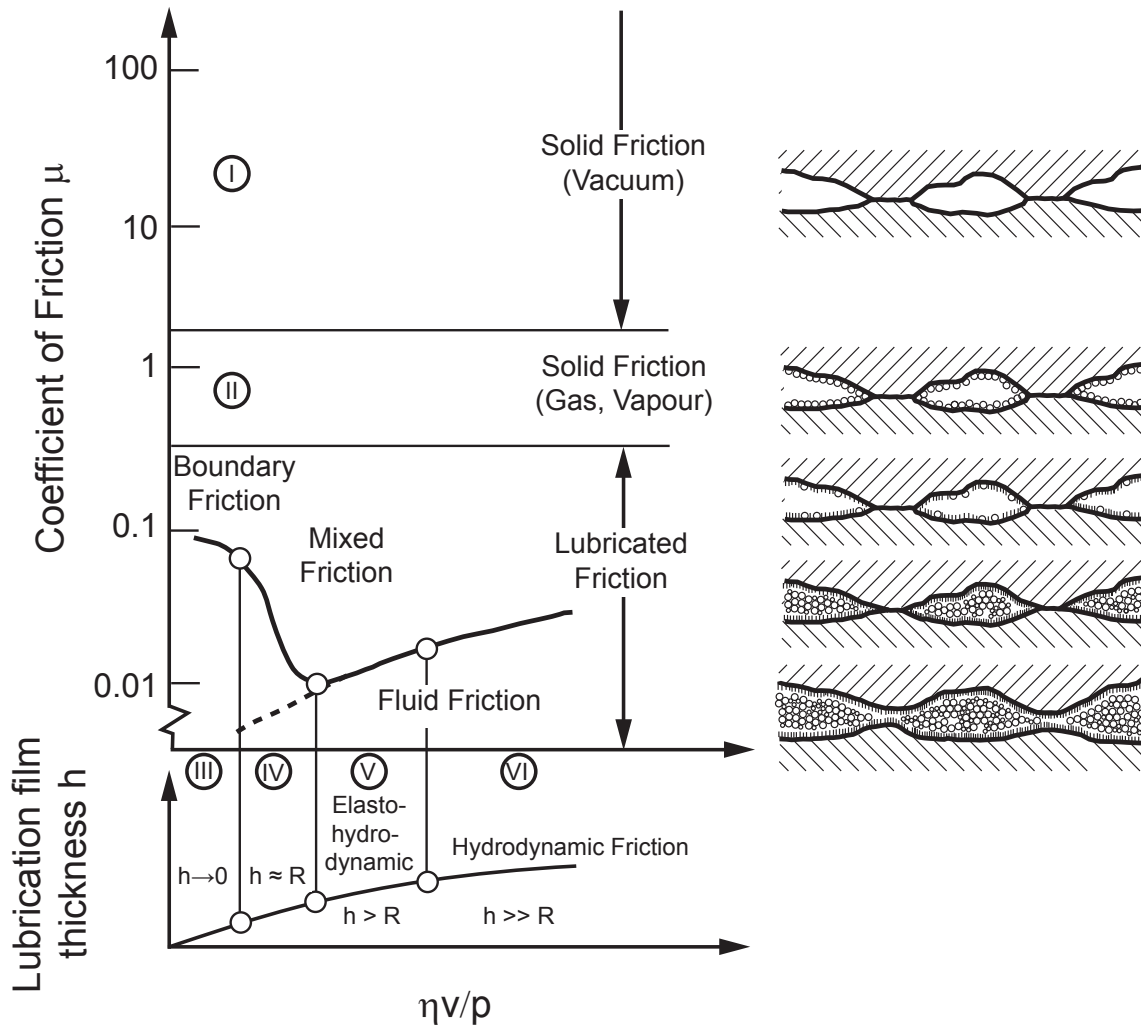
Figure 2.3 demonstrates common friction states in a radial sliding bearing. In addition to the above mentioned friction states, a further classification of fluid friction into elastohydrodynamic (EHL) and hydrodynamic (HL) friction can be identified. In both cases the solid friction partners are entirely separated by the lubricant. HL friction features lubricating film thicknesses that are considerably higher than the roughness peaks. Also in elastohydrodynamic friction the solid friction partners are segregated by the lubrication film, however the film thickness is not as distinct and the base material deforms elastically under the imposed stresses. [Czichos and Habig, 1992, p. 199] The specifications, fulfilling requirements, causes and effects of these lubricated friction states are described by the science branch of lubrication. Due to the limited scope of this paper, lubrication will not be further discussed in the following sections.

2.3.3 Mechanisms of Friction

The mechanisms of friction have been introduced above as being a subset of the tribological processes. As already stated, they are caused by the stress collective acting on the TTS and appear as motion hemming and energy dissipating processes. The main mechanisms of solid friction are presented in this section.

Adhesive Bond Shearing

In general adhesive bond shearing can be described as the formation and destruction of atomic and molecular bonds between the two friction partners. It takes place in the real contact area (A_{real}) between two solids. As the contact area migrates under relative motion and varies due to changing normal forces, also the bonds reform and break up continuously, causing energy to dissipate. Influencing factors are the ductility of the interacting materials, the density of free electrons in the contact area, surface layers and of course intermediate



η ... Viscosity of lubricant; v ... Relative velocity between the two friction partners; p ... Pressure per unit
 h ... Film thickness; R ... Roughness

Figure 2.3: Friction states as a function of the lubricating film thickness in a radial sliding bearing (Stribeck curve) [Sommer et al., 2010, p. 13]

Table 2.2: Variation of friction coefficient of different material pairings that can be attributed to adhesion [Czichos and Habig, 1992, p. 80]

Material Pairing	Coefficient of Friction (μ)		
	Solid Friction in Vacuum	Solid Friction in Air (humid)	Boundary Friction Mineral oil
Copper/Copper	> 100	1.0	0.08
NaCl/NaCl	1.3	0.7	0.22
Diamond/Diamond	0.9	0.1	0.05
Sapphire/Sapphire	0.8	0.2	0.2
Glass/Glass	0.5	1.0	0.28

and surrounding media.

A low formability, like in hexagonal closest packed (hcp) metals (for example Zn, Mg), leads to small real contact areas and subsequently to low adhesive bond shearing. Also materials with a low density of free electrons in the friction interface, as in transition metals (like Fe, Co, Ni), are less prone to this friction mechanism. [Czichos and Habig, 1992, pp. 75-79]

The adhesion narrowing influence of existing oxidation layers and separative media is obvious and needs no further clarification.

Table 2.2 highlights the variation of the friction factor μ with different material and environmental combinations. It demonstrates again that the coefficient μ is not a material pairing constant, but rather a function depending on the system structure and tribological loads.

Plastic Deformation

Two solid bodies with distinct roughness profiles under normal loads and relative motion are subjected to plastic deformation in the contact area, thus energy is dissipated.

Abrasion

Abrasion takes place as the asperities of two solids with different hardnesses are moved relatively to each other. Peaks in the surface roughness or even already formed particles are forced into the softer material. The resistance of the deformed material adds to the friction component.

Hysteresis Losses in Elastic Deformation

Elastic deformation is stored as intrinsic distortions inside the material structure. Ideally, the shape of a material should return to its original dimension once the deforming mechanical load is removed. However, in real applications a hysteresis is observed, as in addition to the distortions also vibrations are introduced into the lattice.

2.4 Wear

Wear is the progressive material loss in the contacted surface region of a solid body. It is induced by mechanical loads that are generated by the relative motion of two contacting bodies. [GfT, 2002][DIN 50320]

It is the, in most cases, undesirable material incline or surface disturbance due to tribological strains.

2.4.1 Wear Types

Defining the types of wear can be done according to different aspects. On the one hand the friction type can serve as a point of reference. Sliding friction generally leads to sliding wear, rolling friction accordingly causes rolling wear. Such an approach is adequate when two solids interact without foreign particles involved. If the TTS includes foreign particles a further differentiation according to the involved materials is usually made. In this context it is often referred to erosion processes (hydroerosion, gas erosion, fluid erosion). Sometimes the wear type is also classified according to its underlying physical mechanism (abrasive wear, adhesive wear, fatigue wear, tribochemical wear). [GfT, 2002]

Either way, listing all types of wear in a complemented and comprehensible way is not possible. Especially because real technical applications are not limited to the idealistic motion types and feature many combinations of them instead. In addition wear types and their underlying mechanisms can change over a period of time, due to altered contact geometries and the influence of already formed wear products.

See Appendix A for an elaborate list of wear types. Figure 2.4 illustrates the main wear types based on predominant tribological strains. Besides practical examples that can be assigned to the specific wear type, also an overview on the effective wear mechanisms is given. Please note that this is solely a suggestion. Even specialized literature deviates when comparing the exact wear processes of these idealized tribological configurations. Compare GfT [2002, p. 14], Czichos and Habig [1992, p. 101] and Sommer et al. [2010, p. 15].

2.4.2 Wear Mechanisms

Adhesion

Adhesion denotes the formation and destruction of atomic bonds in the contact zone. The bonds can form because protecting surface layers are removed by other wear mechanisms or because of the nature of the process itself (for example during machining). Active material zones are pressed against each other and form adhesive bonds that often possess higher strength characteristics than the original materials. So when a relative movement forces the separation of the two materials, the rupture does not occur in the prior contact area, but rather above or underneath the bonding course. Thus material is transferred from one friction partner to the other (see Figure 2.5). Influencing factors correspond with the causes for adhesive friction (formability, electron density, protective layers, surrounding/intermediate media). [Czichos and Habig, 1992, pp. 111-112]

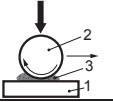
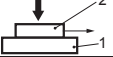
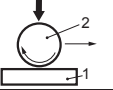
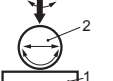
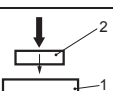
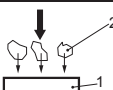
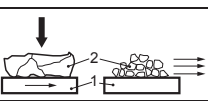
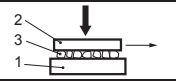

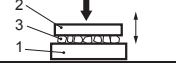
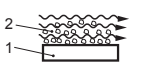
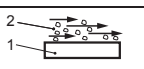
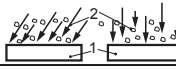
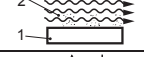

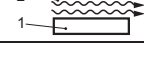
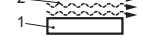
Elements of System Structure 1... Base body 2... Opposing body 3... Intermediate medium	Tribological Load	Type of wear	Example	Effective Wear Mechanisms			
				Adhesion	Abrasion	Surface Fatigue	Tribo-chemical Wear
1) Solid body 3) Intermediate m. Complete separation 2) Solid body 2	Sliding Rolling Bouncing Impacting 		Sliding bearing, Rolling bearing, Gears, Cam shafts	●			○
1) Solid body 2) Solid body (Solid friction Boundary lubrication Mixed lubrication)	Sliding 	Sliding wear	Cylinder liner	●	○	○	●
	Rolling Revolving 	Rolling wear	Rolling bearing, Gear, Cam shaft, Wheel/Rail	○	○	●	●
	Oscillating 	Fretting wear	Fitting surface, Bearing seat	●	●	●	●
	Impacting 	Impact wear	Valve needle	○	○	●	●
1) Solid body 2) Particles	Impacting 	Two-body abrasion	Impact plate, Impact mill	○	●	●	○
	Sliding 		Excavator bucket, Rock drill	○	●	○	
1) Solid body 3) Particles/ Loose material 2) Solid body	Sliding 	Three-body abrasion	Impurities in bearings and guidances	○	●	●	○
	Rolling 		Roller mill	○	●	●	○
	Impacting 		Jaw crusher	○	●	●	
1) Solid body 2) Fluid and particles	Flowing 	Hydroerosion	Pumps, transmission pipes		●	●	○
1) Solid body 2) Gas and particles	Flowing 	Abrasive erosion	Pneumatic conveyer systems	○	●	●	○
	Sliding Impacting 	Oblique impact erosion, Impact erosion		○	●	●	○
1) Solid body 2) Fluid	Flowing Vibrating 	Cavitation erosion	Pumps, valves, water turbines			●	○
	Impacting Sliding 	Drop erosion	Rotor blades, steam turbines			●	○
	Flowing 	Fluid erosion	Pumps, valves, pipes			○	●
1) Solid body 2) Gas	Flowing 	Gas erosion	Gas turbines, thermal shield				●

Figure 2.4: Wear types based on different tribological loads [Sommer et al., 2010, p. 15]

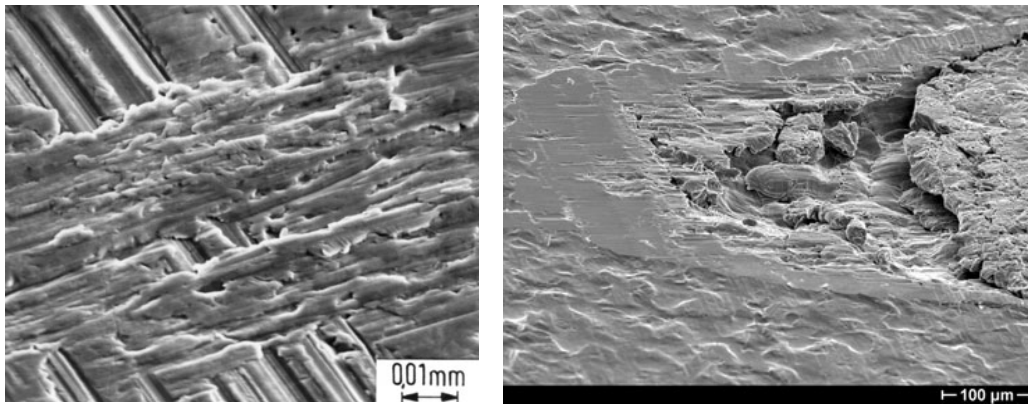


Figure 2.5: Left: Characteristic adhesive material transfer on a hardened striker;
 Right: Shear cracks on a disk (HC260LA) [Sommer et al., 2010, p. 17]

In the context of adhesive wear it is often referred to micro welds (frettings) that lead to scuffings, galling areas, holes, plastic shearings and material transfer. [Grote and Antonsson, 2009, p. 306]

Abrasion

Abrasive wear can be attributed to the concurrent existence of pronounced roughness asperities and dissimilar material hardnesses of the elements in a TTS. The increased hardness can be featured by the opposing body itself, the particles in the intermediate medium or the already formed wear fragments.

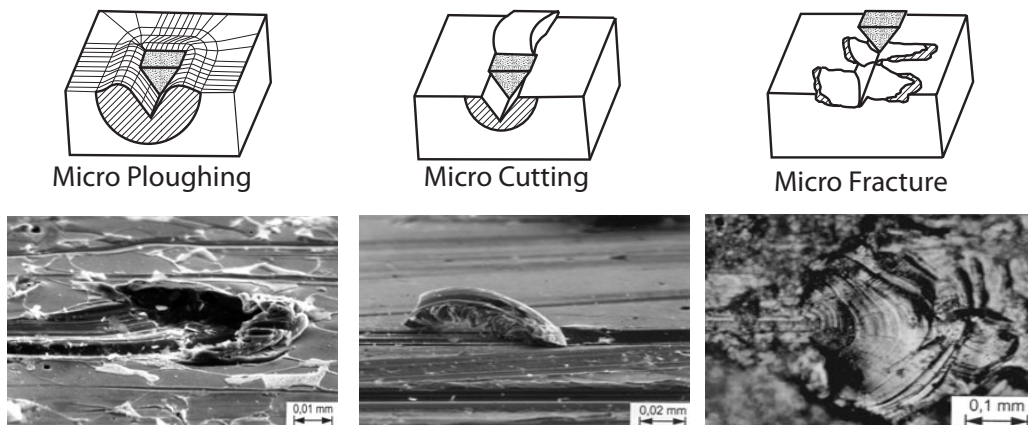


Figure 2.6: Examples of abrasive micro ploughing, micro cutting and micro rupture [Sommer et al., 2010, p. 376][Czichos and Habig, 1992, p. 109]

Depending on the behaviour of the base body when it is penetrated by the harder friction

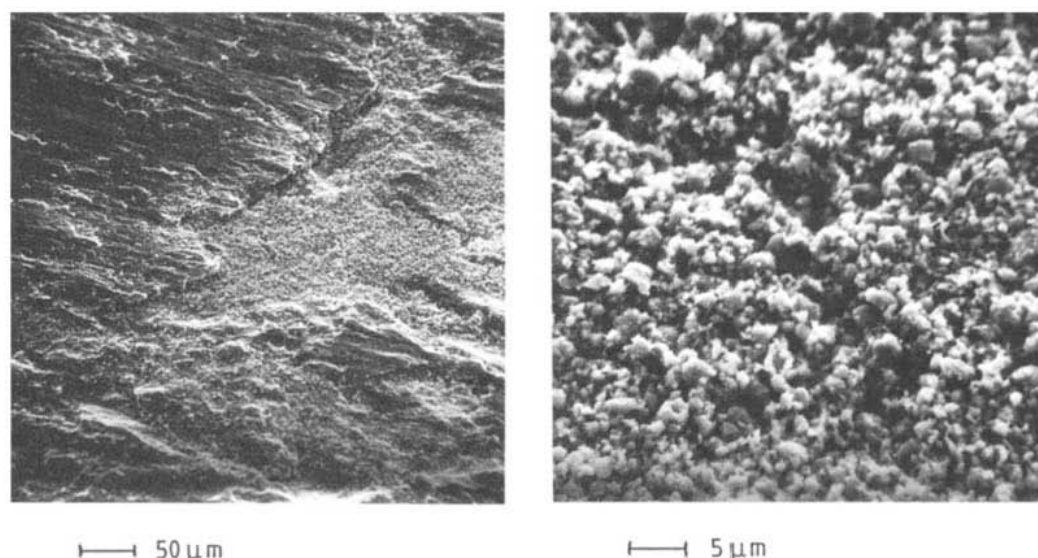


Figure 2.7: Exemplary appearance of tribochemically formed wear particles
[Czichos and Habig, 1992, p. 128]

partner, four types of abrasive wear can be differentiated. *Micro ploughing* is highlighted by the plastic deformation of the base body. In ideal cases no material removal takes place. *Micro cutting* on the other hand results in an immediate material removal, as chips are formed by the abrasive roughness peaks/particles. The inclination angle of the engaged abrasive partner primarily determines whether micro ploughing or micro cutting is more likely to take place. A process that can also be allocated to the wear mechanism of surface fatigue is *micro fatigue*. It is triggered by local material fatigue due to repeated contact with harder roughness peaks/particles. *Micro fracture* is caused by the local exposure of the base body to a critical load and is especially observed in brittle materials. [Czichos and Habig, 1992, pp. 108-109] Scratches, grooves and ripples are observed consequences of abrasive wear. See Figure 2.6 for examples.

Tribochemical Wear

Tribochemical wear is caused by chemical reactions of the base and/or counter body with the surrounding and/or intermediate medium. The reactivity of metals is increased by thermal and mechanical activation during the triboprocess. In metals especially oxidation takes place in the micro contacts. The formed metal-oxides are very prone to brittle rupture if the loaded stress exceeds a critical value. This produces wear particles with altered characteristics that contribute to abrasive wear. On the other hand it is also a so formed oxidation layer that can prohibit adhesive wear. [Czichos and Habig, 1992, p. 115]

Figure 2.7 illustrates a characteristic surface exposed to tribochemical wear.

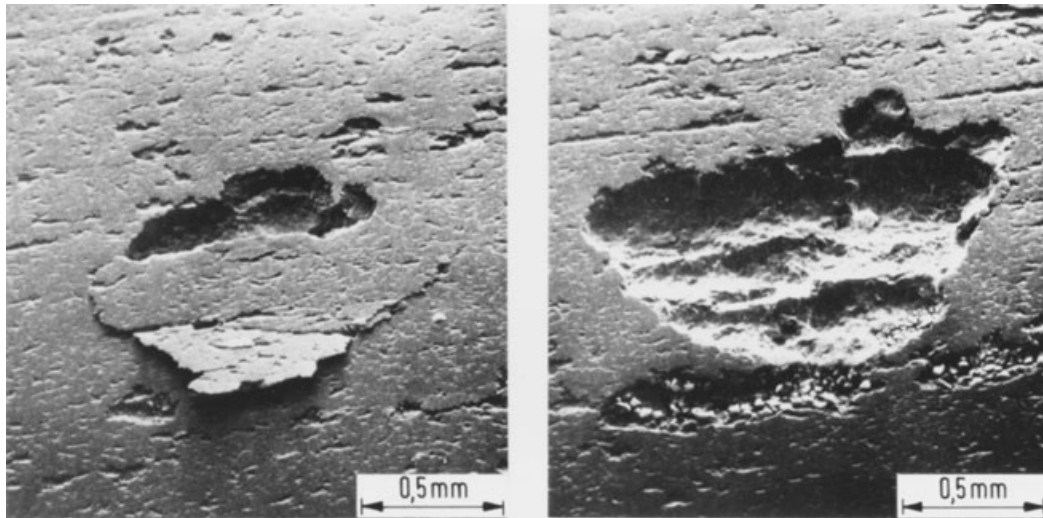


Figure 2.8: Progressing pit mark on a tooth flank that is caused by surface fatigue [VDI 3822, Blatt 5]

Surface Fatigue

Tribotechnical systems are often exposed to periodically changing and alternating stresses. If the changes between multiaxial tensile and compressive stresses exceed the material specific tensile strength or lower intermittent stresses are applied over a long period of time, surface fatigue will lead to a decrease in strength and the formation of cracks in surface-near areas. Eventually, a material loss takes place in form of cracks, pittings or flakings (compare Figure 2.8).

Operating experiments show that surface fatigue is especially common in Hertzian⁴ contact zones. It has been also observed that elasto-hydrodynamic friction results in cracks that originate underneath the surface, while mixed and boundary friction are susceptible to cracks on the surface that advance inwards. Surface fatigue can be phased into an incubation period, during which lattice defects accumulate, the formation of first submicroscopic cracks and their development to micro cracks, the crack extension combined with the merging of cracks and of course the final rupture of the material. Properties that slow progressing surface fatigue are internal compressive stresses, homogeneous structural conditions and increased material hardnesses. [Habig, 1980; GfT, 2002; Sommer et al., 2010; Czichos and Habig, 1992]

2.4.3 Wear Quantification

All of the above findings conclude that wear ultimately results in a removal of material. Accordingly the quantitative assessment of wear is based on investigating the lost material. Several characterizing values describing wear have been formulated and can be further divided into direct and indirect parameters.

⁴See also Figure 5.3 ‘Contact mechanics according to Hertzian theory’ on page 48.

- Direct Wear Characteristics
 - *Wear amount* - Mass loss [kg], linear dimension change [m], volume loss [m³]
 - *Wear resistance* - 1/(Wear amount) [1/m, 1/m³, 1/kg]
 - *Wear rate* - (Wear amount)/(Time or travelling distance) [m/m, m³/m, kg/m, m/s, m³/s, kg/s]
 - *Wear coefficient* - (Wear rate)/(Normal force) [m³/Nm]
- Indirect Wear Characteristics
 - *Wear-limited service life* - For example number of parts of a cutting tool before it fails.
 - *Wear-limited throughput* - Used primarily for the transport of abrasive material and is measured in number of parts or kg before failure.

The most direct method to gain the material mass deviation is weighing the parts before and after the tribological strain is applied. However, this measuring technique is highly prone to errors. As explained above, a material transfer between elements of the TTS is very common. So is the formation of oxidation layers. Both mechanisms will distort the values captured through balancing as they actually increase the mass of the worn part. In addition, the applicability of balancing is limited to wear processes with a mass change larger than 1 mg in a specimen not heavier than 0.5 kg, due to the sensitivity of the balance. If the wear progress needs to be monitored over a period of time an additional problem arises: in order to weigh the specimens several times during the course of wear a repeated disassembly/reassembly can not be avoided. The chance that the contact zone and consequently the predominant wear mechanisms are altered and corrupted are extremely high.

In comparison, retrieving data on dimensional changes seems to be more accurate. The predominant method is to measure the distance between the mounting fixtures of the two tribo elements. One major advantage is the ability to monitor the wear progress continuously without interruption. Nevertheless, also in this method the wear mechanisms impose specific peculiarities that require a thorough interpretation. Figure 2.9 gives an example of an alumina ball sliding continuously on an alumina disc. The graph shows that the displacement increases consistently at the first third of the monitored process. This would suggest a *negative* wear. The results can be explained by an accumulation of wear products of the larger friction scar (disk) on the smaller friction scar (ball), thus increasing the distance between the measuring points. When the wear particles break off, the distance decreases abruptly, followed by new friction particles amassing in the contact area. The change in friction force can be attributed to modifications of the surface interactions as well as increasing contact areas.

Another way to assess the material removal directly is to calculate the volume loss. Of course this can be achieved by considering the material mass and density. However, the measuring faults described above persist. In addition eventual material coatings or surface treatments influence the density in a way that reliable results can not be expected anymore. Calculating volume changes based on dimensional changes is more preferable. For simple configurations and in the particular case that only one friction partner is subjected to material loss, elementary equations are available that retrieve the volume loss on basis of simple linear

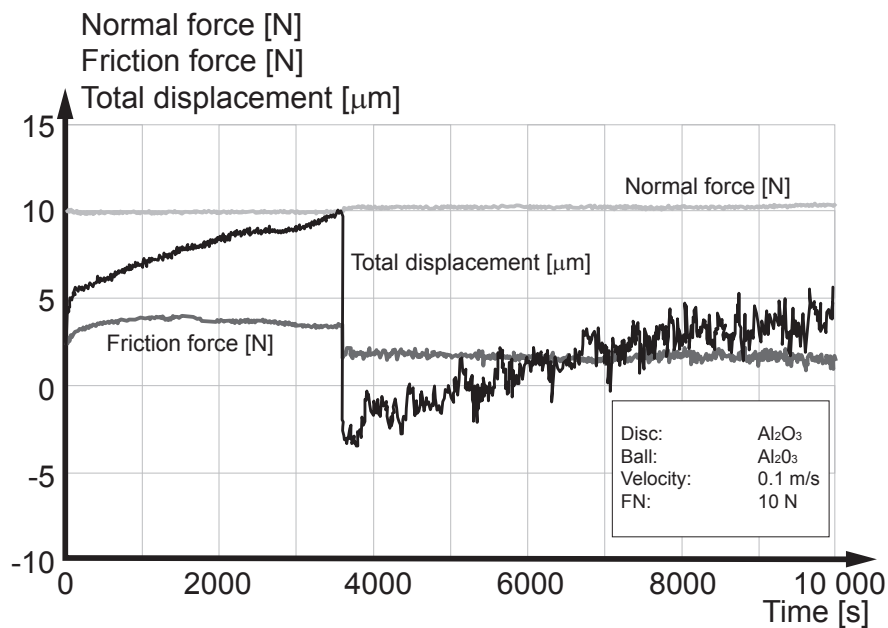


Figure 2.9: Example of on-line measurement of linear wear (total displacement of ball relative to disc) and friction force during continuous sliding [Saito et al., 2006, p. 700]

measurements. For example, the wear volume of a ball can be calculated by

$$W_{v,b} = (\pi d_a^2 d_p^2 / 64r). \quad (2.3)$$

With d_a and d_p standing for the diameter of the wear scar on the ball perpendicular (d_a) and parallel (d_p) to the sliding direction and r for the radius of the ball specimen. Naturally, also this technique faces limitations. Especially regarding the ability to monitor the wear progress *online* (continuously).

Most accurate results can be achieved by the topographic acquisition of three-dimensional profile changes. However, such an approach is only advisable if the resulting wear scar is distinctively deeper than the surrounding roughness and if an offline consideration is sufficient. [Saito et al., 2006, p. 201]

2.5 Testing Equipment

In the previous sections all significant mechanisms responsible for the degradation of performance, efficiency and value of tribological elements have been listed. For every individual process mathematically formulated laws can be found in literature that adequately describe the function and can predict its outcome to some degree. However, and this needs to be stressed, the dissipative, non linear and highly dynamic nature of the combination of all occurring processes can not be mathematically anticipated at the moment. Thus the experimentally determination of information on the behaviour of friction and wear is still

Table 2.3: Categories of tribological testing configurations [GfT, 2002]

Cate- gory	Testing type Stress collective	System structure		
I	Operational or operation- related trials	In-situ tests	Entire engine/ Entire facility	
II		Field tests	Entire engine/ Entire facility	
III		Bench test includes entire engine or facility	Original parts	Entire engine/ Entire facility
		Bench test includes aggregate or assembly group	Entire aggregate/ Assembly group	
IV	Small scale trials	Trials with original parts or reduced assembly group	Extracted parts/ Downsized assemblies	
V		Similar stresses imposed on test samples	Model samples	Parts with similar strains
VI		Model trials with simplified specimens		Simple geometries

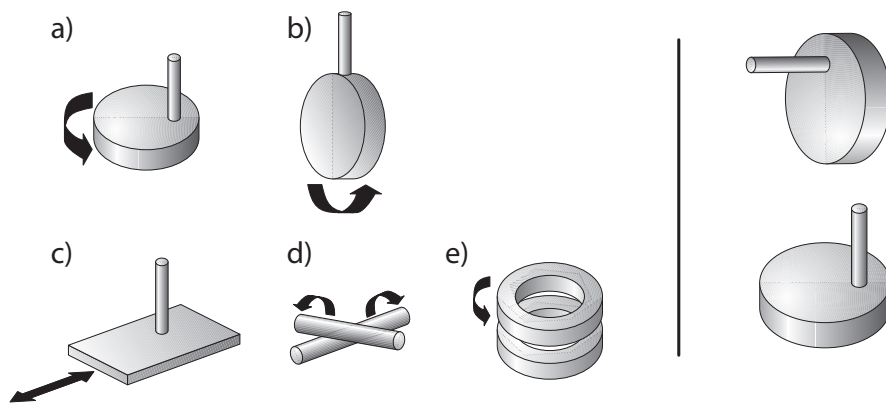
indispensable today. The specific functions of tribologically focused testing procedures vary to a great extent, just as the scopes of particular examinations do. The following section gives an overview of different scopes of tribo-testing and a summary of prevalent testing configurations on a laboratory scale.

2.5.1 Reasons and Categories of Tribological Testing Techniques

DIN 32322 lists several reasons to engage in tribological testing:

- Detection of wear related influences on the overall function of engines
- Monitoring of wear affiliated functionality of engines
- Operation mode diagnostics
- Optimization of parts or tribosystems to ensure a desired service life
- Creation of data and specifications for maintenance purposes
- Preselection of materials and lubricants for practical applications
- Quality control of materials and lubricants
- Wear research, mechanism oriented wear testing

Derived from the above objectives, DIN 50322 differentiates between six categories of testing techniques that are distinguished by featuring different levels of simplification. The single classifications are summarized in Table 2.3. As you go through the defined categories, they become more and more abstract and lose some of their significance to the considered application. However, the overall costs for testing applications IV - VI, as well as the complexity of the testing configuration, decrease proportionally too.



a) Pin on disc; b) Pin on ring; c) Pin on flat; d) Crossed cylinders; e) Thrust washers

Figure 2.10: **Left:** Commonly applied sample geometries for sliding wear tests;
Right: Different assembly types of *Pin on Disc* configuration
 [Gee and Neale, 2002]

As this paper aims at designing and building a testing device on a small scale that should feature a high degree of control and low complexity, the following chapter focuses on category VI.

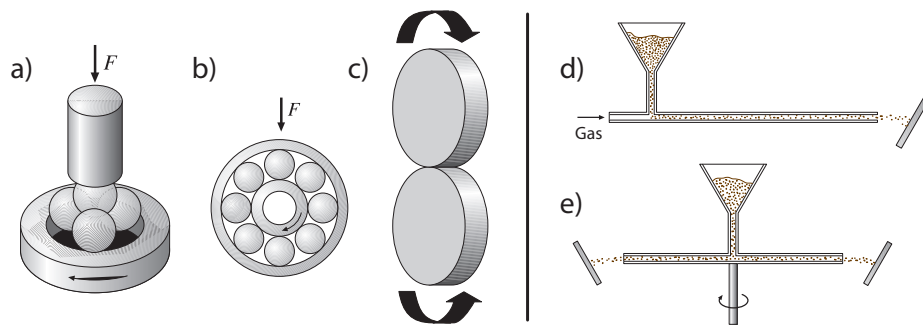
2.5.2 Tribometry

A tribometer is a testing configuration that can be attributed to categories IV - VI. This means the system structure is highly simplified and the actual parts and assembly groups have been replaced by samples of simple geometric shapes. This section gives a rough overview of tribometers that are used in modern-day applications.

Even after excluding all testing configurations that are not allocated to the last category (VI), giving a complete compilation of currently applied tribometers is not easily achieved. A NPL (National Physical Laboratory) report from 1997 summarizes a total of 424 different standards and guidelines for wear testing procedures that were collected in eleven industrialized countries. [Owen-Jones and Gee, 1997] It can be assumed that the number of testing techniques has been further increasing since this publishing. Not included in this figure are the numerous adaptations of processes that individual institutions generate to meet their specific demands and can either not be assigned to one standard procedure or are simply not found in published literature. Saito et al. [2006, pp. 693-670] suggest the differentiation of this vast number of accumulated techniques according to their main wear types, in order to gain a clearer view of the current state of the art.

Sliding Wear

Tribometers featuring sliding motions are still omnipotent among laboratory testing apparatuses. During the *International Conference on Wear of Materials* in 1995, 75 % of all presented testing modifications could be associate to sliding motion. [Owen-Jones, 1997]



a) Four ball test; b) Balls in bearing race; c) Roller on roller; d) Gas-blast test; e) Centrifugal accelerator

Figure 2.11: Left: Examples of common wear tests involving rolling motion; Right: Erosion by solid particles [Saito et al., 2006, p. 695]

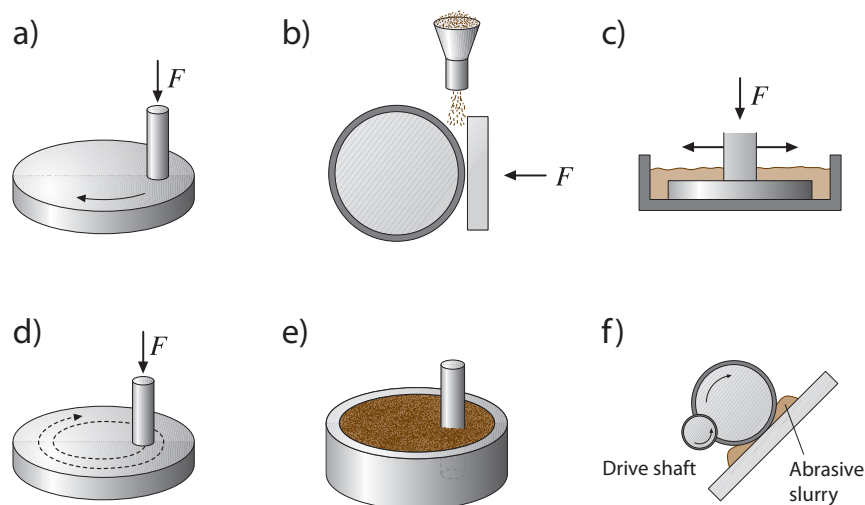
In general there are two types of sliding tribometers. Tribometric applications in which the extent of the relative motion is comparatively large, so that every contact point of at least one friction partner is out of contact at some point during the testing period, are in contrast to configurations in which the two bodies are in contact at all times. The type of motion varies between rotating and reciprocating. Figure 2.10 shows common sample configurations in sliding wear tests. The pictured pin sample is often replaced by balls or blocks. As depicted in Figure 2.10 (right), the assembly of the chosen sample geometries has also great impact on the test results. While in the second case the produced wear debris is trapped in the contact area, further influencing the behaviour, it can easily escape in the first variant.

Rolling Wear

Figure 2.11 highlights commonly used wear tests involving rolling motion. Bearing races are a particular case in tribological research, as the original parts feature simple geometries and can therefore be investigated with rather simple means on a laboratory scale. Due to the multiple balls the degree of complexity is higher and the controllability is lower than in comparable applications (compare Four Ball Test, Roller on Roller in Figure 2.11) and might be substituted by them.

Abrasive Wear

As stated by Czichos and Habig [1992, p. 694], the simplest variant of abrasive wear testing is the adaptation of sliding tribometers with abrasive coated paper (Figure 2.12 a, d). Due to permanent contact, however, the paper is damaged and the test results might be compromised due to its debris. By exposing the test samples to a continuous flow of abrasive particles this problem can be eliminated (Figure 2.12 b, c, e, f). Whether these particles recirculate within the system (Figure 2.12 c, e, f) or are replaced by new abrasive media, depends on the purpose of the test and needs to be considered carefully before deciding on a specific variant.



a) Pin on rotating abrasive disc; b) Plate against rotating wheel with feed of abrasive; c) Block on a moving plate in a bath of slurry; d) Pin on rotating abrasive disc with spiral track; e) Wear of pin in rotating pot of slurry; f) Micro-scale abrasion test with rotating ball on plate in presence of abrasive

Figure 2.12: Common test configurations for abrasive wear [Saito et al., 2006, p. 694]

Erosive Wear by Solid Particles

As illustrated in Figure 2.4 ‘Wear types based on different tribological loads’ on page 15, erosion wear is caused by loose abrasive particles, flowing gas or liquid as well as the combination of both. The specific design depends on the kind of erosive medium, the adjustable particle (impact) speed and the angle of collision. Figure 2.11 (d,f) gives an example of two different methods for abrasive erosion simulation.

Based on a typical *Pin on Disc* configuration, an example shall be given on how much the scopes of applied technologies can vary in modern day applications. When comparing two *Pin on Disc* tribometers from two different suppliers, the ranges between simple and therefore economically maintainable configuration to high-tech solutions are demonstrated best. A rather simple *Pin on Disc* tribo-tester is provided by *TRIBOtechnic*. It features adjustable normal forces by adding/removing weights to the deflection arm that also measures the coefficient of friction during the test period. By measuring the disc wear track profile and the diameter of the worn pin surface, a provided software calculates the wear rate of both friction partners. The applicable friction force is limited to 6 N, with rotation speeds from 2 rpm - 300 rpm. [Tribotechnic Tt, 2012]

The same basic tribological structure - in a more elaborate way - is supplied by *CETR*. This tribometer is able to test several different sample geometries, in different relative motion types, that are subjected to controlled environmental conditions. The adjustable normal force can mount up to 1,000 N, with rotation speeds from 0.1 rpm - 3,000 rpm. Another highlight

is the adaptability of temperature (-25 °C - 150 °C) and humidity (10 % - 95 % RH). In order to observe all these parameters, several sensors are included (force sensors ranging from 1 mN to 1 kN, 6-D sensors for measurement of 3 forces and 3 torques in X, Y and Z axes, high-frequency acoustic emission sensors, temperature and humidity sensors). [CETR, 2012]

Please note that variant one is in no way dated or obsolete - both solutions represent state-of-the-art technology, but on different scales.

Trends and Ongoing Research

Based on a survey of 234 applied laboratory tribometers in 1976, Czichos and Habig [1992, p. 155] identified the basic geometry combination applied in tribometers.

- Ball-Ball contact (Multiple)
- Crossed Cylinders
- Pin-Disc (Alternating or linear movement)
- Flat-Flat (Alternating or linear movement)
- Rotating Pin on Disc
- Rotating Disc on Pin
- Cylinder-Cylinder
- Rotating Cylinder on Pin
- Rotation Cylinder on Block
- Disc on Disc

By comparing this list of predominant sample geometries with the examples of test configurations given above (Figures 2.10, 2.11 and 2.12), it can be seen that in a period of 30 years no significant changes took place in terms of the basic structure of tribometers. Also the consideration of presented papers at the *European Conference on Tribology* in 2011 suggest that the focus of tribometry research is not on the substitution of system structures. Instead, studies concentrate on the augmentation of measurement accuracy and the online detection of friction and wear parameters by designing more effective sensors and measuring methods (compare Markova et al. [2011]; Ronkainen et al. [2011]; Korres et al. [2011]).

In general the development can be summarized by an increasing level of automatisation and accuracy. A lot of research focuses on measuring techniques that enable a reliable monitoring and recording of friction and wear parameters on site and in real time. Furthermore, progress is made versus applications in nano scales. A significant part of tribology is now concentrating on the interaction of technical components within the human body, investigating artificial joints, their wear behaviour and the effects on the patient's health.

A rather new topic is the idea of *hot tribology* - the tribological behaviour of systems at elevated temperatures. The knowledge gained from this branch of research - today still in its fledging stages - will especially be of interest for hot forming applications.

Chapter 3

Forming Technologies

Forming technologies comprise all manufacturing techniques that permanently deform solid bodies into new shapes while preserving the material's cohesion and mass.

This chapter gives an overview on the prevalent forming techniques, their physical fundamentals, as well as a succinct review on the historical development, before going into further detail regarding deep drawing applications and prevalent coating methods.

3.1 Introduction

3.1.1 Historical Development

First evidences of forming applications can be traced back to prehistoric times. Archaeological finds prove already existing forming knowledge in the period between 5000 and 4000 B.C.. Within this epoch gold and copper were hammered into distinct shapes. In 1400 B.C. primordial sheet metal presses were introduced - metal sheets were put on dies, weighed down with leather or wood and pressed into shape.

Further milestones:

- 900 B.C (Begin of Iron Age): More complex dies for the sheet forming are introduced.
- Roman Empire - 13th century: No considerable enhancements of techniques - continuous spreading of existing knowledge.



Left: Greek bronze die (700 B.C.) Right: Roman forging illustration on vase

Figure 3.1: Historic evidence of forming applications [Doege and Behrens, 2010, p. 2]

- 14th - 18th century: The importance and applicability of iron processing increases consistently.
- 15th century: First appearance of pile-driving machines.
- 15th century: Forging becomes competitive regarding casting for the first time.
- 18th century: First hydraulic press (England, 1789).
- End of 19th century: Industrialization of the - up to that time - rather manual applications.

For further information on the historic development of forming technologies see Doege and Behrens [2007, 2010].

3.1.2 Economic Relevance

Fritz and Schulze [2010, pp. 390-391] summarize some evident advantages of forming technologies in general, all of which result in significant economic benefits.

Improved material efficiency In direct comparison to machining processes, modern forming technologies need 10 % to 50 % less material.

Reduction of processing times Reduction of processing times up to 30 %, when considering conventional manufacturing techniques, are not uncommon. This can be accredited to higher output rates due to accelerated stroke rates and automated loading and unloading apparatus, paired with multiple machine operations.

Quality refinement of processed part Increased dimension accuracy and surface quality. Some forming techniques are able to realize very narrow tolerances. Impact extrusion, for example, succeeds in creating wall thickness deviations of ± 0.01 mm (at $\varnothing 600$ mm).

Increase of material strength Several cold forming techniques result in significant strength raises due to work hardening processes. Cold extrusion methods may increase the steel strength by up to 120 %. Of course also this aspect has an immediate effect on the economic relevance, as low strength - and therefore cheaper - raw parts can be purchased and used for high-strength applications as well.

Shape stability Unlike cutting techniques, forming technologies do not destroy the grain flow in materials. As it stays homogeneous throughout the part's geometry, a distinct increase in the shape stability as well as a reduction in the susceptibility to notch effects can be observed.

3.1.3 Classification of Forming Technologies according to DIN 8582

DIN 8580 specifies that forming techniques are technologies that modify the shape of manufactured parts, while preserving material cohesion.

A further categorization of forming technologies is suggested by DIN 8582, dividing the methods according to the present stress conditions (see also Figure 3.2).

Forming under Compressive Conditions

- Rolling
- Open Die Forming
- Closed Die Forming
- Coining
- Extrusion

Forming under Tensile-Compressive Conditions

- Drawing or Stripping
- Deep Drawing
- Flange Forming
- Spinning
- Upset Bulging

Forming under Tensile Conditions

- Extending by Stretching
- Expanding
- Stretch Forming

Forming by Bending

- Bending with Linear Die Movement
- Bending with Rotary Die Movement

Forming under Shearing Conditions

- Displacement
- Twisting

Besides the above described itemization of forming technologies, a certain method is also commonly classified as either bulk (also massive) or sheet metal forming as well as hot or cold forming technique. The refinement between massive and sheet metal forming is obvious. The distinction between cold and hot forming technologies, however, needs further explanation. The general classification is often made according to occurring forming temperatures. If the temperature is higher than the recrystallization temperature of the formed part, the forming method is referred to as hot forming technology. Even though this definition seems well-defined, it might be subject to misunderstandings. As highlighted by Klocke and König [2006, p. 15], hot forming temperatures are reached at both 450 °C (Iron; $T_S = 1536$ °C) as well as 3 °C (Lead, $T_S = 327$ °C).

In order to distinctively classify hot forming applications, the forming velocity is examined as well. If the recrystallization velocity is faster than the forming velocity - no work hardening occurs, as the microstructure reforms continuously - hot forming takes place.

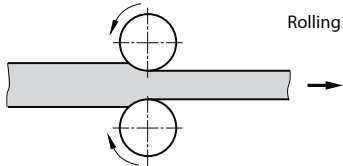
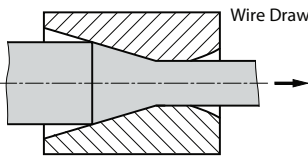
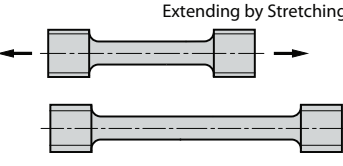
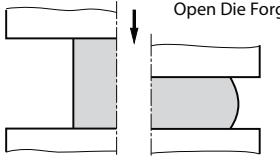
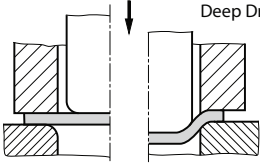
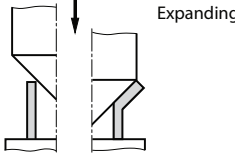
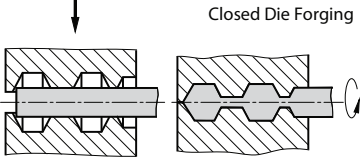
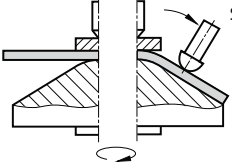
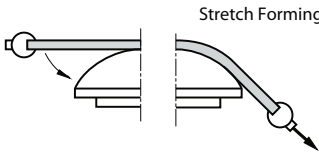
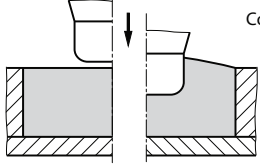
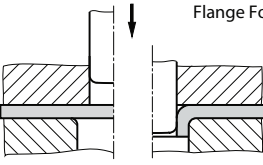
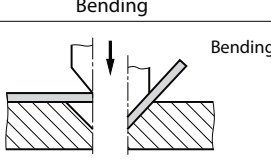
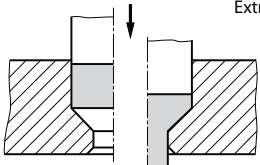
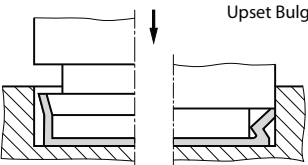
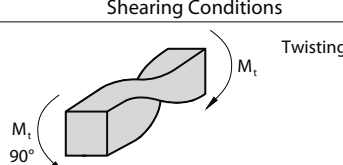
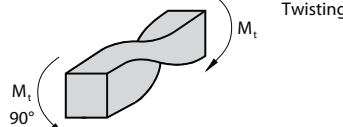
Compressive Conditions	Tensile-Compressive Conditions	Tensile Conditions
 <p>Rolling</p>	 <p>Wire Drawing</p>	 <p>Extending by Stretching</p>
 <p>Open Die Forging</p>	 <p>Deep Drawing</p>	 <p>Expanding</p>
 <p>Closed Die Forging</p>	 <p>Spinning</p>	 <p>Stretch Forming</p>
 <p>Coining</p>	 <p>Flange Forming</p>	 <p>Bending</p>
 <p>Extrusion</p>	 <p>Upset Bulging</p>	 <p>Shearing Conditions</p>
		 <p>Twisting</p>

Figure 3.2: Forming techniques according to DIN 8582 [Fritz and Schulze, 2010, p. 390]

3.2 Deep Drawing

DIN 8584 characterizes deep drawing as the forming of a planar sheet metal (foils, plates) into a hollow shape under prominently tensile-compressive stresses, without the intended decrease of the wall thickness. Often several forming steps are necessary for the generation of a required shape.

Deep drawing occupies an exceptional position among the sheet metal forming techniques, as it is the most significant manufacturing technology for the production of three-dimensional sheet parts. It is omnipresent; in high volume production branches (automotive industry) as well as in small series (aviation industry).

3.2.1 Procedural Principle

The process of a deep drawing operation can be explained regarding Figure 3.3, where a drawn cup is formed out of a plain metal sheet. The configuration always consists of a

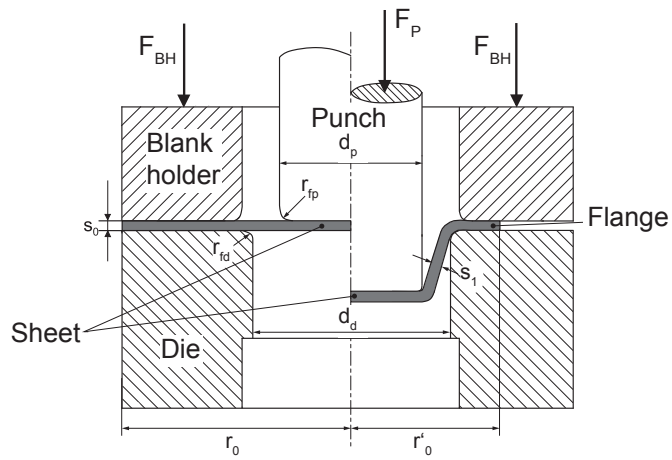


Figure 3.3: Principle of deep drawing [adapted from Grote and Antonsson, 2009, p. 595]

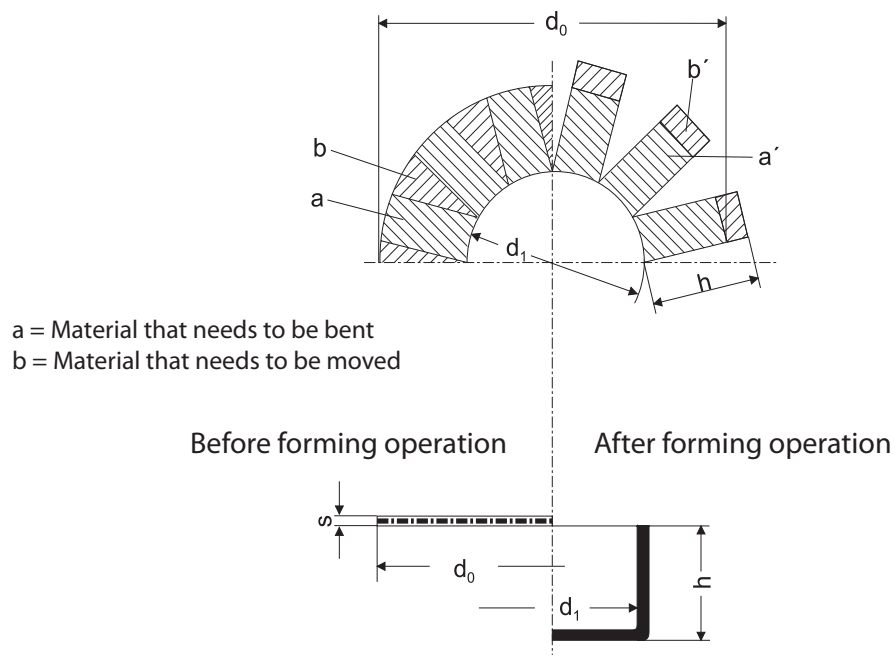


Figure 3.4: Resulting material reallocation during the drawing of a cup [Klocke and König, 2006, p. 324]

drawing punch, a drawing die and blank holders. The - in this case circular - blank is formed by the rigid punch into the die cavity. As the punch is lowered, the sheet material is drawn into the die, reducing the outer diameter of the blank. The blank holders allow the material to flow inwards and mainly serve to make sure that there are no wrinkles forming in the area of the flange. The determination of the right blank holder forces is one of the challenges in controlling the process.

Figure 3.4 demonstrates how the material has to *relocate* in order to form a drawn cup. Sections *a* are bent up to form the cup's frame, pushing sectors *b* upwards into positions *b'* ($A_b = A_{b'}$). During this rearrangement of material the rim area is both stretched and compressed, while the bottom part of the cup is hardly deformed.

The punch force acts on the plastic deformation indirectly, as it is introduced through the bottom of the cup while the deformation takes place in the flange and rime area. This leads to a very distinctive stress condition and subsequent wall thicknesses that are illustrated in Figure 3.5.

3.2.2 Characterizing Parameters

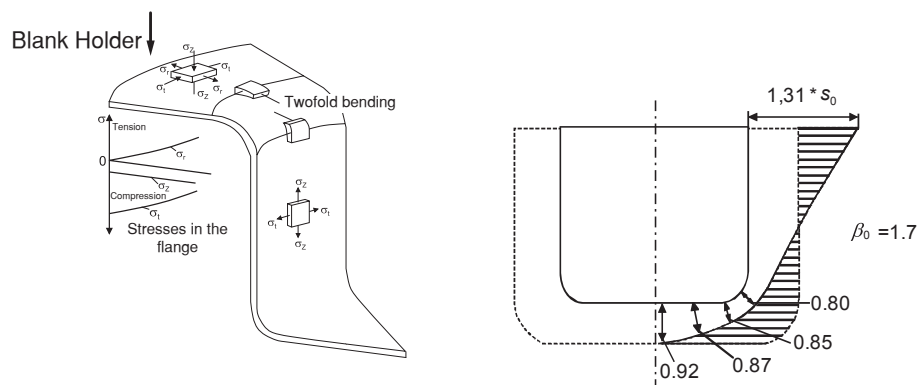


Figure 3.5: **Left:** Stress conditions of a volume element in a deep drawn cup [Klocke and König, 2006, p. 327]; **Right:** Variation of wall thickness [Doege and Behrens, 2010, p. 287]

Stress Conditions and Effective Strain

Figure 3.5 (left) shows a volume element and its corresponding stress conditions during the drawing progress. At the beginning of the process, when the volume element is in the flange area, it is subject to tensile stress in radial direction and compressive stresses in tangentially and - if blank holder forces are applied - axial direction. In the intersection between flange and frame the element is bent twice. First, the sheet is bent over the die radius (r_{fd}), and then it is reversely bent into the cylindrical frame of the cup. The tensile stress condition present in the cup frame is a result of the radial stresses in the flange, the bending stresses caused

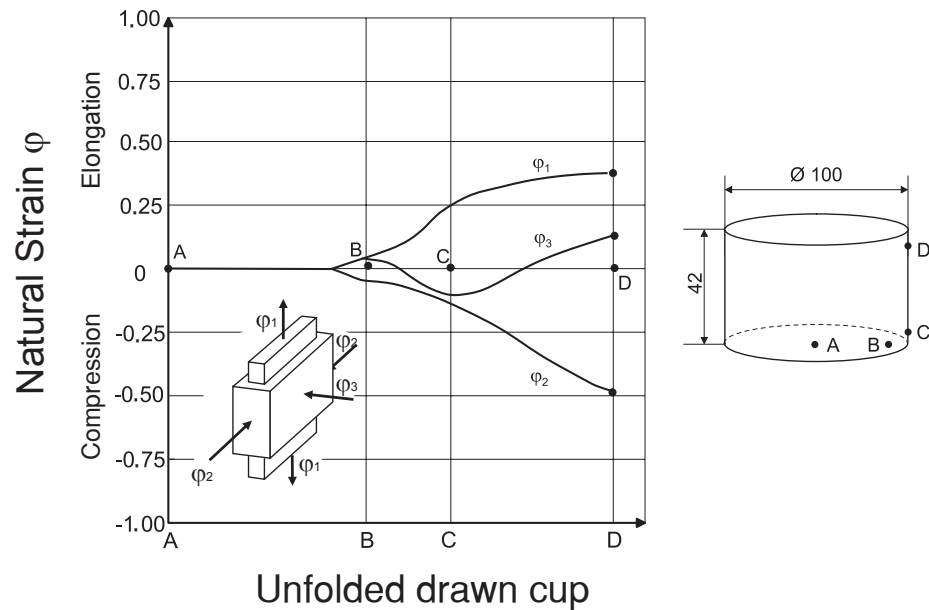


Figure 3.6: Natural strain distribution of drawn cup [Klocke and König, 2006, p. 328]

by the die radius and the interfering friction forces. This uneven exposure to different stress conditions leads to unequal natural strains (φ) in the specific cup areas. The initial shape thickness s_0 is only maintained in the middle of the cup base. It decreases in direction of the base edge, with a minimum within the range of the punch radius. This is consequently the section most prone to cracks. Once the blank has entirely taken the shape of the forming punch, a tensile-compressive stress condition arises, causing the wall thickness to increase with increasing cup height. The maximum of the wall thickness ($s_{max} > s_0$) is located at the upper edge of the cup frame (see Figure 3.5 b).

This rather simple configuration and its locally varying stress conditions suggests that more complex geometries are much harder to anticipate and maintain a constant material flow. As the local strains can not be anticipated and the sheet thickness is very difficult to measure, sample parts with applied measuring grips are formed from which the radial and tangential deformation can be obtained. Figure 3.6 shows the main natural strains of a deep drawn cup in relation to the developed view. With the main normal strains the effective strain can be determined, and - by considering a flow curve of the applied material - assumptions of the strength behaviour can be gained. [Klocke and König, 2006, pp. 326-330]

Drawing Ratio

Equation 3.1 represents the drawing ratio, with d_0 being the blank diameter before forming and d_1 being the inner diameter of the drawn cup (equal to the punch diameter).

$$\beta = \frac{d_0}{d_1} \quad (3.1)$$

It is a parameter that describes the degree of deformation of a deep drawing application. The drawing ratio is limited, as the material will fail eventually with too high drawing depths. Accordingly, β_{max} describes the maximum drawing ratio that must not be exceeded. For non-alloy steels and initial drawing steps, a maximum drawing ratio (β_0) of 2.0 can be achieved. Subsequent drawing steps reach maximum drawing rates (β_n) of 1.3 (without work annealing) and 1.7 (with intermediate annealing process). The drawing ratio depends highly on the friction conditions and decreases with increasing punch diameter. [Klocke and König, 2006, p. 330]

Anisotropism of Sheet Metals

Metals are made up of unit cells that do not possess the same properties when examining different directions. This is especially true for sheet materials. Due to the forming process (casting, rolling) a characteristic texture - and therefore a distinct preference to deform plastically in certain directions - develops and needs to be taken into consideration. The value that gives information on the anisotropism of a specific material is called *vertical anisotropy* r . It is obtained from tensile tests and defined as the ratio between the natural strains regarding the width and thickness of the tested sheet.

$$r = \frac{\varphi_2}{\varphi_3} = \frac{\varphi_b}{\varphi_s} \quad (3.2)$$

For $r = 1$ an isotropic behaviour of the sheet metal can be expected, as the material deforms equally in direction of the width and thickness of the sheet. Accordingly, a value below 1 means that the plastic deformation occurs preferentially in the thickness direction, and vice versa. For deep drawing applications a high value of r is strived for, as the one of the main characteristics of deep drawing is the constant sheet thickness. If the metal sheet features a distinct texture that originates in its production, the anisotropy depends highly on it and varies when considering different orientation of the sample regarding the rolling direction. This effect is acknowledged by the *planar anisotropy*:

$$\Delta r = \frac{r_{0^\circ} + r_{90^\circ}}{2} - r_{45^\circ} \quad (3.3)$$

A pronounced planar anisotropy leads to unfavourable earings in deep drawing applications. [Klocke and König, 2006, pp. 84-86]

Forming Limit Curve (FLC)

Figure 3.5 (left) depicts the varying stress condition of a volume element during the forming process of a symmetrical cup. When keeping this - rather simple - configuration in mind, it is obvious that a more complex part will be subject to a vast number of stress conditions that can differ, both, in type and size. While the drawing ration can provide information on the feasibility of a drawing process in general, it does not distinguish between different areas

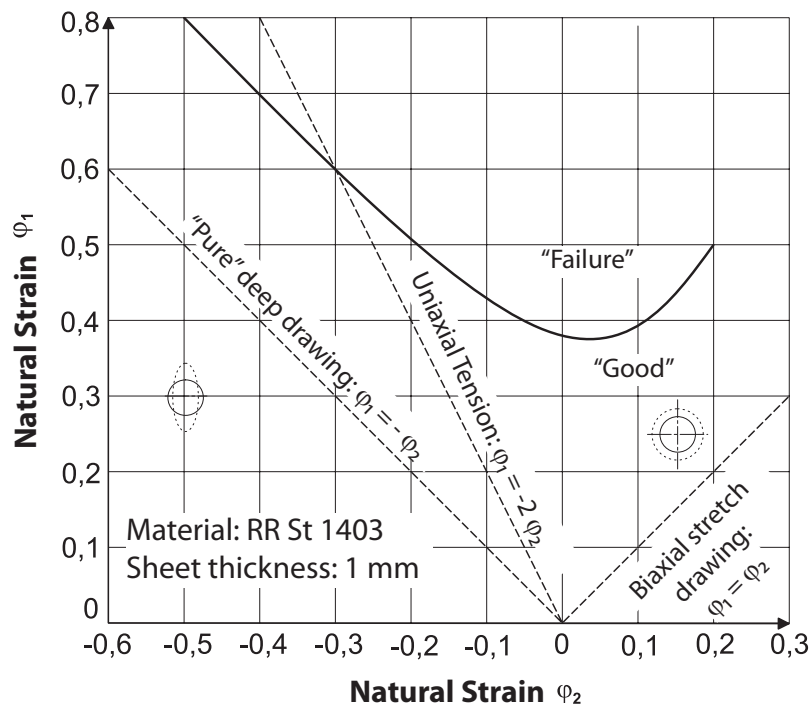


Figure 3.7: Example of a forming limit diagram (FLD) of a cold-rolled sheet metal [Klocke and König, 2006, p. 128]

of the drawn part. In order to identify critical part areas, forming limit diagrams (FLD) are consulted. They are experimentally obtained and indicate forming limitations for different sheet metals. Figure 3.7 gives an example of a FLD for cold-rolled steel strips. The continuous line indicates forming limit and therefore the material failure. Stress conditions that are below that line are tolerated. The FLC is influenced by numerous factors. One parameter that can alter the form and position of the curve is the *forming history* - that means it is different for subsequent drawing steps. Other influencing factors include the temperature, the sheet thickness, the forming velocity, the lubrication, the geometry and so on. [ETH, 2011; Klocke and König, 2006]

3.3 Tribology in Forming Applications

In this section the general knowledge on tribology gathered in Chapter 2 is applied to forming processes.

3.3.1 Tribosystem

As stated in Section 2.2, any technical operation can be described as tribotechnical system (TTS) - the simplified model of a real technical application that detaches all elements involved in friction and wear from their surrounding. Figure 3.8 depicts such a TTS for a

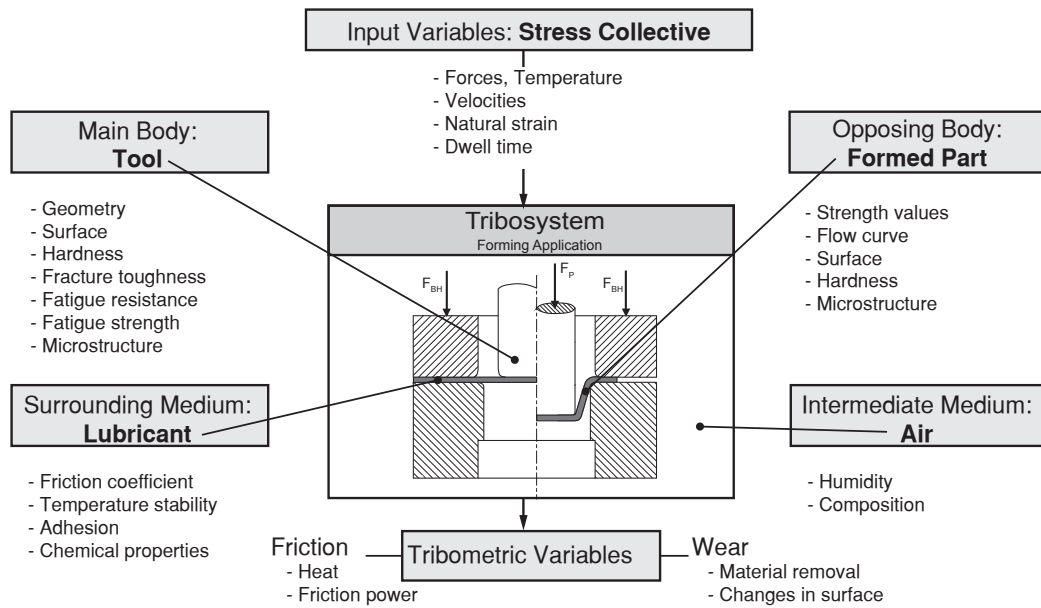


Figure 3.8: Forming process depicted as tribotechnical system
[Czichos and Habig, 1992, p. 454]

forming process.

According to the introduced denomination, a TTS for a deep drawing process consists of the base body (tool - punch, die, blank holders), the opposing body (sheet metal), the intermediate medium (lubricant) and the surrounding medium (air). It is considered an *open*¹ system, because the materials in contact do not stay the same.

3.3.2 Friction

Three distinct areas of friction can be identified, when considering a deep drawing process. These are localized at the contact area between the sheet and the blank holder/drawing ring (A), between the sheet and the die radius (B), as well as the sheet and the punch radius (C). While the occurring friction is disadvantageous in areas A and B (because it increases the needed drawing force), it does have positive effects on the maximum drawing ratio (β_{max}) in region C. In the latter case, the friction force contributes to the deformation of the drawn part and is therefore desired. [Klocke and König, 2006, p. 334]

Accordingly suitable measures (lubricants, functional coatings) are applied to realize high friction forces the punch radius area (C). Low friction forces, on the other hand are aimed for in the areas of the blank holder (A), in order to control the material flow and in area of the die radius (B) to enable an unopposed sliding of the sheet material. [Reissner, 2009, p. 140]

¹See Table 2.1 ‘System structures of tribosystems’ on page 8 for explanation.

3.3.3 Wear

Aside from the physical disruption of a forming tool, tool wear is considered the most important failure mode in forming applications, as it has a direct impact on the dimension accuracy, shape and surface quality of the processed parts.

The wear mechanisms explained in Section 2.4.2 'Wear Mechanisms' on page 14 are now considered regarding the deep drawing process²:

Abrasion

Due to peaks in the surface roughness, the harder friction partner (forming tool) 'ploughs' the softer one (formed part). On reoccurrence, particles are formed that are harder than the forming tool and eventually lead to its abrasion. The resulting consequences are the geometric deviation of the tool and the weakening of tool areas.

Adhesion

Adhesion of forming tools can be caused by two different initiating mechanisms. These initiating mechanisms are the formation of interface bondings and mechanical interlocking. Both lead to a material transfer from the softer (sheet metal) to the harder (tool) friction partner and are briefly explained below: *Formation of interface bondings*: As introduced in Section 2.4.2 'Wear Mechanisms', this process is abrasion in its classical sense. As a consequence of the surface enlargement of the plastically deformed metal sheet, on the one hand, and abrasive wear on the other, the non-metallic surface layers of both friction partners are partly destroyed during the forming process. The direct contact between the metallic compounds, combined with elevated surface pressures, lead to interface bondings that - if higher than the internal cohesion forces - result in a permanent material transfer. *Mechanical interlocking*: High surface pressures squeeze the softer material into potential surface defects of the tool (scratch marks, burrs). Relative movements of the two materials cause the shearing-off of the material.

Both mechanism result in highly roughened tool surfaces - and therefore produce parts of low quality. The uneven material transfer also induces local stress peaks that can lead to a material overload and cause a sudden crack formation in the tool.

Tribochemical Wear

During the forming process energy is introduced into the surface areas of both contact partners. This leads to chemical reactions and thus boundary layers of different chemical compositions. The tool wear is based on the break-away of brittle layers or the abrasive wear of softer ones. Elevated temperatures, as commonly used in press hardening applications, accelerate the chemical reactions and therefore the tribochemical wear even further.

²[Klocke and König, 2006, pp. 141-147]

Surface Fatigue

Surface fatigue is commonly observed in rolling contacts, thus deep drawing application are not prone to this wear mechanism.[Reissner, 2009, pp. 219-222]

All of the above wear mechanism can be slowed down by functional tool coatings.

3.4 Wear Slowing Tool Coatings

Since high-strength and ultra high-strength materials have become a dominant constant in deep drawing operations, the tribological strain on forming tools has been ever increasing. In order to meet these demanding requirements, while maintaining appropriate cost levels, critical tool areas are covered with functional graded coatings.

Kolleck and Pfanner [2008] summarize the reasons for surface modifications of forming tools as follows:

- *Economical aspects*
Economic base materials combined with highly advanced coatings
- *Modification of existing tool surfaces*
Partial coating of excessively stressed areas
- *Repairing of tool surfaces*
- *Functionally graded coatings*
Advantageous variation of physical properties in surface near layers

3.4.1 Surface Treatments of Critical Tool Areas

Lange [1993, pp. 670-683] gives an overview of surface treatments that are commonly used in forming applications:

- Reaction Layers
 - *Nitriding*
 - *Boriding*
 - *Vanadizing*
 - *Ion beam coating*
- Deposited Layers
 - *Hard chromium plating*
 - *Nickel plating*
 - *Welding techniques*
 - *Chemical Vapour Deposition (CVD)*
 - *Physical Vapour Deposition (PVD)*

In general a distinction is made between techniques that enrich the base material (or substrate) with a certain, wear improving element (for example nitrogen, boron, vanadium) and processes that actually deposit new material on the base material.

As it would go beyond the scope of this paper to describe each process elaborately, continuative references to other sources in the literature are made at this point. (Bach et al. [2006], Lange [1993, Chapter 17], Ruge and Wohlfahrt [2002, Chapter 4, 8], Doege and Behrens [2010, pp. 417-425])

3.4.2 Laser Cladding

As the presented master thesis aims at designing a device to pretest laser cladded coatings, this coating technique is described briefly in the following section.

Demarcation from other Surface Treatments

Table 3.1 compares laser cladding to similar coating techniques. The tabulated processes correspond with the processes introduced above that are primarily used for wear slowing tool coatings in forming applications.

Laser cladding can be described as the beneficial combination of laser welding and powder metallurgy. It creates strong bonds between the coating and the substrate, with low heat-affected zones (HAZ) and therefore minimal distortions in the base material. This is due to the characteristics of the laser beam. As the laser beam is very tense and well confined, it can be controlled adequately. This has positive effects on the coated part, as the base material that is effectively subjected to the heat impact is limited to a minimum. Directly related to this aspect is the manipulation of solidification rates of the melted material by adjusting the energy input - this way the formation of the microstructure and ultimately the mechanical properties can be controlled. [Vilar, 1999]

The dilution rate (mixing percentage of the substrate to the produced coating) is higher compared to alternative processes like thermal spray coating, PVD and CVD - where no dilution takes place. However, it is low compared to laser alloying or glazing. [Toyserkani et al., 2005, p. 49]

Disadvantages of the process are the high investment costs and the moderate repeatability of the produced coatings.

Process Principle

Figure 3.9 highlights the process principle of laser cladding. A high-powered laser beam penetrates the base material and melts a thin layer of the substrate. At the same time powder nozzles feed metal/ceramic powders into the melting bath and form pore- and crack-free coatings three-dimensionally. The generated coatings feature high bondage strengths to the base material. This process is quite flexible, as coatings of small, highly stressed areas are feasible - but also the modification of large scale surfaces is possible, as the coating can be expanded by overlapping individual tracks. The generated coating thicknesses vary between 50 μm and 2 mm. Larger thicknesses can be achieved, by layering several coatings on top of each other.

Table 3.1: Distinction between laser cladding and other metallic surface treatments
 [Toyserkani et al., 2005, p. 50]

Feature	Laser Cladding	Conventional Welding	Thermal Spray	CVD	PVD
Bonding strength	High	High	Moderate	Low	Low
Dilution	High	High	None	None	None
Coating materials	Metals, ceramics	Metals	Metals, ceramics	Metals, ceramics	Metals, ceramics
Coating thickness	50 μm - 2 mm	1 mm - several mm	50 μm - several mm	0.05 μm - 20 μm	0.05 μm 10 μm
Repeatability	Moderate - high	Moderate	Moderate	High	High
Heat-affected zone	Low	High	High	Very low	Very low
Controllability	Moderate - high	Low	Moderate	Moderate - high	Moderate - high
Costs	High	Moderate	Moderate	High	High

This generative laser process can be distinguished by the way the powder is supplied. Variations of powder injection, pre-placed powder on the substrate and powder supply by wire feeding exist. The single-step process of powder injection, as described above, has become the prevailing laser cladding technique. Reasons for that are the superior process controllability and reproducibility of this variant. Also, the higher energy efficiency adds to the predominance of laser cladding by powder injection. [Vilar, 1999]

Process Limitations

As already mentioned before, the repeatability of the process is not as distinct as in other coating processes. Fluctuations of operating parameters like laser power, beam velocity and powder feed rate, but also material characteristics such as variations in the absorptivity of the substrate, lead to significant alterations of the processed clad. [Toyserkani et al., 2005, p. 15]

This fact adds to the need for a functional testing device at the T&F to evaluate and verify welding parameters as well as ideal coating combinations before transferring them to large scale deep drawing applications.

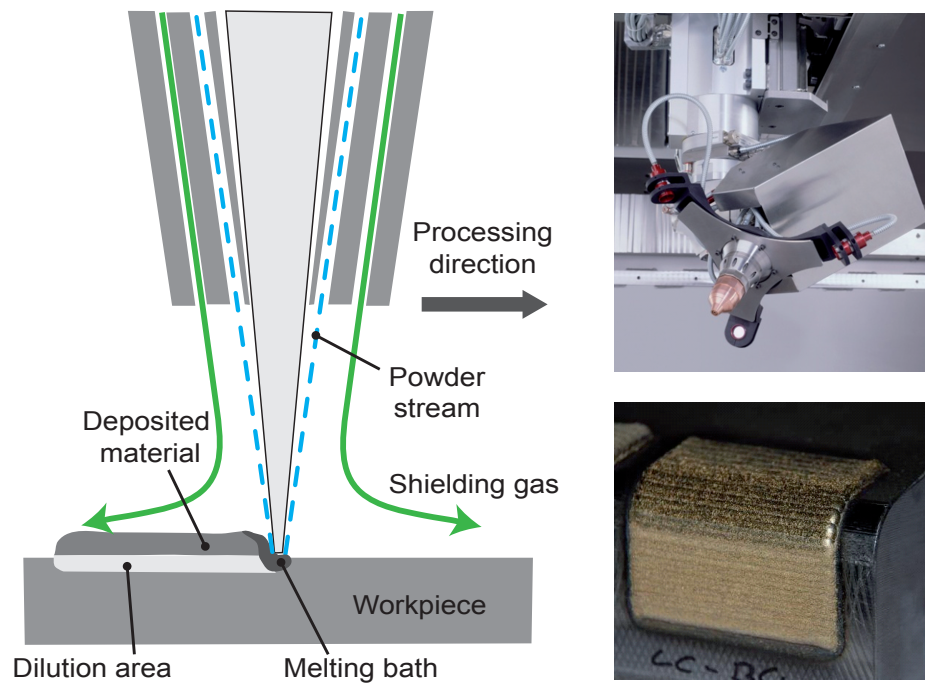


Figure 3.9: Left: Process principle: Laser cladding [Industrial Laser Solutions, 2010];
 Right: Welding nozzle as applied at the T&F, Exemplary laser cladded coating of critical tool area

Chapter 4

Project Content

This project focuses on conceptualizing, designing and assembling a suitable tribological testing device for assessing the wear behaviour of different material pairings that are applied in deep drawing processes. The obtained tribological module ought to be built and utilized at the T&F at the University of Technology Graz and is required to fulfil the following technical demands:

1. Adjustable surface pressures from 0 to 50 MPa
2. Relative movements between friction partners from 0 to 0.15 m/s
3. Consideration of warm and hot forming techniques (temperatures up to $\approx 900\text{ }^{\circ}\text{C}$)
4. Arbitrary friction partners
5. Interexchangeability of friction partners
6. Integrability of the testing tool into an existing device at the T&F

It was agreed on - before the beginning of the project - that existing tribometric equipment was not be taken into consideration during the conceptual phase, in order to maintain a certain degree of impartiality. Finding the most appropriate configuration for the requirements at hand was prioritized over applying standardized solutions. Also, an approach like this implied the possibility to find a new, innovative solution. Consequently, the section on tribometry in Chapter 2 'Tribology' was composed after a concept variant has been decided on and provides an overview of applied testing configurations for the reader.

Based on a morphological matrix, a number of concept variants are generated in order to find a suitable tribometric configuration. Every variant is then individually evaluated for its compliance with the prerequisites listed above. Concepts that lack important features are eliminated, while the remaining ones are compared with each other by applying efficiency analysis. The most promising testing configurations are compared once again, and the most fitting concept is ultimately chosen.

The main focus during the design process is - apart from assuring the requested functionalities - to keep the overall costs down. This economic demand is met by primarily using standardized parts. Chapter 6 'Technical Realisation' illustrates all steps taken to implement the chosen concept variant. A comprehensible and complete chronicle of the design process is

emphasized. In most cases the reasons for selecting a certain component are given along with available alternatives. However, due to the intuitive nature of design processes on the one hand, and the vast number of design possibilities on the other, not every possible choice can be mentioned. All according technical drawings can be obtained from Appendix B ‘Technical Drawings’, and are referred to specifically at the correspondent point in the paper. The thesis is concluded by a thorough description of the experimental set-up in Chapter 7 ‘Test Set-up’.

Chapter 5

Determination of Concept

5.1 Generation of Concept Variants

As pointed out in Section 2.2 ‘Tribotechnical System’, a TTS is highlighted by two bodies in contact that are subjected to a relative motion. Subsequently, the first step to find a suitable tribometric concept is the identification of shapes of the friction partners and the type of relative movement between them.

In order to find a befitting configuration in a well-arranged manner, a morphologic matrix is created. It contains basic geometries that can be either manufactured or purchased easily. These shapes represent the latter friction partners. The third parameter in the matrix is the relative movement between the two geometries.

Figure 5.1 depicts the created morphologic matrix that marks the initial point of the concept finding process. Each parameter is consistently paired with two corresponding elements, creating a list of possible solutions. This procedure eventually results in a total of 80 sample pairings. To make the overview more concise, arrangements that would not make sense are not further considered. Such excluded variants are, for example, the helical (spatial) movement of any sample on anything other than a cylinder. Or the helical (planar) motion on a ring. Furthermore, variants that are too much alike are merged to just one appearance. An example for the elimination because of similarity is the reciprocating motion on a disc, as it has the same properties as a configuration with a meandering sample on a flat.

After this preliminary elimination of inoperable and similar variants, a list of 24 variants is compiled that can be obtained from Figure 5.2.

5.2 Assessment of Concepts

As it would go far beyond the scope of this paper to elaborate every identified variation, the research objectives introduced in Chapter 4 ‘Project Content’ are used to cut the number of possible solutions. For reasons of readability, this list of requirements is iterated below:














VARIANT					
CHARACTERISTIC	a	b	c	d	e
1. Shape of friction partner n°1	Pin 	Ball 	Block 	Counterpart Cylinder 	
2. Shape of friction partner n°2	Disc 	Ring 	Flat 	Cylinder 	
3. Contact movement	Rotational 	Helical (planar) 	Helical (spatial) 	Translational 	Sinuous 

Figure 5.1: Identification of basic testing configurations based on a morphological matrix

1. Surface pressures 0 - 50 MPa
2. Relative movements from 0 - 0.15 m/s
3. Arbitrary friction partners
4. Consideration of warm and hot forming techniques temperatures up to $\approx 900^\circ\text{C}$)
5. Integratability of the testing tool into an existing device

The first demand - the generation of a defined surface pressure - leads to the most rigorous reduction of variants.

A majority of the generated concepts are characterized by a point or line contact between the two friction partners. The elastic contact deformation of such axisymmetric geometries is well documented (see Hertzian theory [Popov, 2010, chapter 5]), making it quite easy to determine the normal force needed to produce a certain surface pressure. However, the local pressure peak in the center (see Figure 5.3) leads to an accelerated material removal because of wear. As the tool wear progresses, the contact surface increases continuously. This results in decreasing surface pressures. Generating a surface pressure that is constant over time would inevitably result in a device that would exceed the intended complexity level of this project by far.

As a consequence, all variants that are characterized by point or line contacts are eliminated from any following consideration. Accordingly, variants b, g, h, i-p, q and t-x from Figure 5.2 are omitted.

This drastic exclusion of variants results in a more manageable list of seven concepts (a, c, d, e, f, r, s). The consecutive weighing of this remaining solutions, regarding their ability


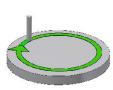
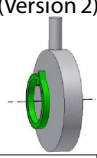
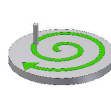
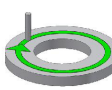
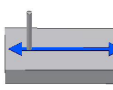
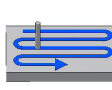
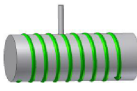
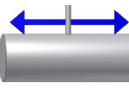

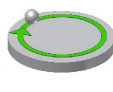
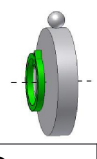

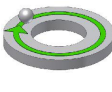
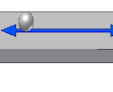
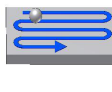
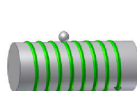
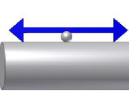

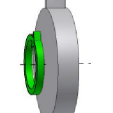
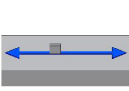
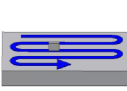
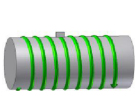
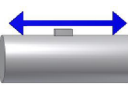
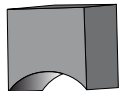
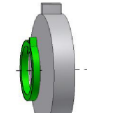
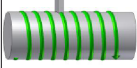
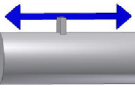
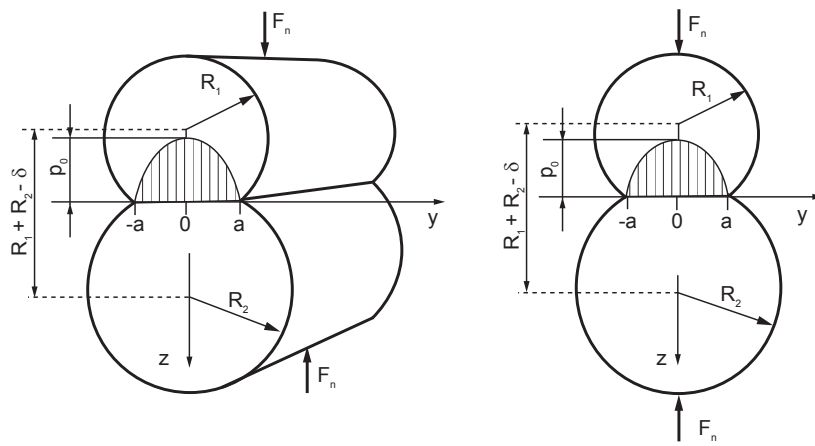
<p>Pin on...</p> 	<p>a Disc Rotational</p> 	<p>b Disc Rotational (Version 2)</p> 	<p>c Disc Helical</p> 	<p>d Ring Rotational</p> 	<p>e Flat Translational</p> 	<p>f Flat Sinuous</p> 
	<p>g Drum Helical</p> 	<p>h Drum Translational</p> 				
<p>Ball on...</p> 	<p>i Disc Rotational</p> 	<p>j Disc Rotational (Version 2)</p> 	<p>k Disc Helical</p> 	<p>l Ring Rotational</p> 	<p>m Flat Translational</p> 	<p>n Flat Sinuous</p> 
	<p>o Drum Helical</p> 	<p>p Drum Translational</p> 				
<p>Block on...</p> 	<p>q Disc Rotational</p> 	<p>r Flat Translational</p> 	<p>s Flat Sinuous</p> 	<p>t Drum Helical</p> 	<p>u Drum Translational</p> 	
<p>Counterpart drum on...</p> 	<p>v Disc Rotational</p> 	<p>w Drum Helical</p> 	<p>x Drum Translational</p> 			

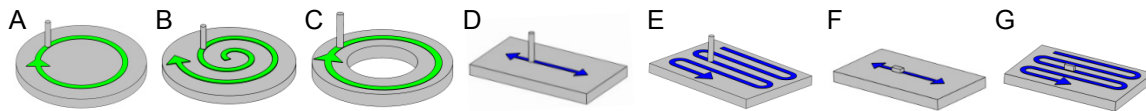
Figure 5.2: Overview of generated concepts after preliminary elimination of inoperable and similar variants



a... Half contact width; δ ... Flattening; p_0 ... Maximal surface pressure

Figure 5.3: Contact mechanics according to Hertzian theory
[Czichos and Habig, 1992, p. 37]

to meet the given requirements, is much more subtle and therefore an efficiency analysis is carried out. The weighing characteristics, including the basic assumptions that led to the evaluation, are listed below, sectioned into groups according to the research demands. For additional clarity, the remaining variants are renamed A-G (see Figure 5.4) and will be referred to accordingly in the following explanations.



A) Pin/Disc rotational; B) Pin/Disc helical; C) Pin/Ring rotational; D) Pin/Flat translational; E) Pin/Flat sinuous; F) Block/Flat translational; G) Block/Flat sinuous

Figure 5.4: Remaining concept variants

Surface pressure

- *Required normal force:* Of course this initial concept phase is too early to make reliable assumptions regarding the required normal force, as there are no dimensions agreed on. Generally it can be said that - due to its smaller cross section - a round profile will require less normal force in order to produce the same surface pressure, compared to a prismatic profile with the same diameter. Because of their linear relation, the same premise can be made when considering the resulting friction force. The difference is small however, leading to an insignificant differentiation of variants.

Relative movement

- *Drive system:* The considerations concerning the drive system are obvious. To realize variant A, the simplest form of drive systems (one constant rotational speed) will be sufficient. Of course this is only true if the end dimensions allow the adjustment of the relative movement - within the given velocity specifications - by alternating the radial position of the pin on the disc. In variant B the ring form of the second friction partner has a positive effect on the moment of inertia and therefore the driving torque. At the same time it calls for a drive mechanism with adjustable rotational speed in order to realize different relative velocities. Variants D and F also need a drive system that provides alterable rotational speeds. In addition, the system must include a gear unit to transfer the rotational movement of the motor into the desired translational movement. The implementation of Variant B necessitates two adjustable drives for both - linear and rotational - movements. Variants E and G require two linear actuators, one of which has to be continuously adjustable.
- *Velocity regulation:* It can be presupposed that an adequate drive system, paired with a suitable control unit, will be able to realize any demanded velocity (within certain limitations), regardless of the chosen solution. Nevertheless, configuration A enables the regulation of velocity only by varying the position of the pin on the disc at a constant rotational speed. The same mechanism leads to an increasing relative speed in variant B, as the pin progresses towards the disc's edge, which makes the realization of a constant relative speed more difficult.
- *Stop/Go:* Having the actual application area in mind - that is the deep drawing of sheets - a stop and go ability should be given some acknowledgement. Again, with the right driving system every solution can simulate this sequence of acceleration, steady speed and deceleration. But all variants with either translational or sinuous movement possess this characteristic naturally and are evaluated accordingly.

Arbitrary friction partners

- *Massive (tool):* If the second friction partner should represent the massive tool material, any configuration that varies its location continuously (B,E,G) will not be suitable. As the whole testing device aims at evaluating innovative laser cladded coatings, a singular penetration of the surface coat will not lead to any significant observation other than the outcome of a simple scratch test. And this information could be gathered more easily by other test settings.
- *Thin walled (metal sheet):* The above conclusion is completely reversed when the applicability of metal sheets as one friction partner is contemplated. Assuming that the second friction partner is realized as metal sheet and the corresponding friction partner (pin or block) is laser cladded in the contact surface, a single repetition of the contact movement has no assessable effect on the coated pin/block, as it is the harder friction partner in this constellation. A progressional running of the test in recurring contact areas will lead to a worn through metal sheet by the time the relevant friction partner shows signs of wear. Of course this setting could also result in a possible

Table 5.1: Qualitative evaluation of the remaining concept variants according to efficiency analysis

Category	Group		Sub W.	Sub													
	W.	Subcat.		A	B	C	D	E	F	G							
Surface pressure	10	Required normal force	10	4	40	4	40	4	40	4	40	4	40	4	40	4	40
		Drive system	15	5	75	2	30	4	60	3	45	1	15	3	45	1	15
Relative motion	40	Velocity regulation	15	5	75	1	15	3	45	3	45	3	45	3	45	3	45
		Stop/Go	10	2	20	2	20	2	20	4	40	4	40	4	40	4	40
Arbitrary friction partners	40	Massive material	20	5	100	1	20	5	100	5	100	1	20	5	100	1	20
		Metal sheet	20	1	20	5	100	1	20	1	20	5	100	1	20	5	100
Other	10	Lubrication	10	2	20	4	40	2	20	2	20	4	40	2	20	4	40
	100		100		350		265		305		310		300		290		280

damage of underlying components (drive system, heating device, etc.) and therefore has to be dismissed. This leaves variants B, E and G as only suitable possibilities to include a metal sheet into the test configuration.

Other

- *Lubrication:* The distinguishing characteristics between the different variants regarding the lubrication is based on the following assumptions: while all variants with recurring contact points (A, C, D, F) require a proper lubrication mechanism (which shall not be decided upon here), the remaining models allow a single application of lubricant prior to the test run.

Table 5.1 shows the numeric translation of the explications listed above. First, the single categories are weighed according to their importance to the overall function of the tribometer. The reason why the *Surface pressure* category is comparatively rated lower is that the adjustment of the surface pressure is already assured by all variants. All additional assumptions have little impact on the functionality of the device. Also the *lubrication* aspect is not prioritized, because it is not a main focus in this thesis. The assigned category weight is then broken down into subweights for each element. The allocation of subweights is, again, based on the perceived importance of the specific subgroup to the functionality of the device. Assessing the compliance of each concept variant with the defined project requirements leads to the individual *degree of performance*. This rate is represented by the grey numbers in Table 5.1. By multiplying each degree of performance with the correlating subweight and adding up all numbers belonging to one variant, the qualitative ranking of the remaining vari-

Table 5.2: Direct comparison of last remaining concept variants

	Pin/Disc Rotational + Helical	Pin/Flat Reciprocating + Meandering
Drive System	Required drives slightly favourable	2 translational movements
Velocity	Easiest for rotational mode	Can be realized easily by drive systems
regulation	Most complex for helical mode	
Stop/Go	Has to be realized by drive system ↑ complexity	Occurs naturally
Pin wear	Uneven	Even
Infinite loop	Restricted in helical mode	Realizable in sinuous mode

ants can be obtained. With the assumptions defined above, the efficiency analysis leads to the conclusion that variant A (Pin/Disc rotational) should be favoured, followed by configuration D (Pin/Flat translational) and C (Pin/Ring rotational).

However, when concentrating on findings in category *Arbitrary friction partners*, it can be seen that the performance of all variants is exactly reversed in the two subcategories. Concepts that manage to simulate the tribological strain on massive materials to a high degree will fail when it comes to the operation including metal sheets - and vice versa. This observation inevitably calls for the merging of single concept variants in order to fully meet the defined requirements. Such combinations will feature two operation modes, depending on whether the second friction partner is massive or thin walled. With the collection of remaining concepts it seems obvious to combine the conceptual functions of variants A and B (Pin/Disc rotational + helical), D and E (Pin/Flat translational + sinuous), as well as F and G (Block/Flat translational + sinuous). Variant C is not capable of operating in a different mode and is therefore excluded from further considerations.

As the above assumptions are still valid, the suitability of these combined variants can be compared by adding up the gained totals from Table 5.1. This consideration leads to the following ranking:

1. Pin/Disc (615 points)
2. Pin/Flat (610 points)
3. Block/Flat (570 points)

While the combinations of Pin/Disc and Pin/Flat scored comparably and need further examination, the Block/Flat variant is far behind regarding its efficiency points and can therefore be eliminated.

5.3 Selection of Concept

Before the final decision on the tribometric concept is made, the remaining two concepts are compared directly to each other (see Table 5.2).

Individually seen, the Pin/Disc configuration in a rotational mode is most favourable. Yet,

the combination with the helical mode - to ensure the applicability of sheet metals - leads to a tremendous increase in complexity. The determining factor in the decision making process is the feasibility of experiments during an extended period of time, when operating with metal sheets. The Pin/Disc (helical) configuration is ultimately limited by the size of the metal sheet. With a suitable loading system that continuously feeds the metal sheet, the Pin/Flat (sinuous) concept can be extended infinitely and is therefore going to be realized.

Chapter 6

Technical Realisation

It is decided that integrating the tribometric device into the milling centre *SHW UniSpeed* is most favourable. Due to the constituted contact area and the small resulting forces, an assimilation into the numerically controlled machine practically suggests itself. The meandering of the test pin on the counter body can be easily controlled numerically, and the vertical position of the test unit can be thoroughly set.

A modular design approach is strived for. This way also a possible extension of the module, to a self-contained tribometer, in the future stays feasible.

This chapter documents the generation of the basic module of the tribometric device and is sectioned into fundamental functions demanded by the system. All corresponding technical drawings can be obtained from Appendix B.

6.1 Determination of Basic Dimensions

One of the main requirements of a tribometer is to adjust specific surface pressures. As the chosen Pin/Disc constellation features a plane contact area, the needed normal force (F_N) can be derived easily from the equation that defines the surface pressure:

$$p = \frac{F_N}{A} \left[\frac{N}{mm^2} \right] \quad (6.1)$$

In order to keep the resulting forces to a minimum, a small contact area is constituted. The chosen pin radius (r) is 2.5 mm and results in a contact area (A) of 19.63 mm². Inserting A and the required surface pressures (10 – 50 MPa) into Equation 6.1, gives an adjustable normal force range of 196 N to 981 N.

To make a rough estimate of the resulting friction force (F_R), a friction coefficient (μ) of 0.6 is chosen. - This value is based on experimentally obtained friction coefficients of different steel on steel pairings in sliding motions by Czichos and Habig [1992, p. 501]. It is very high compared to the commonly used value of 0.2 for dry friction of steel pairings (compare Künne [2007, p. 223]). Using the higher friction coefficient includes a significant safety factor in all following calculations. The above assumptions result in a maximum friction force of 589 N.

Figure 6.1: Castigliano's theorem:

Verification of
pin diameter.

With:

$$d = 5 \text{ mm}$$

$$l = 10 \text{ mm}$$

$$A = 19.63 \text{ mm}^2$$

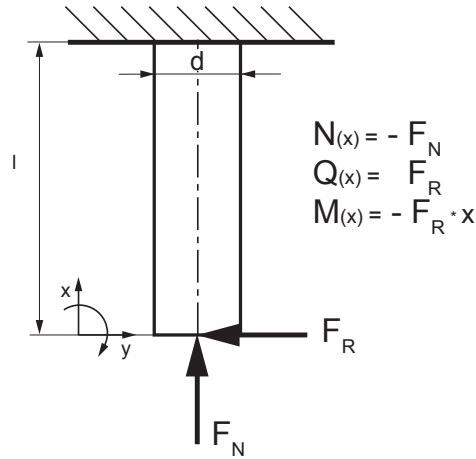
$$E = 210,000 \text{ N/mm}^2$$

$$I = 30.68 \text{ mm}^4$$

$$G = 79,300 \text{ N/mm}^2$$

$$F_N = 1000 \text{ N}$$

$$F_R = 600 \text{ N}$$



Basic strength calculations are used to explain why the pin diameter is ultimately increased to 20 mm: The pin resembles a clamped beam with a constant cross section and two applied forces (F_N , F_R). Castigliano's theorem is applied to anticipate the horizontal displacement of the pin in the contact area. The theory states that the partial derivative of the strain energy, with respect to an applied force, equals the displacement in direction of the specific force (see Equations 6.2 and 6.3).

$$U = \int_{x=0}^l \frac{N^2(x)}{2E \cdot A} dx + \int_{x=0}^l \frac{M^2(x)}{2E \cdot I} dx + \int_{x=0}^l \frac{Q^2(x)}{2G \cdot A} dx \quad (6.2)$$

$$\frac{\partial U}{\partial F_i} = u_i \quad (6.3)$$

$$u_y = \frac{\partial \left[\int_{x=0}^l \frac{-F_N^2}{2E \cdot A} dx + \int_{x=0}^l \frac{-F_R^2 \cdot x^2}{2E \cdot I} dx + \int_{x=0}^l \frac{F_R^2}{2G \cdot A} dx \right]}{\partial F_R} \quad (6.4)$$

The configuration shown in Figure 6.1 results in Equation 6.4. Accordingly, a dislocation of the pin in the contact area of $u_y = 34.8 \mu\text{m}$ can be obtained. An increase of the pin diameter to 20 mm reduces the horizontal displacement to $0.3 \mu\text{m}$ ($A = 314.16 \text{ mm}^2$, $I = 7,853.99 \text{ mm}^4$).

In order to combine the benefits of a small contact surface with a minimum of horizontal displacement, a pin with a diameter of 20 mm that is tapered at the end is utilized (compare Figure 6.2).

6.2 Holding Fixture

The holding fixture needs to be a detachable connection. In addition it has to guarantee a simple mounting/demounting and require a minimum of pin preparation before testing. Keyed and crimped connections, as well as joints with feather keys are disadvantageous because the assembly and disassembly is more time-consuming compared to other basic detachable

joints. Screwed, tapered and bolt connections, on the other hand, require additional preparation of every individual test pin (thread, taper, borehole).

For the given requirements a clamped joint connection is most favourable. Ultimately, a clamped joint consisting of a collet and a clamping nut (according to DIN 6499), like it can be found in milling and drilling devices, is decided on. It features a high degree of operator convenience, consists of standardized parts, and can be easily upgraded for cooling purposes. Moreover, this setting allows to test other pin diameters by adapting solely the collet to a fitting size.

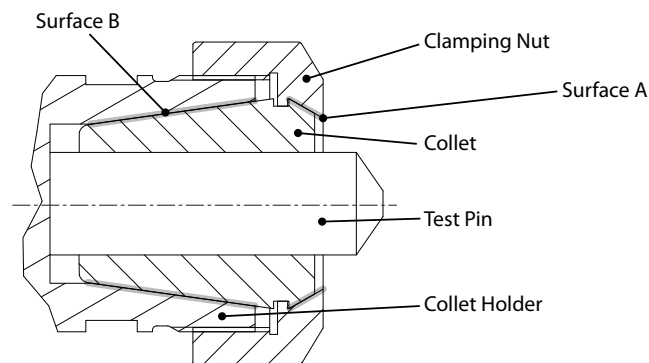


Figure 6.2: Detail drawing: Holding fixture - for a complete drawing see Appendix B-B6

The functioning of this holding fixture is best explained while observing Drawing 6.2: When the clamping nut is tightened, surface A pushes the collet into the tapered surface B of the collet holder. This compresses the alternately slotted collet and therefore clamps the pin. When the nut is loosened, an eccentric actuator in the nut pulls the collet out and releases the pin.

As the test pin is axially supported by the holder and no torques are transmitted, the holding fixture's purpose is only to secure the pin radially and prevent its vertical displacement when no normal forces are applied. Therefore, a recalculation of clamping forces is not necessary.

6.3 Adjustment of Surface Pressure

As already mentioned above, a reliable adjustment of defined surface pressures is crucial for the presented tribological device. In order to keep the complexity low, the module does not feature a continuous recording of the applied normal force. This makes a periodic readjustment of the surface pressure impossible. Consequently, a proper spring system that compensates irregularities in the friction partners, as well as a suitable scaling system for the initial adjustment of the surface pressure, need to be incorporated into the design.

Spring System

Any technical system can be described as a combination of serial and parallel connected parts. When subjected to external loads, these components exhibit the same properties as a very stiff spring.

For the presented application such a behaviour would be very disadvantageous. Once the desired surface pressure is adjusted and the test run begins, a slight peak in the contact partner - or for that matter, an accumulation of wear debris in the contact surface - will cause a sharp increase in the surface pressure. A deepening, on the other hand, will lead to a local plummeting of the pressure.

In order to prevent such implications, an actual spring, with thoroughly defined characteristics, is added serially. This component will absorb the fluctuations in the surface pressure.

It is decided that for vertical variations of ± 0.1 mm normal force deviations of $\pm 2\%$ are acceptable .

A (helical) compression spring is chosen to be implemented into the system. It is the most commonly used type of spring¹, features an almost linear load deflection curve and its temperature dependency is manageable. Temperatures up to $250\text{ }^{\circ}\text{C}$ are operational, however, service temperatures below $100\text{ }^{\circ}\text{C}$ are recommended in order to guarantee a linear spring behaviour.

There are two characteristics that need to be acknowledged when dimensioning this type of spring: The usable spring deflection is limited to 62% of the nominal deflection in order to ensure creep resistance. Also, a minimal initial load (between $13 - 30\%$) is necessary to ensure the linear load deflection behaviour. This value depends on the maximal spring deflection. [Fibro, 2012, F8]

It is not possible to find a standard compression spring that covers the whole range of requested normal forces, and that also meets the operational demands listed above. Hence, the range is divided and a combination of two springs is aimed for.

By virtually pairing different springs, a combination of identical springs - but of different capacity load groups - is found that fulfils all requested demands, and additionally features similar deflections when simulating the whole force range.

Table 6.1: Chosen combination of compression springs to meet all requirements

#	R [N/mm]	S_n [mm]	F_{\max} [N]	F_{\min} [N]	$F_{\min\text{Allowed}}$ [%]		$S_{\max} - S_{\min}$ [mm]	ΔF [N]	ΔF [%]
1	84.4	32.5	1000	430	13	375	$(11.8 - 5.1) = 6.8$	8.44	1.96
2	38.3	39.0	450	200	13	194	$(11.8 - 5.2) = 6.5$	3.83	1.92

Table 6.1 shows the combination of the two chosen helical compression strings. S_n is the nominal spring deflection and represents 100% of the possible compression length, F_{\max}

¹[Meissner and Wanke, 1993, p. 188]

and F_{min} are the normal forces that are generated with the according springs. F_{max} has a direct impact on the minimum pretension value, below which the generated normal force must not fall. In addition, the deflection range ($s_{max} - s_{min}$) is tabulated. It can be seen that it is nearly the same for both springs. This has a positive effect on the quantification of the surface pressure. It is also demonstrated that a deviation of ± 0.1 mm in the contact zone results in force discrepancies smaller than 2% of F_{min} .

To prevent friction losses between the spring and the mandrel, lubrication grease is applied. As no torques are transmitted, a felt ring is introduced to seal the spring area - see Appendix B-B6.

Quantification

The normal force, and therefore the exerted surface pressure, is adjusted by altering the vertical position of the tribo-module in reference to the contact zone. Before the module engages in actual testing procedures, it needs to be calibrated. For this purpose, a scaling pin is integrated into the design. It is attached to the test unit and moves upwards (in relation to the housing) as the surface pressure increases.

For calibration, a load cell is implemented instead of the friction partner. Then, the desired normal force range is generated stepwise and the position of the scaling pin, in dependence of the normal force, is marked on the housing. When the scaling function is tested and verified, a proper scale is laser marked on the housing.

As there are two springs that need to be exchanged to simulate the complete range of surface pressures, also two separate scales are necessary - see Figure 6.3.

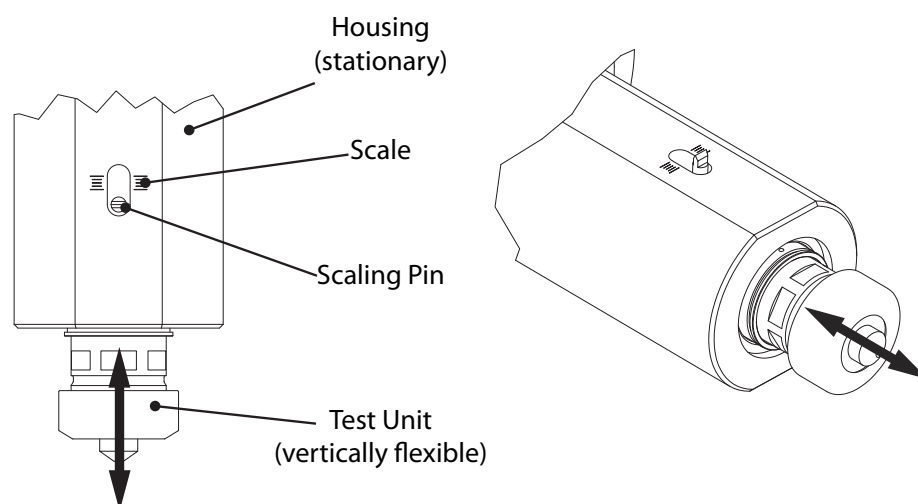


Figure 6.3: Detail drawing: Scaling unit

The scaling pin also secures the test unit vertically prior to and after a test sequence.

6.4 Guiding System

As a direct consequence of the spring system - and its demand for the unhindered translational motion of the system - the necessity for a linear guidance system arises. A linear rolling bearing soon becomes the guidance of choice. As highlighted by Brecher and Weck [2006, p. 358], rolling bearings are characterized by a smooth running (due to rolling friction), the elimination of stick-slip, an economic installation, little need for maintenance and the availability as standardized parts. The respective disadvantages linked to this type of bearing, like the minor damping ability perpendicular and parallel to the guidance direction, can be tolerated for this application. All of these benefits and flaws derive from the direct comparison to sliding bearings.

A configuration consisting of a guide pillar, a ball bearing cage and a guide bush is chosen.

In order to compact the design and to ensure the positioning of the guiding system near the test zone, an integration of sub-functions is decided on. This results in the merging of the clamping, guiding and spring system into one customized part. Figure 6.4 emphasizes this aggregation of functions. Now, the adapted guide pillar also holds the collet and features a thread into which the guide bolt for the compression spring is integrated.

In Figure 6.4 it can be seen that also the cooling system is held by the guide pillar. The additional space between the cooling connections and the clamping system is needed for the ball bearing cage to move upwards and downwards.

6.5 Cooling System

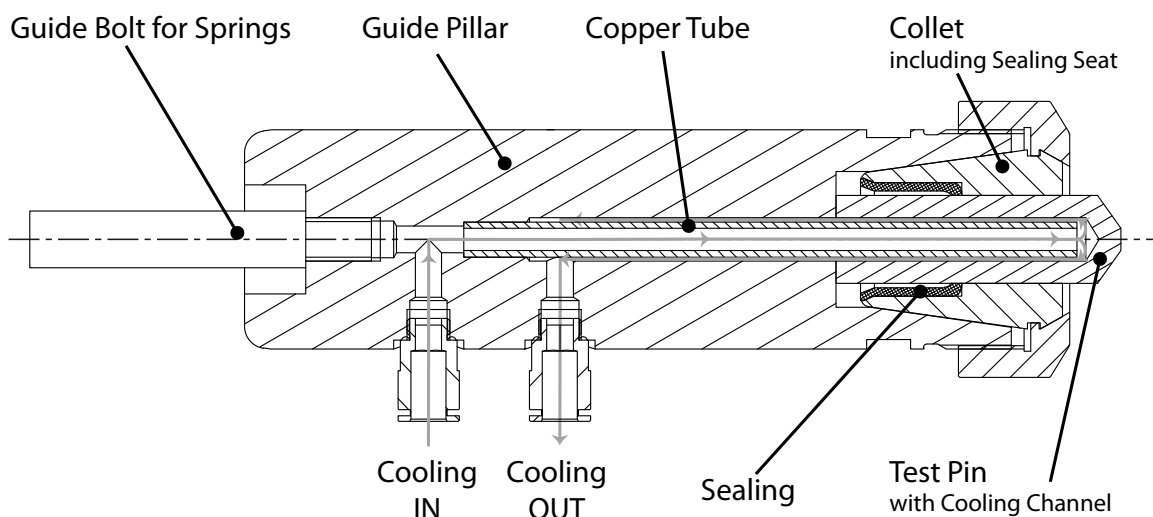


Figure 6.4: Detail drawing: Cooling - for a complete drawing see Appendix B-B6

Hot forming technologies, like press hardening, have become a dominant factor in deep

drawing applications. Especially for the presented test configuration, and its small test sample, a functional cooling system is essential when operating with heated metal sheets. The chosen approach integrates the cooling channel into the guide pillar. The test pin is also equipped with a surface-near cooling hole and can therefore be cooled directly. Beside the upgrade of the collet to a version with a sealing seat - and the according sealing - no changes are made regarding the applied parts. As it can be obtained from Figure 6.4, the cooling channel goes through the whole pillar, thus facilitating the manufacturing process. The left opening is closed by a bold needed for guiding the compression spring. The separation of cooling inlet and outlet is realized in a way that does not require a seal. - Due to manufacturing limitations, the seat that holds the left end of the copper tube is tapered in the end. This slight interference leads to a tight fit between tube and pillar and therefore substitutes an actual sealing.

Another advantage of the *SHW UniSpeed* is the existing cooling system. This way, only matching connections need to be integrated into the designed tribo-module. This is ensured by adding plug-in connections that fit the existing cooling pipes.

The dimensions of the copper tube and the corresponding cooling channels are based on the demand that the surface area of the inlet (A_{in}) equals the surface area of the outlet (A_{out}), which ultimately results in a constant flow stream. As standardized copper tubes and manufacturing tools interfere with this request, it is mitigated. In the end a copper tube with a diameter of 8 mm and a wall thickness of 1.5 mm is applied. This results in an A_{in} of 19.63 mm^2 and an A_{out} of 28.27 mm^2 .

6.6 Housing

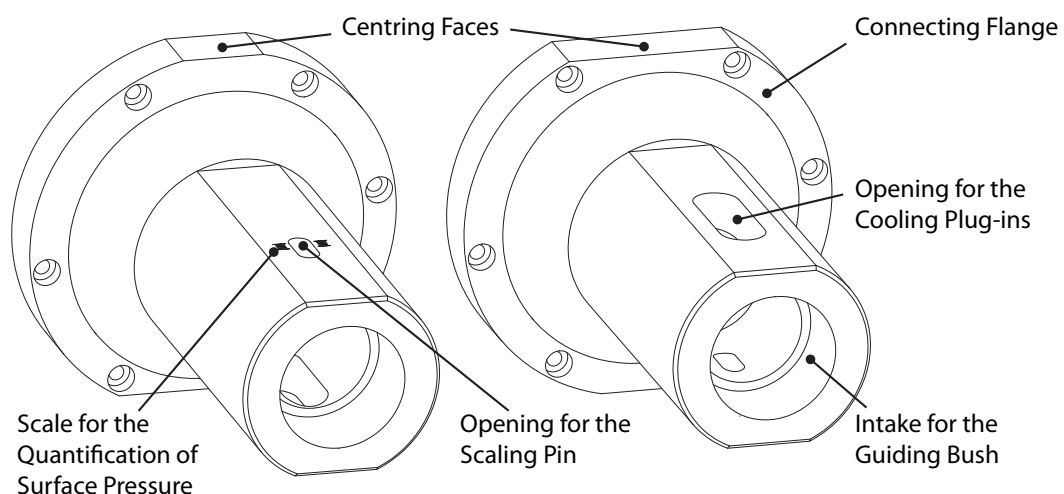


Figure 6.5: Detail: Housing - for a detailed drawing see Appendix B-B4/B6

The design of the housing results from all above considerations. Figure 6.5 depicts the consequent housing. It features longitudinal grooves for the scaling and the cooling equipment and an intake for the guide bush. The connection flange and its corresponding pockets result

from the mounting dimensions of the milling centre. For centring purposes two according faces are incorporated into the housing.

Due to manufacturing limitations the housing has to be opened in the flange area (see Appendix B-B4). In order to provide a supporting surface for the compression spring, a thrust plate is integrated into the housing.

Because of the high density of the material ($\rho = 7.85 \text{ kg/dm}^2$), a slender housing is constituted. Strength analyses - similar to the calculations carried out for the pin diameter (see Section 6.1) - lead to a vertical dislocation of $2.7 \mu\text{m}$. As this value is based on a very high friction coefficient ($\mu = 0.6$), it is tolerable.

Chapter 7

Test Set-up

During the initial test set-up, a pilot test run is performed in order to verify the basic functions of the designed tribo-module.

7.1 Pin Preparation

As described in the previous chapter, the test pin is tapered at the end to ensure small resulting forces and, therefore, minimum distortions in the contact area. At the same time, this diminution of the pin diameter has a positive effect on the laser cladded coating that is ultimately tested. Due to the nature of the laser cladding process, inhomogeneities and vertical exaggerations can be expected in the peripheral areas of the generated coatings. These irregularities are due to the direction inversion (movement of nozzles) during the welding process, and can be avoided by tapering the coated pin before testing it.

The tribo-module is calibrated based on the vertical displacement of the test unit regarding the housing. Thus, the actual height of the tested laser clad is not of importance. It is, however, crucial that the produced coating is planar and perpendicular to the axis of the test unit, in order to ensure a constant surface pressure in the contact area.

The applied test pin is not laser cladded for the pilot test run. Instead, a 1.2210 (DIN 115CrV3) bar stock is tapered and applied as *dummy*. As the actual evaluation of laser cladded coatings is not part of this master thesis, this simplification is of no consequence. On the contrary, the results obtained from the pilot test run highlight impressively why wear resistant coatings are essential in any forming process.

The diameter of the applied round bar features a fit tolerance of $h9$ ($20^{+0}_{-0.052}$ mm). This corresponds with the clamping tolerance of the collet (20^{+0}_{-1} mm).

Accordingly, the test pin is not required to be machined prior to the test run.

7.2 Fixation of Metal Sheet

For the initial test sequence a deep drawing sheet metal is chosen as opposing body in the created TTS. Beside the obvious wear resistance, the corrosion-resistant steel (1.4034,



Figure 7.1: Test pin *dummy* clamped by collet and nut during pilot test sequence

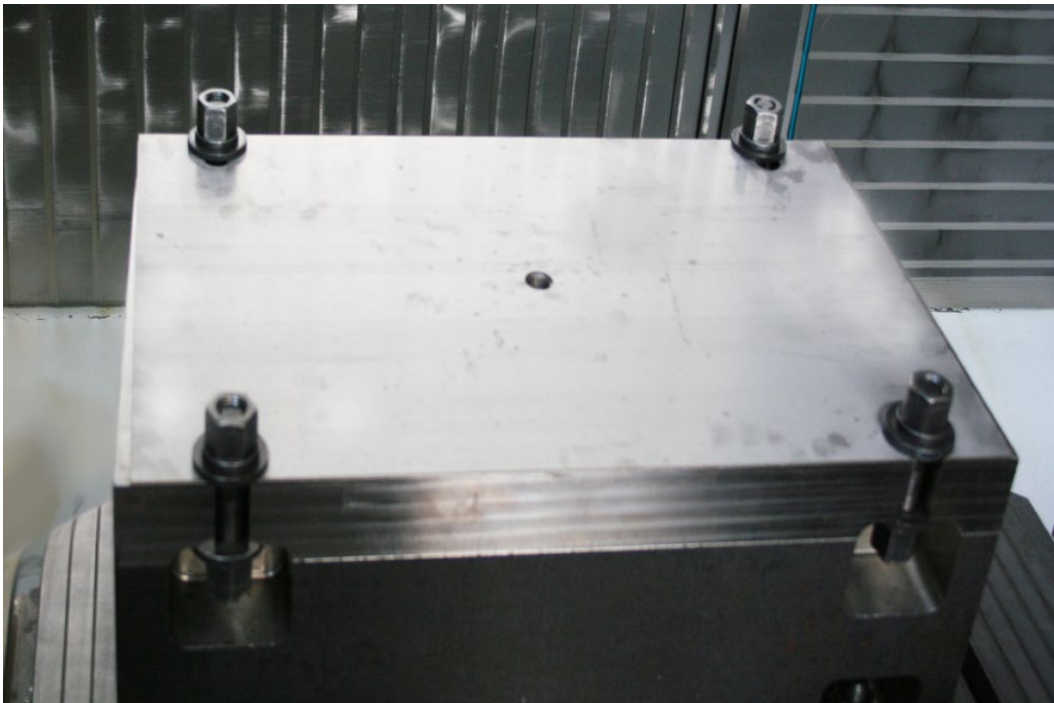


Figure 7.2: Fixation of sheet metal on existing tool chuck



Figure 7.3: Overview of basic components of the tribo-module

X46Cr13) features a good response to hardening processes, as well as favourable wear behaviour. Further tests with different sheet grades are planned. For the fixation of the metal sheet an existing chuck at the T&F is utilized. In order to firmly clamp the sheet metal, it is laser cut to fit the dimensions of the block (See Picture 7.2).

The outside dimensions of the tested sheet are 388 mm x 610 mm and result in a maximal wear path of approximately 20 m. For a legitimate test sequence, the metal sheet will have to be exchanged several times (depending on the the wear resistance of the applied laser clad). Thus, a modified sheet fixation that features a larger contact area should be considered in the future.

In addition, it would be highly favourable to conceptualize a sheet fixation that does not require the accurate cutting of each individual metal sheet.

7.3 Assembly of Tribo-Module

Picture 7.3 shows the basic components that assemble the tribo-module. The guide bush is glued into the housing at the very beginning of the assembly, in order to give it time to affix. The felt ring needs to completely shape into the lining groove. Therefore, it is incorporated into the housing very early and drenched in lubricating oil. Another part that is already fixed to the housing is the thrust plate. It locks the upper opening of the housing that was created for manufacturing purposes only. Accordingly, those three components are not highlighted in Picture 7.3.

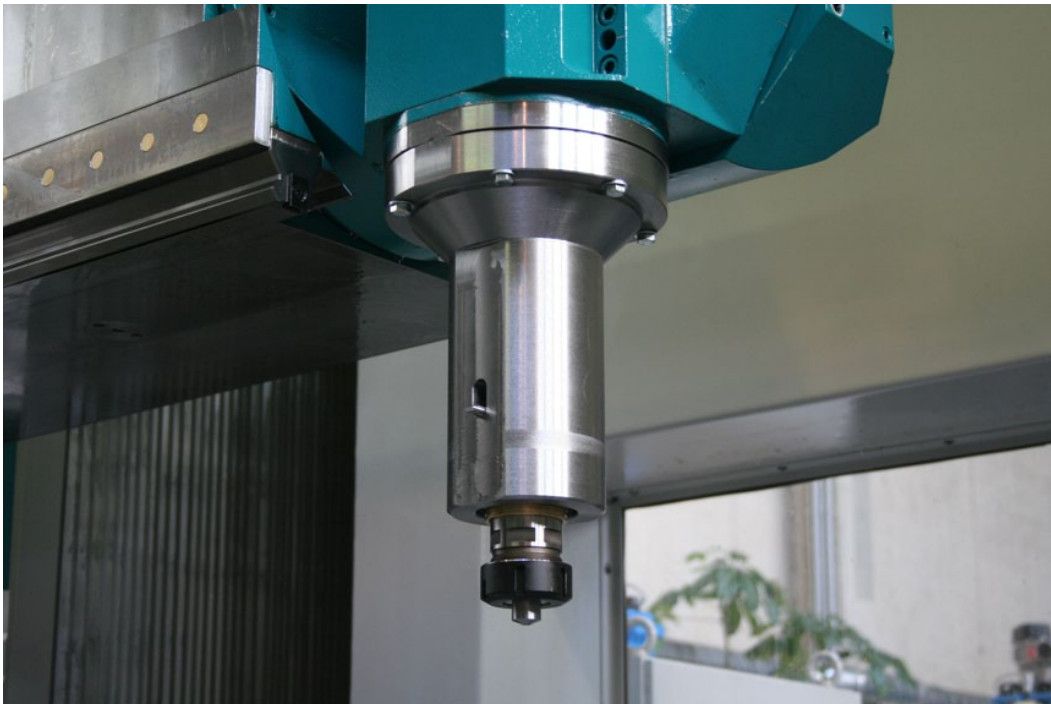


Figure 7.4: Assembled and mounted tribo-module

All following steps are elementary and therefore the repeated assembly/disassembly is guaranteed to be unproblematic. First, the guide bolt is attached to the upper ending of the customized guide pillar, while bounteously applying lubrication grease. The friction between the stationary housing and the vertically moveable test unit primarily takes place between the felt ring and the guide pillar. Also, the friction between the compression spring and the guide bolt needs to be considered. While the complete elimination of the friction is not possible, this lubrication does diminish it to some extent.

After the compression spring is imposed to the guide bolt, the test unit is inserted into the housing. In order to linearly guide the tribo-module, the ball bearing cage is placed between the test unit and the housing. One characteristic of ball guide systems is that the ball bearing cage *travels* half the amount of the actual dislocation between the two guided components. This fact is taken into consideration, by aligning the lower edge of the ball bearing cage with the lower edge of the housing when considering the starting position (the compression spring is in contact with the thrust plate). This way, the ball bearing cage is still positioned in the guide push, while the maximum dislocation (approximately 15 mm) is realized. See also Appendix B-B7 for the technical drawing of the two end positions. Once the test unit is successfully positioned, the scaling pin is inserted in order to secure the test unit vertically.

These are all steps necessary to assemble the tribo-module. Now, the device can be mounted to the *SHW UniSpeed*. This is facilitated by the two centring faces introduced in Section 6.6 ‘Housing’. Picture 7.4 shows the mounted tribo-module.

The insertion of the test pin (including collet and nut) is standardized and should be familiar. Nevertheless, some guidelines are given: The collet should never be placed into the



Figure 7.5: Calibration of tribo-module with a load cell

collet holder without the prior connection to the nut. In addition, the collet must not be clamped without an inserted test pin, because this could lead to permanent deformations of the clamping collet. When placing a test pin into the clamping fixture, it should not be inserted less than two thirds of the collet bore length. The maximum tightening torque of the nut is 176 Nm and must not be exceeded. In order to firmly close the nut, hexagonal flats are incorporated into the guide pillar, to fixate the test unit while tightening the nut. [RegoFix[®], 2011]

7.4 Calibration

Before the actual test run can begin, the acting normal forces need to be calibrated with a load cell. Picture 7.5 demonstrates the calibration process, where the the tribo-module is positioned in relation to the load cell by the numerically controlled mill centre. The vertical dispositions of the module and the corresponding normal forces are recorded.

Figure 7.6 depicts the obtained results for normal forces between 400 – 1,000 N. The presented hysteresis effect can be attributed to friction forces between the test unit and the housing. This friction is composed of the friction between the parings compression spring/guide bolt, felt ring/guide pillar, and ball barrier cage/guide pillar respectively ball barrier/guide bush. For the initial test procedures, a recalibration is suggested because the hysteresis is expected to change slightly. This is mainly due to the adaption of the felt ring that will absorb more lubricant and therefore minimize the friction.

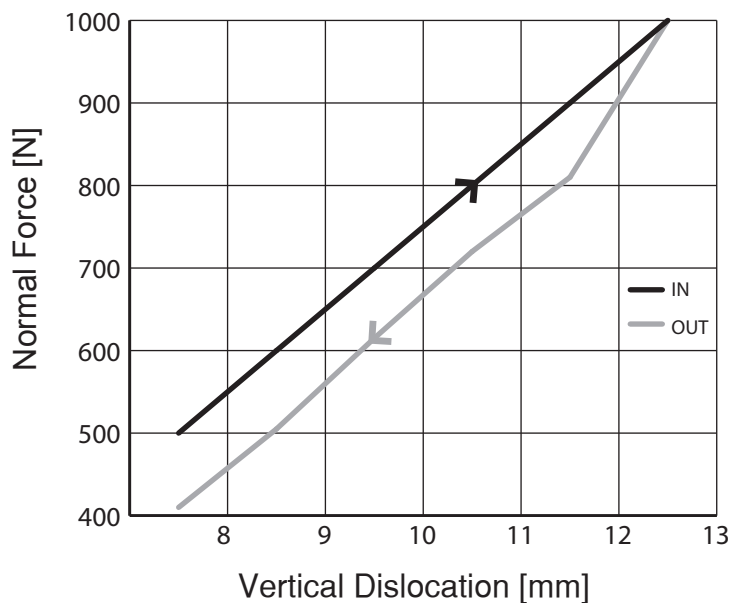


Figure 7.6: Hysteresis effect during loading and unloading of tribo-module

But also after a certain running-in period, this discrepancy between the achieved normal forces, based on the in- or outfeed of the system, will be observed and must be acknowledged accordingly.

The documented hysteresis also emphasizes the desired linear force-deflection behaviour of the introduced compression spring.

7.5 Pilot Test Sequence

For the initial test run the conceptualized (see Picture 7.7), meandering relative motion is substituted with a number of single, consecutive parallels, in order to verify the stability of the system before putting a biaxial strain on it. With the incorporation of the tribo-module into the *SHW UniSpeed*, the feasibility of any motion is guaranteed anyway and does not have to be validated at this point.

A normal force of 500 N is increased linearly at the beginning and end of each slope in form of a vertical dislocation. The offset between individual lines is actualized when the tribo-module is not in contact with the sheet metal. After the operation at tentative feed rates confirmed the functionality of the designed testing device, further test runs at maximum required speed (150 mm/s) are carried out successfully.



Figure 7.7: Engaged module during pilot test sequence

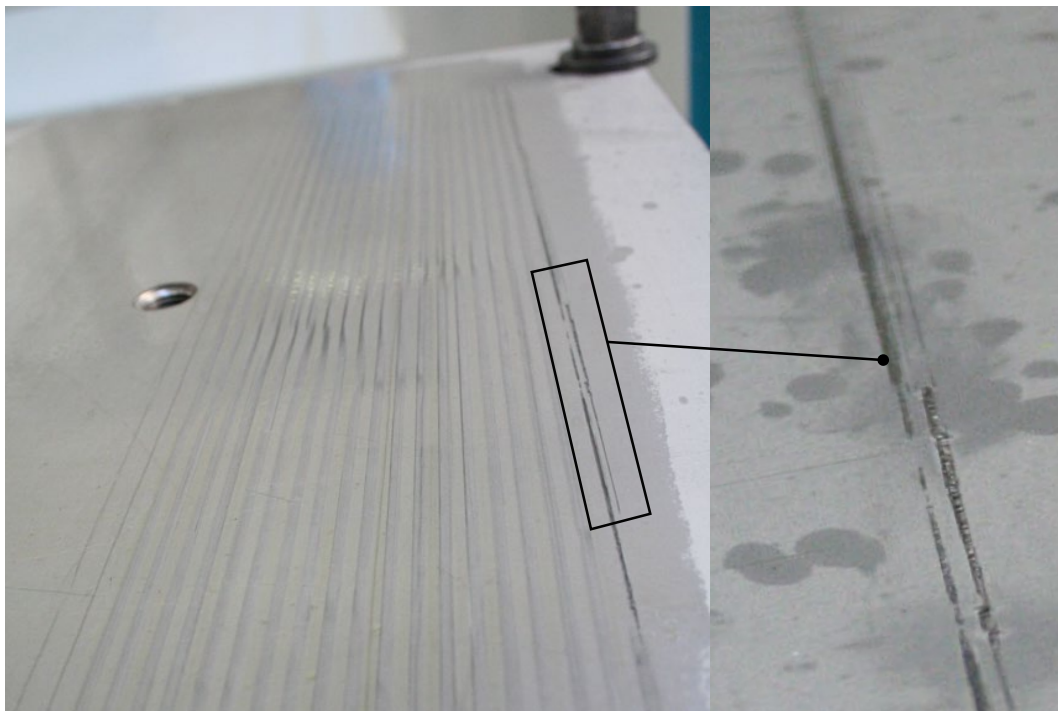


Figure 7.8: Generated wear on tested sheet metal

7.6 Obtained Results

Picture 7.8 emphasizes the resulting wear effects on the engaged metal sheet. The first lane (on the very right) is very distinct in comparison to the remaining wear paths. This is due the fact that the first tribological encounter was realized without any applied lubrication. As a direct result, frettings and severe material transfer in general could be observed. For the following sequence, the metal was coated with oil, which resulted in a tremendous improvement of the obtained wear behaviour. The test pin also showed severe signs of were and had to be polished during the test sequence to ensure a planar contact. Even though the pilot test was only conducted to substantiate the basic functions of the tribo-module, these results also demonstrate the overall need for wear slowing tool coatings.

Chapter 8

Concluding Remarks and Outlook

All presented findings coincide when it comes to the necessity of tribometric testing engagements in order to simulate and anticipate tribological behaviour of technical systems. Even though many scientific projects focus on the mathematical description of friction processes, and progress has evidently been made, a reliable prediction of friction - and consequently wear - behaviour can not be made. The interdependencies and overlapping of single friction and wear mechanisms still call for an experimental determination of these *system parameters*, and thus, making tribometry and its many variants indispensable.

Having stated this, tribometric configurations also forfeit a large amount of significance because of the high degree of simplification. This is especially true for the simulation of forming operations, because the vast majority of applied tribometers simulate *closed* tribotechnical systems. This means that the two friction partners are repeatedly engaged in the same contact areas. As forming processes possess *open system* features, another portion of validity of the obtained test outcome is lost.

The presented tribo-module emends this system error, while maintaining the low complexity factor that is common to all tribometric equipment. In addition, it mainly consists of standardized parts and therefore also features low investment and maintenance costs. The functionality of the designed device has been verified in a pilot test sequence and the results are very promising.

As stated in Section 2.5.2 ‘Tribometry’, the possibilities to realize a specific tribometric constellation appear endless. The presented instrument is a very basic variation that can easily be upgraded and adapted to extended purposes due to its modular design. Such potential improvements include:

Sheet Fixation

In order to facilitate future wear tests, the enlargement of the sheet metal surface engaged in the test sequence is highly recommended. Even though the clamping mechanism, as presented in the previous chapter, is efficient, a substitutional system that does not require the accurate cutting of the sheet metal would be favourable as well.

Feeding System

Another aspect related to the handling of the metal sheet is the possible introduction of an expedient feeding system. By introducing a coiler/decoiler system, for example, the performed wear tests would not be limited in the realized distance (*wear path*), and the test sequence would not have to be interrupted for the exchange of sheet metals.

Hot Tribology

As presented in Chapter 6 ‘Technical Realisation’, the tribo-module features a system that cools the entire test unit, including the engaged test pin. The applied connections fit the utilities of the engaged *SHW UniSpeed milling centre*. In order to simulate state-of-the-art hot-forming processes, however, the sheet metal has to be heated to temperatures up to 900 °C. Realizing such a temperature increase, in a controlled way, is complex as it is. Adding a functional heating device into the milling centre, while shielding all relevant components from the heat impact, is demanding.

The incorporation of the heating system is the optimization aspect that should be focused on primarily in the near future, as *hot tribology* is thought to be highly viable in the fields of tribological research.

In conclusion, it can be said that the overall project demands have been met and a functional, economic tribometric device, with a low degree of complexity, has been generated in the course of this master thesis. It is believed that the designed module bares great potential, especially regarding ongoing research in the fields of *hot tribology*.

Appendix A

Wear related Terms and Definitions

Name	Cat.	Definition
Abrasion Abrasion	WM	Material removal caused by furrowing or scratching strain.
Abrasive erosion Gleitstrahlverschleiß	TW	Special form of <i>solid particles erosion</i> , with a stream of particles that is nearly parallel to the solid's surface.
Abrasive wear Abrasiveverschleiß	TW	Wear type caused by <i>abrasion</i> .
Adhesion Adhäsion	WM	Formation of interface bondings Friction mechanism as well as wear mechanism.
Adhesive wear Adhäsivverschleiß	TW	Wear type caused by <i>adhesion</i> .
Amount of wear Verschleißbetrag	WI	Length, surface, volume or mass changes in the wearing body.
Bearing area Tragbild	WA	Distinctive friction surface that was formed due to changes in the surface morphology during a tribological process.
Blunting, Truncating Abstumpfung	WA	Unwanted deformation, for example of a cutting edge.
Bouncing Prallen	SC	<i>Impacting</i> perpendicular to the solid's surface.
Cavitation Kavitation	Misc	Formation and implosion of cavities in liquids, when local pressures are smaller than the vapour pressure. This can lead to micro jets with high velocities that penetrate the solid's surface.

Misc... Miscellaneous, **SC...** Stress Collective, **SS...** System Structure, **TW...** Type of Wear

WA... Wear Appearance, **WI...** Wear Indicator, **WM...** Wear Mechanism, **WT...** Wear testing procedure

Name	Cat.	Definition
Cavitation erosion Kavitationserosion	TW	Material removal caused by micro jets.
Chatter marks Rattermarke	WA	Periodic alterations of surface topography, caused by <i>stick slip</i> or vibrations.
Chipping, Flaking Abplatzer	WA	Comparatively large flakes lost from a surface.
Component wear test Bauteil- Verschleißprüfung	WT	Wear test examining original parts in one aggregate.
Corrosion-erosion Erosions-Korrosion	TW	Concurrence of <i>erosion</i> and <i>corrosion</i> . Usually <i>corrosion</i> can progress because protective layers are destroyed by <i>erosion</i> .
Craze cracking Brandriss	WA	Cracks near surfaces, caused by simultaneous shear stresses and heat impact; e.g. during boundary friction or at beginning <i>seizure</i> .
Delamination Delamination	WA	Stripping off of (surface) layers due to mechanical or thermal overload.
Drop erosion Tropfenschlagerosion	TW	Material removal caused by the <i>impingement of drops</i> .
Electroerosive wear Elektroerosiver Verschleiß	TW	Material removal that is induced by electric discharge.
Embedding Einbettung	WA	Embedding of hard foreign particles into softer base or opposing body.
Erosion Erosion	Misc	Influence of loose abrasive particles, flowing gases/liquids and their combination on solid bodies.
Erosive wear Erosionsverschleiß	TW	Material removal induced by <i>erosion</i> .
Fatigue wear Ermüdungsverschleiß	TW	Wear due to material disruption (- caused by periodic tribological strain).
Field wear test Betriebs- Verschleißprüfung	WT	Wear test examining the entire engine or facility under realistic conditions.
Flake, Spill, Sliver Schuppe	WA	Surface lamination by tangentially material deformation or adhesive material transfer.
Flaking Ausbruch	WA	Surface damage that leads to an interface with fracture characteristics.

Misc... Miscellaneous, **SC...** Stress Collective, **SS...** System Structure, **TW...** Type of Wear

WA... Wear Appearance, **WI...** Wear Indicator, **WM...** Wear Mechanism, **WT...** Wear testing procedure

Name	Cat.	Definition
Flash temperature Blitztemperatur	Misc	Temporary temperature increase within a microscopic area of a friction surface.
Fluid erosion Flüssigkeitserosion	TW	Material removal caused by flowing liquids.
Fluid erosion wear Spülverschleiß	TW	Trough-shaped and sinuous material removal caused by erosive media.
Formation of craters Auskolkung (Kolk)	WA	Trough-shaped form of wear appearance, e.g. in conveying systems caused by abrasive bulk materials or on the chip surface of cutting tools.
Fretting corrosion Reibkorrosion/ oxidation	WM	Material removal of contacting bodies under small oscillating relative motions with the presence of corrosive media. Special form of tribochemical reaction.
Fretting debris Passungsrost	WA	Powdery, oxidized <i>wear debris</i> or coating that is caused by <i>fretting wear</i> and can be attributed to tiny relative motions in fitting.
Fretting wear Schwingungsverschleiß	TW	Wear between two contacting bodies with an oscillating relative motions of small amplitude.
Friction martensite Reibmartensit	WA	Very hard and brittle layers at steel surfaces, which were formed by local exceeding of austenitising temperatures due to friction heat.
Fusion of low melting phases An-, Ausschmelzung	WA	Friction induced form of wear appearance caused by the melting of material components.
Gas erosion Gaserosion	TW	Material removal due to flowing gases.
Hydroabrasive wear Hydroabrasivverschleiß	TW	Wear that is caused by solids or particles that are carried by a flowing liquid.
Impact Stoßen	SC	Mechanical interaction during a short period of time, with an impulse and energy transfer between the colliding bodies.
Impact wear Stoßverschleiß	TW	Wear caused by <i>impacting</i> .
Impingement, Impact erosion Prallstrahlverschleiß	TW	Special form of <i>solid particles erosion</i> , with a stream of particles that is nearly perpendicular to the solid's surface.
Impingement of drops Tropfenschlag	SC	Impact loading of a solid surface by impacting liquid drops.

Misc... Miscellaneous, **SC...** Stress Collective, **SS...** System Structure, **TW...** Type of Wear

WA... Wear Appearance, **WI...** Wear Indicator, **WM...** Wear Mechanism, **WT...** Wear testing procedure

Name	Cat.	Definition
Indentation Eindrücken (Eindruck)	WA	Surface deformation caused by particles that are pressed into the base or opposing body.
Initial pitting Einlaufgrübchen	WA	Pittings that are caused by initial stresses.
Operating variables Beanspruchungskollektiv	Misc	Stress collective that acts upon a tribological system.
Oblique impact wear Schrägstrahlverschleiß	TW	Special form of <i>solid particles erosion</i> , with a stream of particles at an oblique angle (0° - 90°) to the solid's surface.
Oscillation, Vibration Schwingen	SC	Oscillating relative motion (sometimes of very small amplitudes).
Overlap ratio Eingriffsverhältnis	SC	Ratio between contact and friction surface.
Particle plowing Teilchenfurchung	TW	Surface damages in the form of <i>ripples</i> , caused by the sliding motion of free moving particles.
Permanent wear Dauer-Verschleiß	WI	Wear after <i>running in</i> occurred.
Pitting Grübchen	WA	Shell-shaped deepening (caused by material removal) that can be attributed to <i>surface fatigue</i> .
Reaction layer Reaktionsschicht	WA	A solid layer of reaction products at the surface of solids, formed by tribochemical reactions.
Ripple, Corrugation Rides Riffel	WA	Periodic, sinuous surface alterations, perpendicular to the direction of motion.
Rolling abrasion Kornwälzverschleiß	TW	Wear caused by two rolling bodies, with abrasive particles in between them.
Running in Einlaufen	Misc	Alteration of geometry as well as physical, chemical or mechanical properties of surface areas of two friction partner under initial stresses.
Running in wear Einlaufverschleiß	Misc	Slightly increased wear that emerges during <i>running in</i> and that is often desired.
Scar Narbe	WA	Irregular deepening, caused by <i>fretting corrosion</i> , <i>cavitation</i> , <i>erosion</i> or locally limited plastic deformations.
Score, Groove Riefe	WA	Long, linear surface damages in sliding direction, caused by hard roughness peaks of opposing body or harder particles.

Misc... Miscellaneous, SC... Stress Collective, SS... System Structure, TW... Type of Wear

WA... Wear Appearance, WI... Wear Indicator, WM... Wear Mechanism, WT... Wear testing procedure

Name	Cat.	Definition
Scouring abrasion Furchungsverschleiß	TW	<i>Abrasive Wear</i> induced by roughness peaks or hard particles in sliding contacts.
Scrape Anschürfung	WA	Roughening of bearing surfaces caused by the sliding instead of the rolling of rolling elements.
Scuffing Fressverschleiß	TW	<i>Adhesive wear</i> - on a macroscopic scale.
Seizure Fressen	TW	Destruction of friction surface by <i>adhesion</i> - on a macroscopic scale.
Solid particles erosion Strahlverschleiß, Festkörperverschleiß	TW	Wear caused by a stream of solid particles.
Spalling, Flaking Ablätterung	WA	Flaking of flat particles from surface areas, because of material defects, processing errors or overstressing.
Standstill marks Stillstandsmarkierungen	WA	Surface damage that occurs while system stands still. It can be caused by external vibrations, corrosive exposure, mechanical loads or by passages of current through the system.
Stick slip Ruckgleiten	SC	Fitful intermitting motion between sliding bodies, caused the release of elastic energy in the contact area.
Surface fatigue Oberflächenzerrüttung	WM	Material fatigue and formation of cracks in surface-near areas, which can cause material removal.
Thermal wear Thermischer Verschleiß	TW	Material loss due to softening, melting or evaporation during sliding or rolling motions.
Three body abrasion Kornleitverschleiß, Dreikörperverschleiß	TW	Wear caused by two sliding bodies with abrasive particles between each other.
Total life Gesamtgebrauchsdauer	WI	Total period of time (including down times) after which a part loses its functionality due to wear.
Tribochemical reaction Tribochemische Reaktion	WM	Chemical reactions in a TTS between the base body, the opposing body and the intermediate/surrounding media that are activated by the exerted friction.
Tribooxidation Triboxidation	WM	Special case of a <i>tribochemical reaction</i> . Oxidation reaction in a TTS.
Washout Auswaschung	WA	Material removal caused by flowing media, usually due to the formation of turbulences.

Misc... Miscellaneous, SC... Stress Collective, SS... System Structure, TW... Type of Wear

WA... Wear Appearance, WI... Wear Indicator, WM... Wear Mechanism, WT... Wear testing procedure

Name	Cat.	Definition
Wear Abnutzung	Misc	Unwanted devaluation of objects due to mechanical, chemical, thermal and/or electric energy impact.
Wear coefficient Verschleißfaktor, Verschleißkoeffizient	WI	Empirically determined proportionality factor in wear related equations.
Wear debris Abrieb	WA	Material removed from the functional area due to tribological strains.
Wear life Verschleißbedingte Lebensdauer	WI	Total service life without downtimes.
Wear rate Verschleißrate	WI	<i>Amount of wear</i> in relation to suitable reference parameters (like loading time or distance).
Wear reserve Verschleißreserve	WI	Amount of material that can be worn out until the functionality of the TTS is no longer guaranteed.
Wear resistance Verschleißbeständigkeit	WI	Resistiveness of the TTS and the relevant parameters of its elements to wear. The <i>wear resistance</i> is given by the inverse of the <i>wear rate</i> .

Table A.1: List of wear definitions in alphabetical order [GfT, 2002]

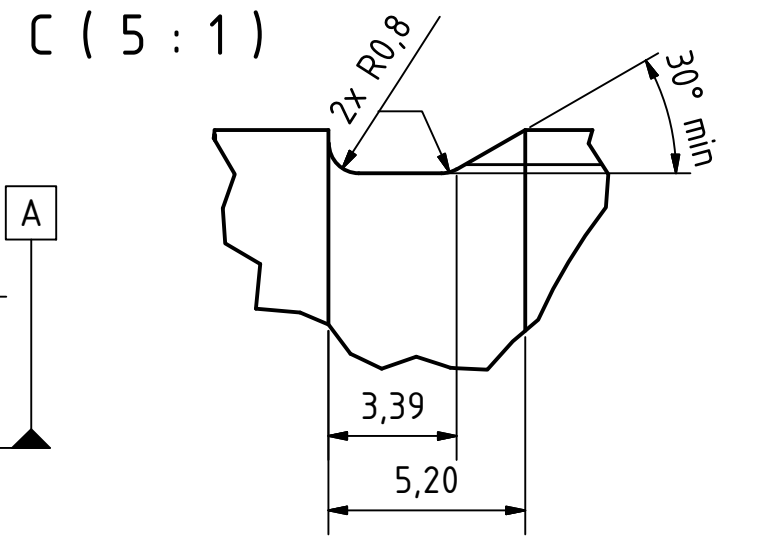
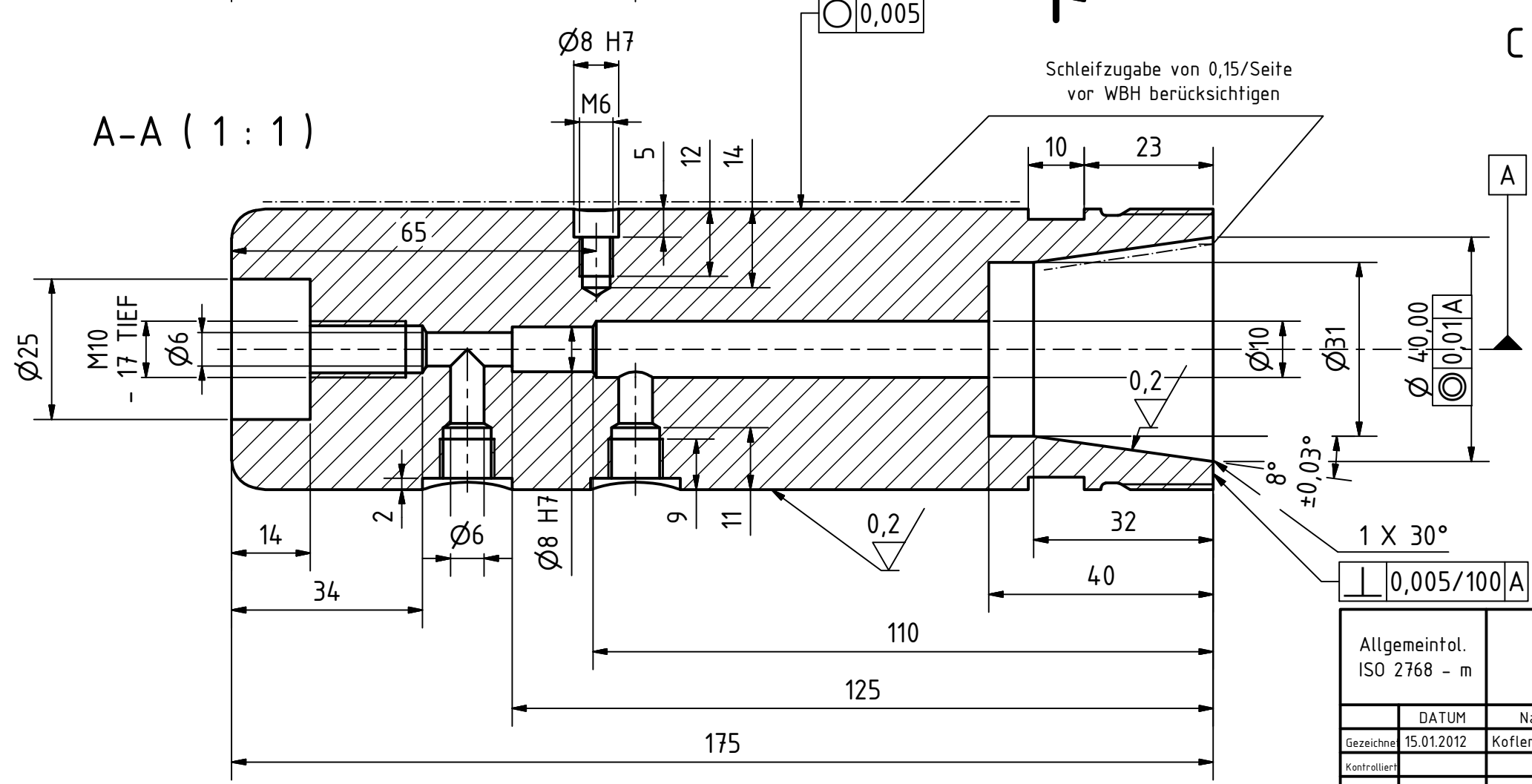
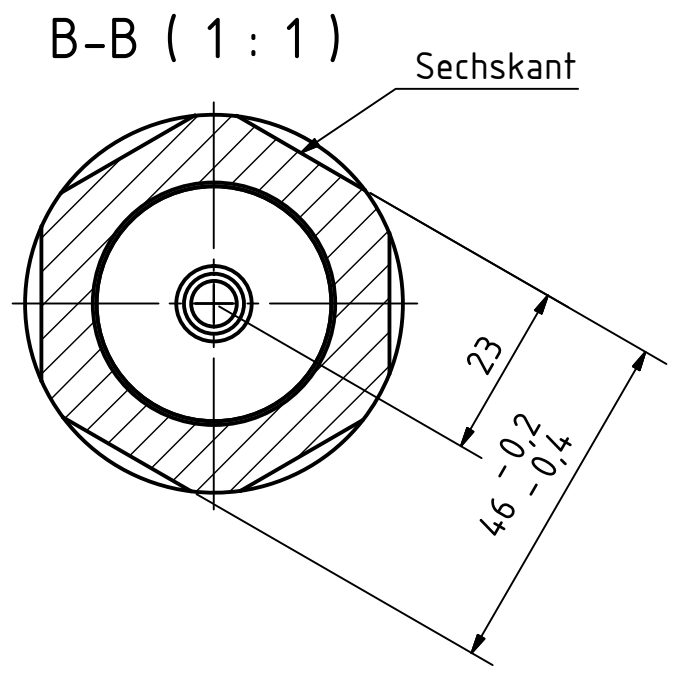
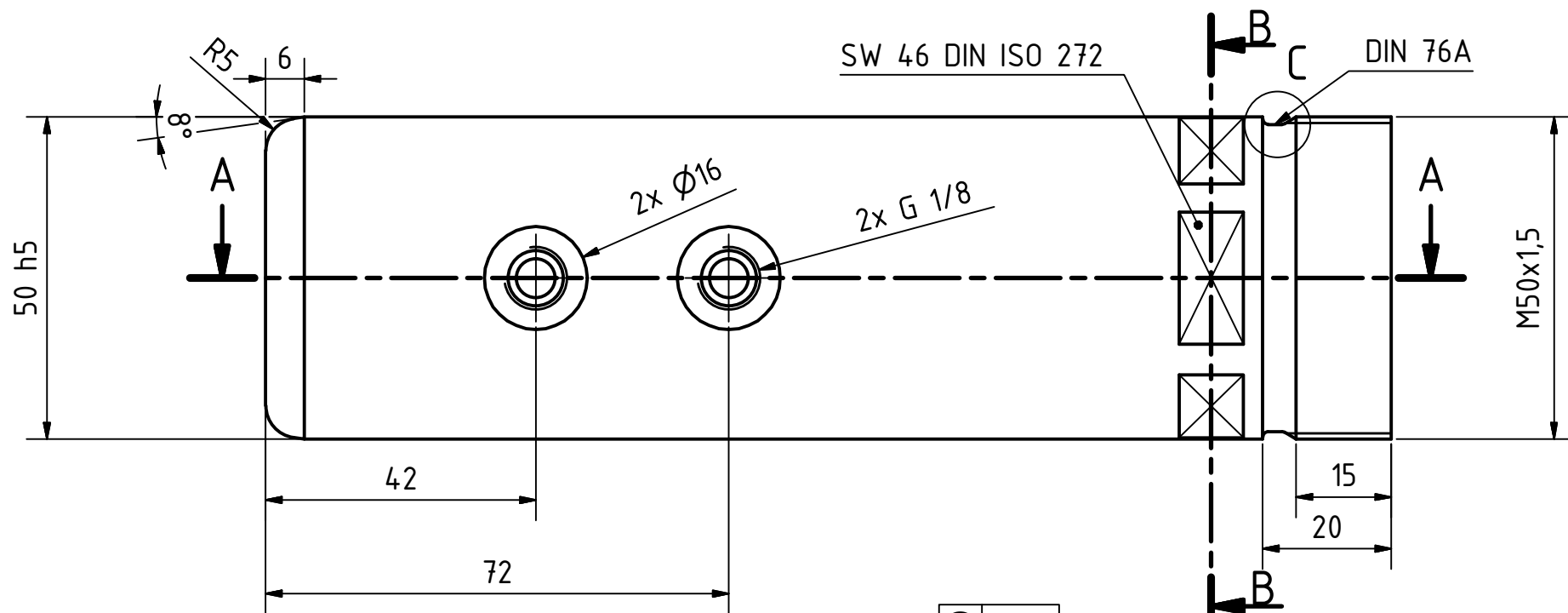
Appendix B

Technical Drawings

Please find attached all technical drawings according which the tribo-module was manufactured. All referenced standards can be obtained from Appendix 'Bibliography'.

Table B.1: Overview of attached technical drawings

No	Manufactured Part	Semi-finished Product	Supplier	Weight
B1	Guide pillar	Round bar 60/250/2379	Meusburger	2.237 kg
B2	Scaling pin	Shoulder screw E 1240	Meusburger	0.015 kg
B3	Test pin (+ cooling channel)	Round bar 20/800/2210	Meusburger	0.015 kg
B4	Housing	Round bar 205/250/1730	Meusburger	16.768 kg
B5	Thrust plate	Round bar 81/20/2312	Meusburger	0.048 kg
B6	Assembly drawing (+ parts list)	-	-	-
B7	Overview end positions	-	-	-



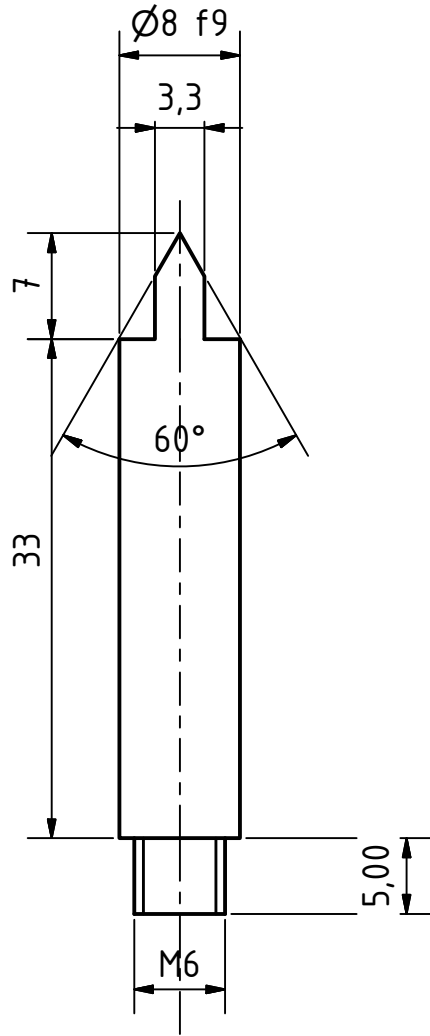
1,6 / (0,2 /) gehärtet und angelassen
60 + 3 HRC

Alle unbemaßten Kanten: 0,5x45°

Übersetzungstabelle		
Passmaß	Höchstmaß	Mindesmaß
8 H7	8,015	8,000
50 h5	50,000	49,989

1 X 30°
0,005/100 A

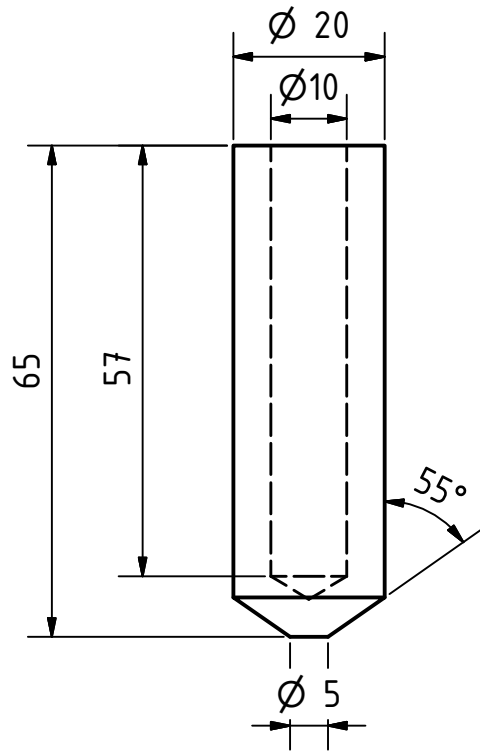
Allgemeintol. ISO 2768 - m	Maßstab: 1:1	Gewicht: 2,237 kg
	Material: X 155 CrVMo 121 - 1.2379 Meusburger Rohmaterial: 60/250/2379 Rundstab	
DATUM	Name	Component drawing
Gezeichnet 15.01.2012	Kofler M.	
Kontrolliert		
Norm		
B1 Guide pillar		1
		A3




Übersetzungstabelle		
Passmaß	Höchstmaß	Mindestmaß
8 f9	7,987	7,951

Alle unbemaßten Kanten: 0,5x45°

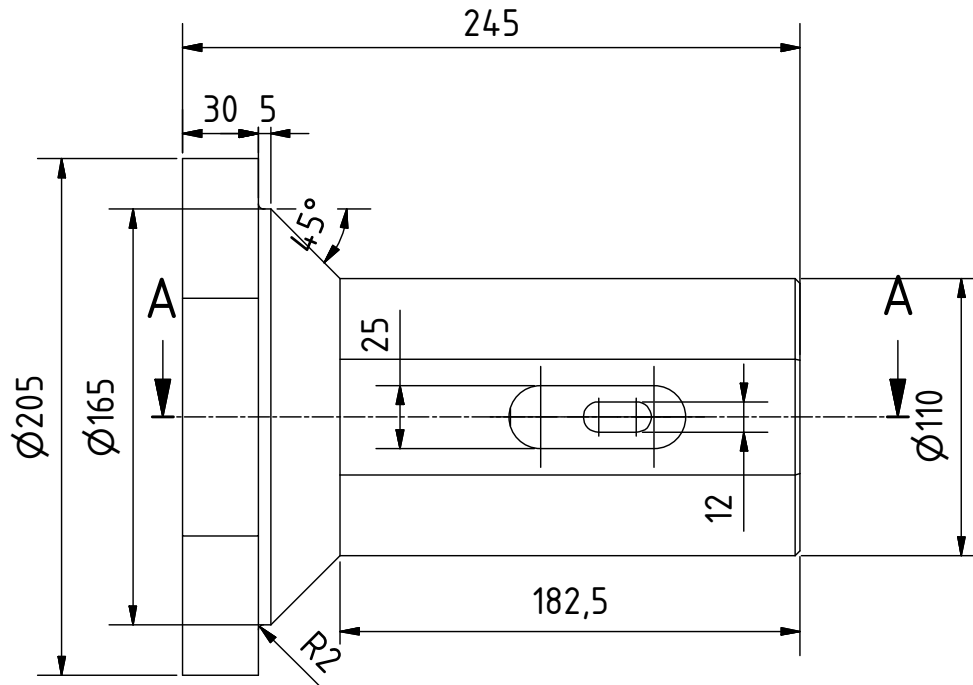
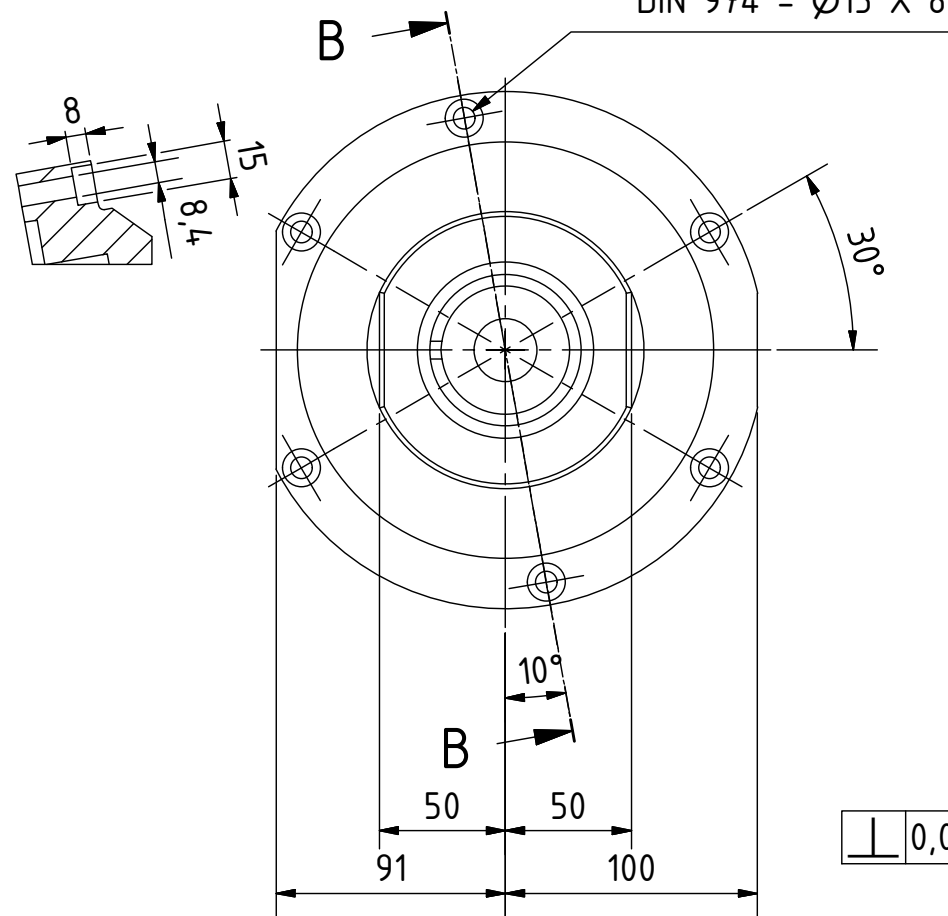
Allgemeintol. ISO 2768 - m		1,6	Maßstab: 1:1	Gewicht: 0,015 kg
Gezeichnete		DATUM	Rohmaterial: Schulter-Passschraube 8 x 70 - Meusburger E 1240	
Kontrolliert		Name	Component drawing	
Norm		15.01.2012		
		Kofler M.		
			B2 Scaling pin	
			1	
			A4	



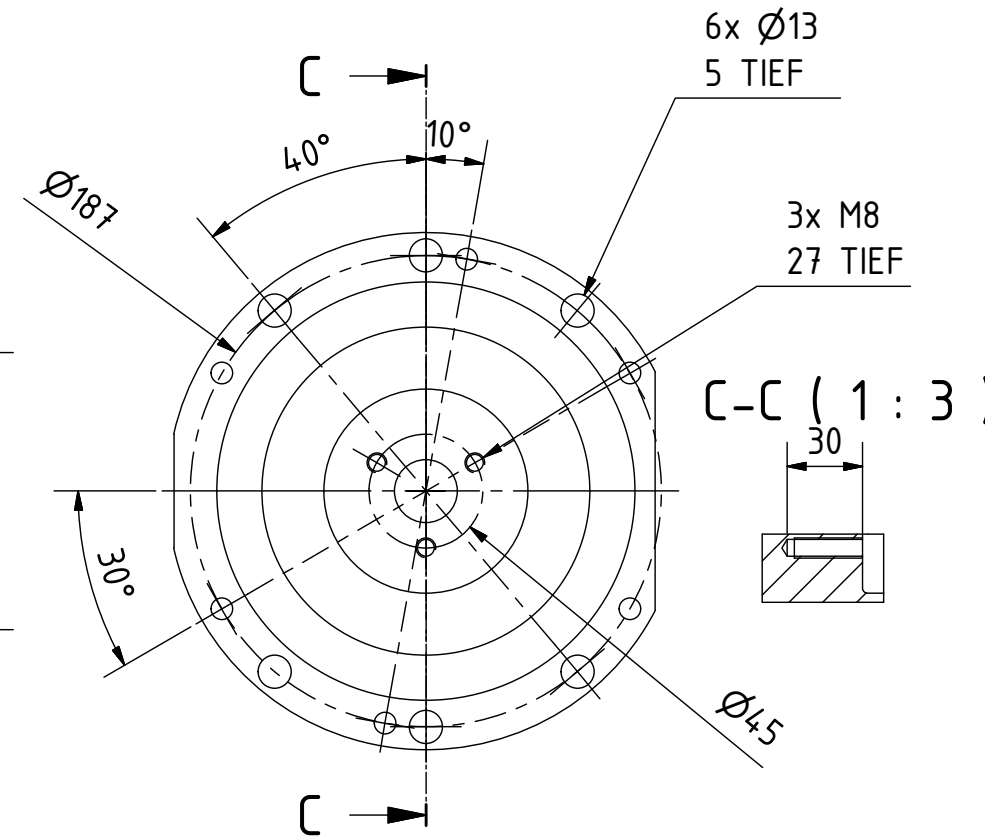
Alle unbemaßten Kanten: 0,5x45°

Allgemeintol. ISO 2768 - m			Maßstab: 1:1	Gewicht: 0,015 kg
			Rohmaterial: Rundstab 20 x 800 - Meusburger 1.2210	
	DATUM	Name	Component drawing	
Gezeichnet	07.03.2012	Kofler M.		
Kontrolliert				
Norm				
			B3 Testing Pin	
			1	
			A4	

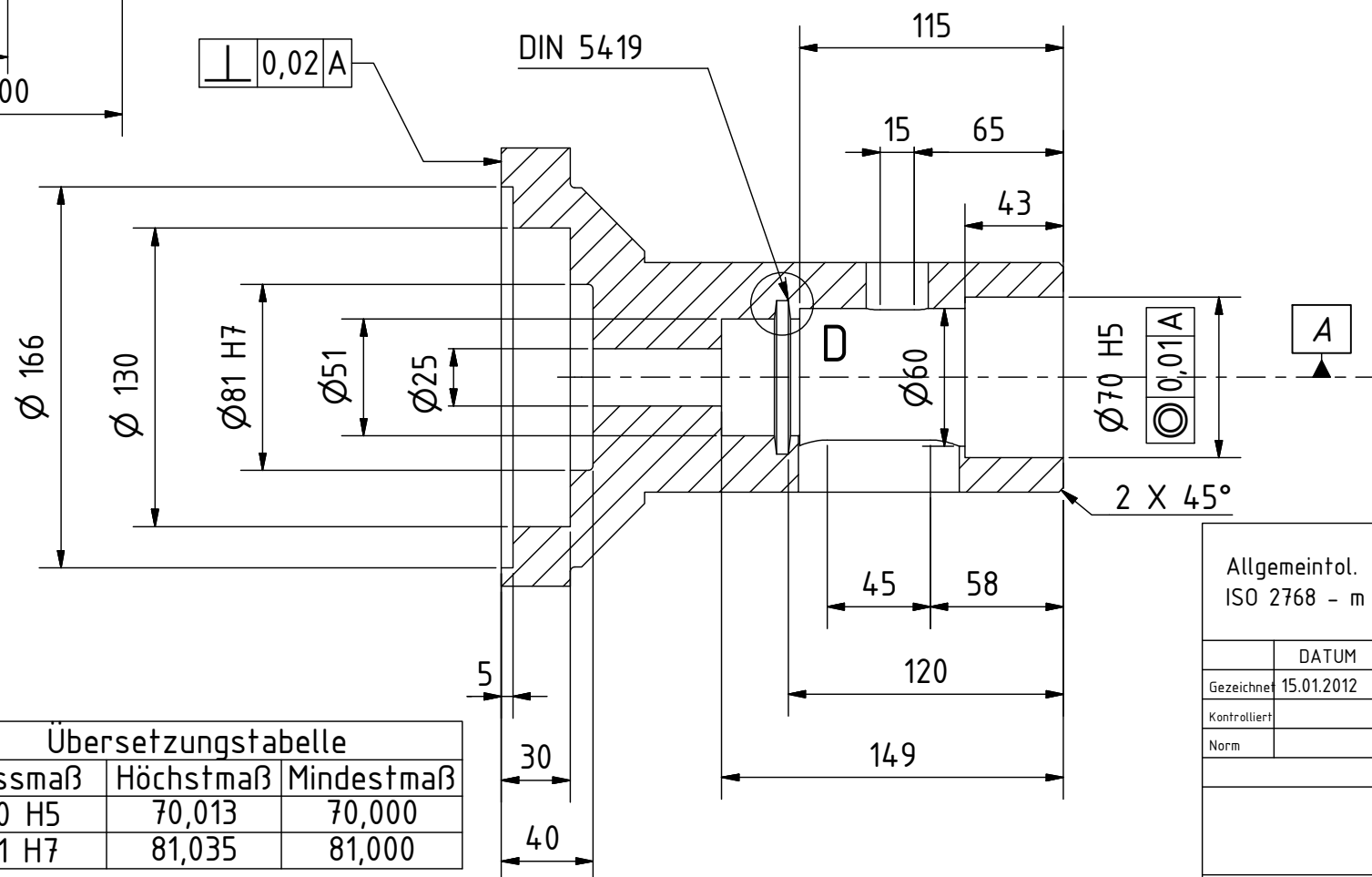
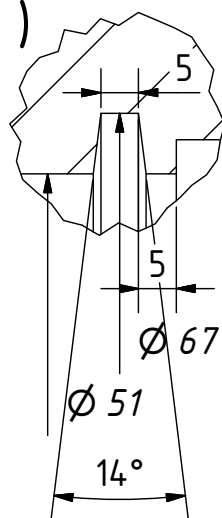
B-B (1 : 3)



A-A (1 : 3)



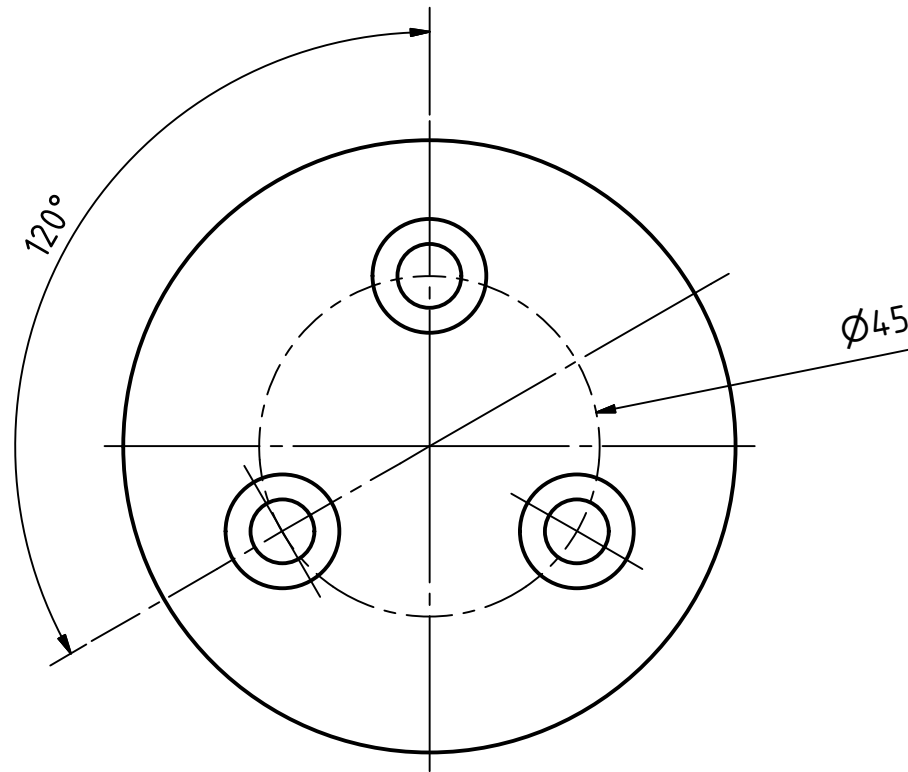
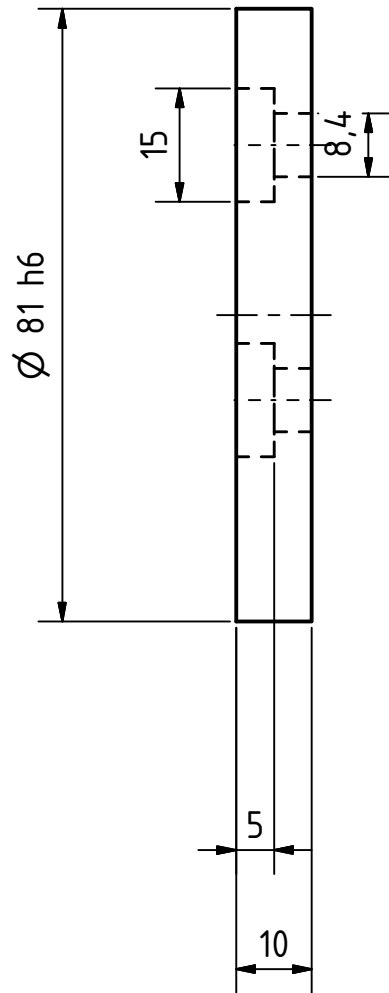
D (1 : 1)



Übersetzungstabelle		
Passmaß	Höchstmaß	Mindestmaß
70 H5	70,013	70,000
81 H7	81,035	81,000

Alle unbemaßten Kanten: 1x45°

Allgemeintol. ISO 2768 - m		1,6	Maßstab: 1:3 (1:1)	Gewicht: 16,786 kg
Gezeichnet 15.01.2012		Name Kofler M.	Material: C 45 U - 1.1730 Meusburger Rohmaterial: NR 205/250/1730 Rundstab	
Kontrolliert		Component drawing		
Norm		B4 Housing		
				1
				A3

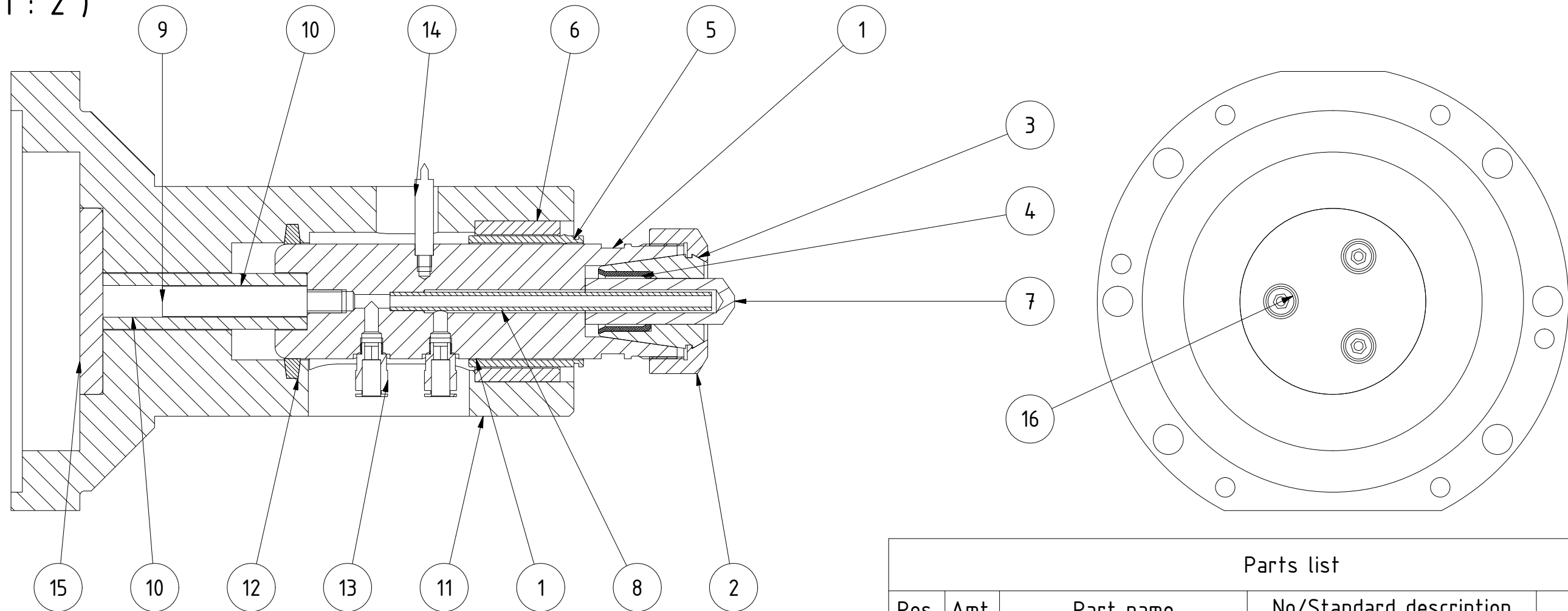


Alle unbemaßten Kanten: 0,5x45°

Übersetzungstabelle		
Passmaß	Höchstmaß	Mindestmaß
81 h6	81,000	80,978

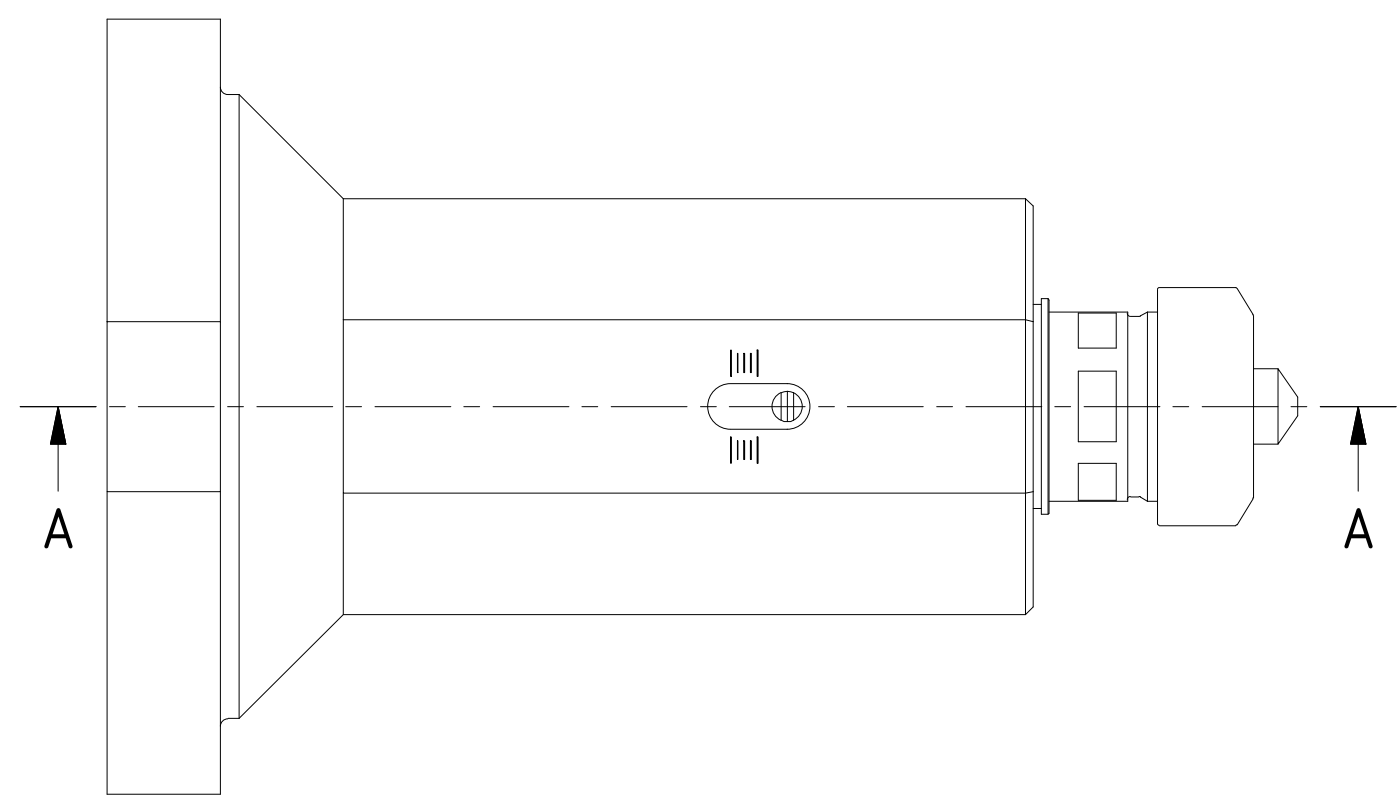
Allgemeintol. ISO 2768 - m		1,6	Maßstab: 1:1	Gewicht: 0,048 kg
Gezeichnete		DATUM	Material: 40CrMnMoS 86 - 1.2312 Meusburger Rohmaterial: NR 81/20/2312 Rundstab	
Kontrolliert		Name	Component drawing	
Norm		Kofler M.		
			B5 Thrust plate	1
				A4

A-A (1 : 2)



Parts list

Pos.	Amt.	Part name	No/Standard description	Remark
1	1	Guide pillar	B1	In-house prod.
2	1	Collet nut	DIN 6499 ER/UM 40	Available
3	1	Collet	DIN 6499 ER 40 (20)	Nann
4	1	Sealing disc	DIN 6499 D-472 E	Nann
5	1	Ball cage	50x50	Fibro
6	1	Guide bush	DIN 9831/ISO 9448-3 50x37	Fibro
7	1	Test pin	B3	In-house prod.
8	1	Copper tube	80x1.5	Zänker & D.
9	1	Guide bolt for springs	DIN/ISO 10069-2 13x63	Meusburger
10	2	Compression spring	DIN/ISO 10243 25x12x89	Fibro
11	1	Housing	B4	In-house prod.
12	1	Felt ring	DIN 5419 F2-50	Filzshop
13	2	Plug-in connection	NPQM G18-Q8-P10	Festo
14	1	Scaling pin	B2	In-house prod.
15	1	Thrust plate	B5	In-house prod.
16	3	Hexagon socket head cap screws with low head	DIN 7984 M8x25	Available



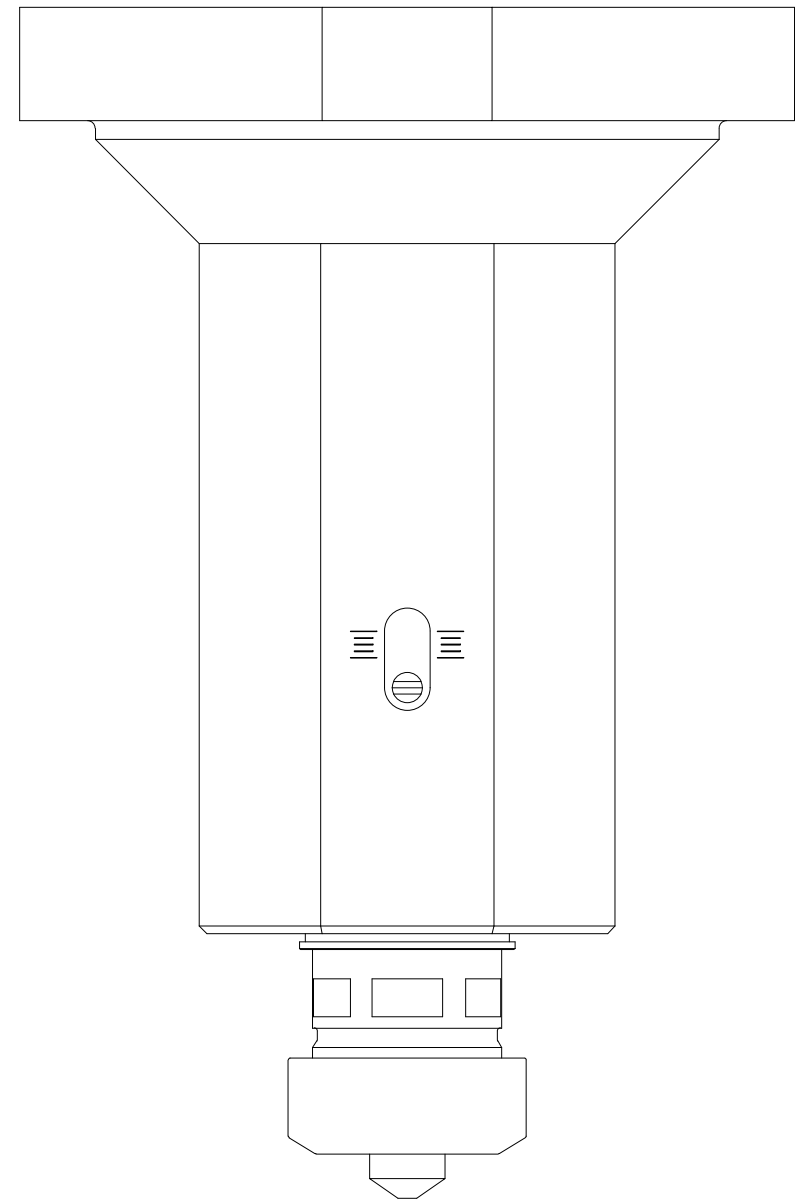
DATUM		Name		Assembly drawing
Gezeichnet	07.03.2012	Kofler M.		
Kontrolliert				
Norm				B6 Tribo Module
				1
				A3

6 5 4 3 2 1

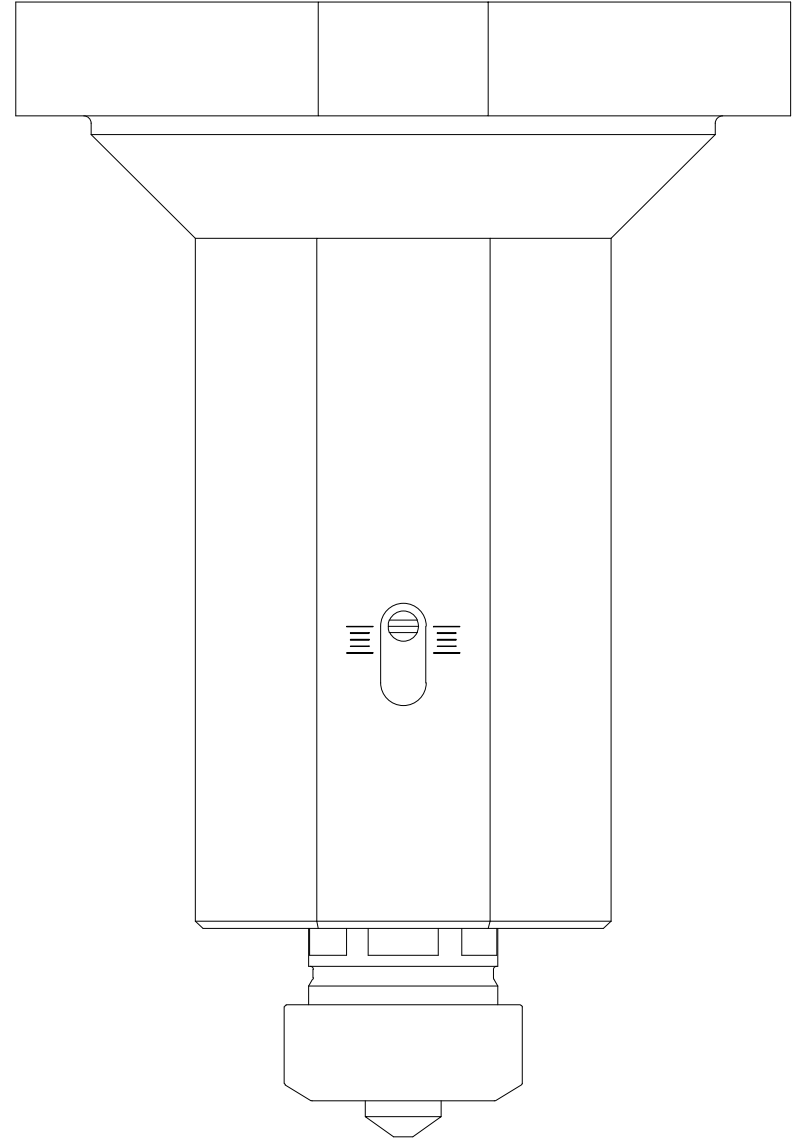
D

D

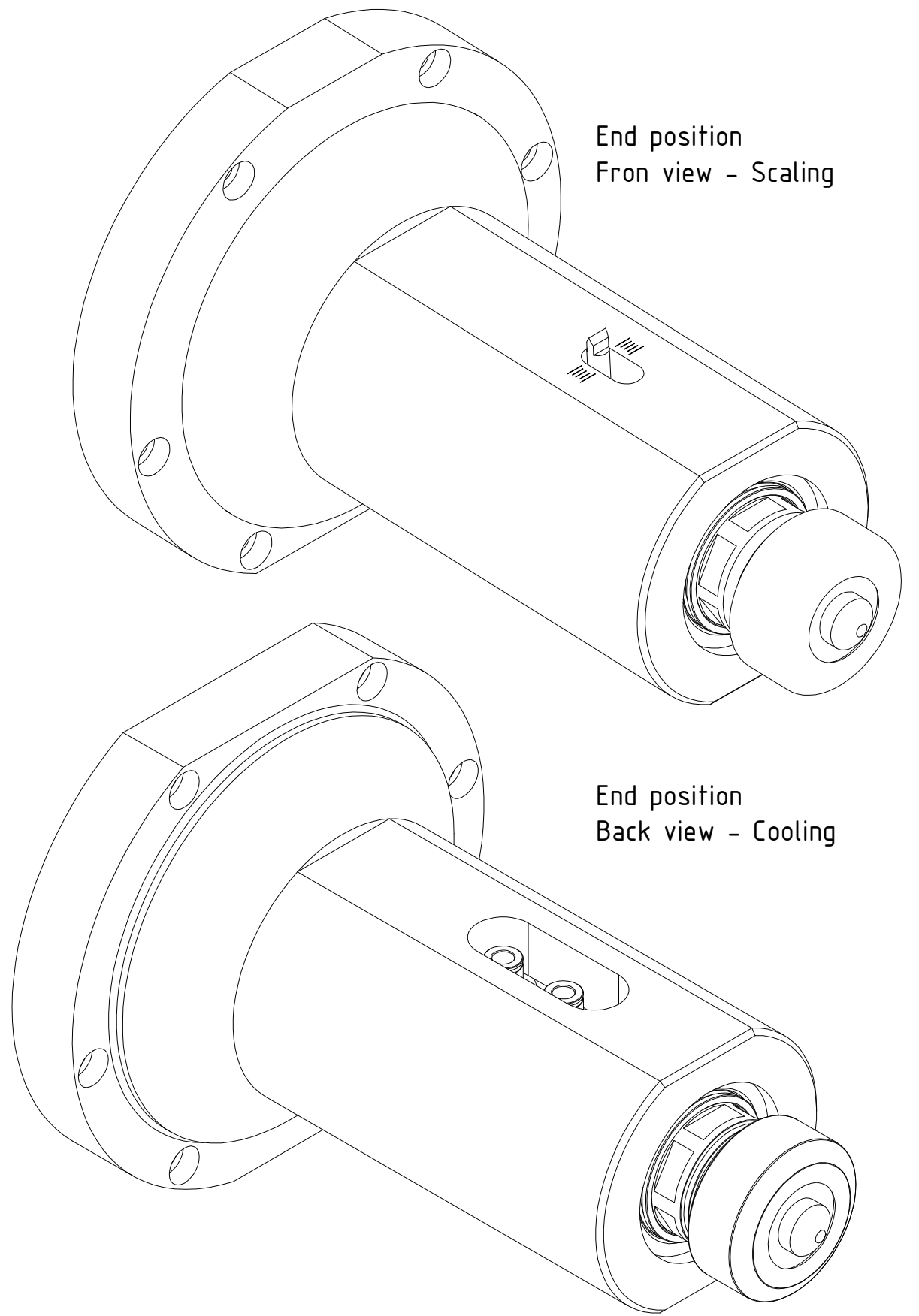
End position
Fron view - Scaling



Starting Position
(without primary tension of
compressiong spring)



End position
(maiximal surface
pressure)



End position
Back view - Cooling

VON EINEM AUTODESK-SCHULUNGSPRODUKT ERSTELLT

VON EINEM AUTODESK-SCHULUNGSPRODUKT ERSTELLT

C

C

B

B

A

A

	DATUM	Name
Gezeichnet	16.03.2012	Kofler M.
Kontrolliert		
Norm		

Assembly Drawing - End positions

B7 TriboModule

1
A3

6 5 4 3 2 1

List of Figures

1.1	Strength-formability relation of common steel grades	2
2.1	Schematic description of a tribotechnical system	6
2.2	Friction according to motion types	10
2.3	Friction states as a function of the lubricating film thickness	12
2.4	Wear types based on different tribological loads	15
2.5	Examples of adhesive wear	16
2.6	Examples of abrasive wear	16
2.7	Examples of tribochemical wear	17
2.8	Example of surface fatigue	18
2.9	Example of on-line measurement of wear	20
2.10	Sample geometries in sliding wear tests	22
2.11	Wear tests for rolling and erosion wear	23
2.12	Sample geometries in abrasive wear tests	24
3.1	Historic evidence of forming applications	27
3.2	Illustration of forming techniques	30
3.3	Principle of deep drawing	31
3.4	Material reallocation during the drawing of a cup	31
3.5	Stress conditions and wall thickness in a drawn cup	32
3.6	Natural strain distribution of drawn cup	33
3.7	Example of a forming limit diagram (FLD)	35
3.8	Forming process as tribotechnical system	36
3.9	Process principle of laser cladding	41
5.1	Identification of basic testing configurations (Morphological matrix)	46
5.2	Overview of generated concepts	47
5.3	Contact mechanics according to Hertzian theory	48
5.4	Remaining concept variants	48
6.1	Verification of pin diameter	54
6.2	Detail drawing: Holding fixture	55
6.3	Detail drawing: Scaling unit	57
6.4	Detail drawing: Cooling system	58
7.1	Test pin <i>dummy</i> clamped by collet and nut during pilot test sequence	62
7.2	Fixation of sheet metal on existing tool chuck	62

7.3	Overview of basic components of the tribo-module	63
7.4	Assembled and mounted tribo-module	64
7.5	Calibration of tribo-module with a load cell	65
7.6	Hysteresis effect during loading and unloading of tribo-module	66
7.7	Engaged module during pilot test sequence	67
7.8	Generated wear on tested sheet metal	67

List of Tables

2.1	System structures of tribosystems	8
2.2	Variation of friction coefficient of material pairings	13
2.3	Categories of tribological testing	21
3.1	Distinction between laser cladding and other surface treatments	40
5.1	Qualitative evaluation of the remaining concept variants	50
5.2	Direct comparison of last remaining concept variants	51
6.1	Chosen combination of compression springs	56
A.1	List of wear definitions in alphabetical order	76
B.1	Overview of attached technical drawings	77

Bibliography

- Bach, F.-W., Möhwaldand, K., Laarmann, A. and Wenz, T. (2006). *Moderne Beschichtungsverfahren*. Wiley-VCH, Weinheim, Second edition. ISBN 3-527-30977-1.
- Brecher, C. and Weck, M. (2006). *Werkzeugmaschinen 2 - Konstruktion und Berechnung*. Springer, [New York], Eighth edition. ISBN 3-540-22502-1.
- Czichos, H. and Habig, K.-H. (1992). *Tribologie Handbuch: Reibung und Verschleiß; mit 115 Tabellen*. Vieweg, Wiesbaden, First edition. ISBN 3-528-06354-8.
- Doege, E. and Behrens, B.-A. (2007). *Handbuch Umformtechnik; Grundlagen, Technologien, Maschinen*. Springer, Berlin, First edition. ISBN 3-642-04248-1.
- Doege, E. and Behrens, B.-A. (2010). *Handbuch Umformtechnik; Grundlagen, Technologien, Maschinen*. Springer, Berlin, Second edition. ISBN 3-642-04248-1.
- Dowson, D. (1998). *History of Tribology*. Wiley, Second edition. ISBN 978-1-860-58070-3.
- ECOTRIB 2011, editor (2011). *3rd European Conference on Tribology*, Vienna. Österreichische Gesellschaft für Tribologie.
- ETH (2011). *Experimentelle Ermittlung von FLCs*, Lecture Notes; Eidgenössische Technische Hochschule Zürich.
- Fibro (2012). *Spezial-Schraubendruckfedern*, Produktkatalog.
- Fritz, A. H. and Schulze, G. (2010). *Fertigungstechnik*. Springer, Berlin, Ninth edition. ISBN 3-642-12878-3.
- Gee, M. G. and Neale, M. J. (2002). *General Approach and Procedures for Unlubricated Sliding Wear Tests*. National Physical Laboratory (NPL), MGPG(51).
- GfT (2002). *Tribologie: Verschleiß, Reibung; GfT-Arbeitsblatt 7*. Available online: http://www.gft-ev.de/pdf/2002_AB_7.pdf.
- Grote, K.-H. and Antonsson, E. K. (2009). *Springer Handbook of Materials Measurement Methods*. Springer, Berlin, First edition. ISBN 3-540-49131-6.
- Habig, K.-H. (1980). *Verschleiss und Härte von Werkstoffen* -. Hanser, München, First edition. ISBN 3-446-12965-0.
- Jost, H. P. (1996). *Lubrication Education and Research - A report on the present position and industry needs*. Her Majesty's Stationary Office, London, 36.

- Klocke, F. and König, W. (2006). *Fertigungsverfahren 4 - Umformen*. Springer, Berlin, Fifth edition. ISBN 3-540-23650-3.
- Künne, B. (2007). *Köhler/Rögnitz Maschinenteile 1*. Teubner, Wiesbaden, Tenth edition. ISBN 3-835-10093-0.
- Kolleck, R. and Pfanner, S. (2008). *Potentials and innovative application areas of direct laser welding for forming and cutting tools*. 9th International Conference on the Technology of Plasticity (ICTP), 9(1).
- Korres, S., Scherge, T. and Dienwiebel, M. (2011). *In-Situ Observation of Metallic Tribosystems*. In ECOTRIB 2011 [2011], page 551.
- Lange, K. (1990). *Umformtechnik. Handbuch für Industrie und Wissenschaft: Band 3: Blechbearbeitung*. Springer, Berlin, Second edition. ISBN 3-540-50039-1.
- Lange, K. (1993). *Umformtechnik. Handbuch für Industrie und Wissenschaft: Band 4: Sonderverfahren, Prozesssimulation, Werkzeugtechnik, Produktion*. Springer, Berlin, Second edition. ISBN 3-540-55939-6.
- Markova, L., Myshkin, N. and Makarenko, V. (2011). *On-Line Magnetoelastic Oil Viscosity Detector*. In ECOTRIB 2011 [2011], page 503.
- Meissner, M. and Wanke, K. (1993). *Handbuch Federn - Berechnung und Gestaltung im Maschinen- und Gerätebau*. Verlag Technik, Berlin, Second edition. ISBN 3-341-01087-4.
- NANN (2012). *Standardspannmittel*, Produktkatalog.
- Owen-Jones, S. (1997). *Summary on wear test methods; Notes on the 10th International Conference on WEAR OF MATERIALS*. National Physical Laboratory (NPL), CMMT (93).
- Owen-Jones, S. and Gee, M. G. (1997). *Wear testing standards database*. National Physical Laboratory (NPL), CMMT(89).
- Persson, B. N. (1998). *Sliding Friction - Physical Principles and Application*. Springer, Berlin, First edition. ISBN 3-540-63296-4.
- Popov, V. L. (2010). *Kontaktmechanik und Reibung - Von der Nanotribologie bis zur Erdbebendynamik*. Springer, Berlin, Second edition. ISBN 3-642-13301-0.
- Pourciau, B. (2006). *Newton's Interpretation of Newton's Second Law*. Archive for History of Exact Sciences, 60(2):157–207.
- Reissner, J. (2009). *Umformtechnik multimedial; Werkstoffverhalten, Werkstückversagen, Werkzeuge, Maschinen*. Carl Hanser, München, First edition. ISBN 3-446-41840-0.
- Ronkainen, H., Hokkanen, A. and Kapulainen, M. (2011). *Multichannel Optical Sensor for Oil Film Pressure Measurement in Engine Main Bearing*. In ECOTRIB 2011 [2011], page 521.
- Ruge, J. and Wohlfahrt, H. (2002). *Technologie der Werkstoffe: mit 280 Abbildungen und 66 Tabellen*. Vieweg, Wiesbaden, Seventh edition. ISBN 3-528-63021-8.

- Saito, T., Czichos, H. and Smith, L. (2006). *Springer Handbook of Materials Measurement Methods*. Springer, Berlin, First edition. ISBN 3-540-20785-6.
- Sommer, K., Heinz, R. and Schöfer, J. (2010). *Verschleiß metallischer Werkstoffe - Erscheinungsformen sicher beurteilen*. Vieweg + Teubner, München, First edition. ISBN 978-3-8351-0126-5.
- Toyserkani, E., Khajepour, A. and Corbin, S. F. (2005). *Laser Cladding*. CRC Press, Boca Raton, Fla, First edition. ISBN 0-849-32172-6.
- ULSAB-AVC (2001). *Body Structure Materials*. Advanced Vehicle Concepts, AVC(6).
- Vilar, R. M. C. (1999). *Laser cladding*. Journal of Laser Applications, 11(2):64–79.

Online Resources

- CETR (2012). *Comprehensive Materials Testing for Mechanical and Tribological Properties*. Available online: <http://www.bruker-axs.com/cetr-umt-ec-comprehensive-tribo-corrosion-tester.html>; last visited February 2012.
- Gesellschaft für Tribologie (2012). *Was ist Tribologie?* Available online: <http://www.gft-ev.de/tribologie.htm>; last visited February 2012.
- GfT (2002). *Tribologie: Verschleiß, Reibung; GfT-Arbeitsblatt 7*. Available online: http://www.gft-ev.de/pdf/2002_AB_7.pdf.
- Industrial Laser Solutions (2010). *Laser metal deposition defined*. Available online: <http://www.industrial-lasers.com/articles/print/volume-250/issue-6/features/laser-metal-deposition.html>; last visited February 2012.
- International Tribology Council (2011). *Tribology is 45 Years Old; ICT Information Sheet No 194*. Available online: <http://www.itctribology.org/itcnews.php>; last visited January 2012.
- Meusburger (2011). *Online Katalog*. Available online: <http://ecom.meusburger.com>; last visited December 2011.
- RegoFix® (2011). *Technische Informationen*. Available online: http://www.rego-fix.ch/ger/katalog/ti/ti_fs.htm; last visited December 2011.
- Tribotechnic Tt (2012). *Tribotester*. Available online: <http://www.tribotechnic.com/contenu.php?page=tribologie>; last visited February 2012.

Referenced Standards and Guidelines

- DIN 50320. Deutsches Institut für Normung e.V. (1979). Verschleiß; Begriffe, Systemanalyse von Verschleißvorgängen, Gliederung des Verschleißgebiets.
- DIN 50322. Deutsches Institut für Normung e.V. (1988). Verschleiß; Kategorien der Verschleißprüfung.
- DIN 50323. Deutsches Institut für Normung e.V. (1988). Tribologie; Begriffe.
- DIN 6499. Deutsches Institut für Normung e.V. (2002). Spannzangen mit Einstellwinkel 8° für Werkzeugspannung - Spannzangen, Spannzangenaufnahmen, Spannmuttern. Withdrawn and replaced by (ISO 15488:2003).
- DIN 76. Deutsches Institut für Normung e.V. (2004). Gewindeausläufe und Gewindefreistriche - Teil 1: Für Metrisches ISO-Gewinde nach DIN 13-1.
- DIN 8580. Deutsches Institut für Normung e.V. (2003). Fertigungsverfahren - Begriffe, Einteilung.
- DIN 8582. Deutsches Institut für Normung e.V. (2003). Fertigungsverfahren Umformen - Einordnung; Unterteilung, Begriffe, Alphabetische Übersicht.
- DIN 8584. Deutsches Institut für Normung e.V. (2003). Fertigungsverfahren Zugdruckumformen - Teil 1: Allgemeines; Einordnung, Unterteilung, Begriffe.
- DIN ISO 2768-1. Deutsches Institut für Normung e.V. (1991). Allgemeintoleranzen; Toleranzen für Längen- und Winkelmaße ohne einzelne Toleranzeintragung.
- VDI 3822, Blatt 5. Verein Deutscher Ingenieure (1999). Schadensanalyse - Schäden durch tribologische Beanspruchungen.